ABSTRACT

Title of Thesis: Design, Analysis, and Testing of a Flapping Wing Miniature Air Vehicle

Degree Candidate: John Gerdes, Master of Science, 2010

Thesis Directed by: Professor Satyandra K. Gupta
Department of Mechanical Engineering, Institute for Systems Research

Flapping wing miniature air vehicles (MAVs) offer several advantageous performance benefits, relative to fixed-wing and rotary-wing MAVs. The goal of this thesis is to design a flapping wing MAV that achieves improved performance by focusing on the flapping mechanism and the spar arrangement in the wings. Two variations of the flapping mechanism are designed and tested, both using compliance as a technique for improved functionality. In the design of these mechanisms, kinematics and dynamics simulation is used to evaluate how forces encountered during wing flapping affect the mechanism. Finite element analysis is used to evaluate the stress and deformation of the mechanism, such that a lightweight yet functional design can be realized. The wings are tested using experimental techniques. These techniques include high speed photography, stiffness measurement, and lift and thrust measurements. Experimentally measured force results are validated with a series of flight tests. A framework for iterative improvement of the MAV is described, that uses the results of physical testing and simulations to investigate the underlying causes of MAV performance aspects; and seeks to capture those beneficial aspects that will allow for performance improvements. Wings and flapping mechanisms designed in this thesis are used to realize a bird-inspired flapping wing miniature air vehicle. This vehicle is capable of radio controlled flights indoors and outdoors in winds up to 6.7m/s with controlled steering, ascent, and descent, as well as payload carrying abilities.

DESIGN, ANALYSIS, AND TESTING OF A FLAPPING WING MINIATURE AIR VEHICLE

By
John William Gerdes

Thesis submitted to the Faculty of the Graduate School of the
University of Maryland, College Park in partial fulfillment
of the requirements for the degree of
Master of Science
2010

Advisory Committee:

Professor Satyandra K. Gupta, Chair/Advisor
Associate Professor Hugh A. Bruck
Assistant Professor Sarah Bergbreiter
Dr. Stephen A. Wilkerson, U.S. Army Research Laboratory

Acknowledgements

Now that I am finished writing this thesis, I am more aware than ever of the importance of certain people to me and their profound impact on who I am. Therefore, this thesis would not be complete without a proper thank you to these people, as this work was created by many more people than just me.

First and foremost, I want to thank Dr. Gupta, who was always a great advisor to me. During my time in his group, I have learned more than I ever thought possible. Every time I thought I would never graduate or I could not answer a question myself, he always had a new idea and a focused plan for my research. And while I certainly did become a more knowledgeable student, some of the most valuable lessons I learned were about life, the workplace, and how to navigate the hectic world of competing goals, funding, bosses, and emerge with everyone feeling satisfied. I feel that I have been well-prepared to start my career with a feeling of confidence and satisfaction with my academic accomplishments.

I want to thank all of my labmates both in AML and CIM lab. There were many long hours spent together, and I was happy to be part of a group that is full of such lively and fun people. Work among friends like these really does not feel like work at all, and for that I feel very lucky.

I have to offer a big thank you to Drew Wilkerson of Army Research Laboratory, because he may be the one person who has shaped my academic and career choices the most. If I had never met the group out on 'the island' run by Drew four summers ago, I would be doing something very different right now. Over the years, Drew has always had only the very best intentions for me and for all of his students, and in my case, great benefits have resulted. I never could have imagined the opportunities that would open up to me before I met Drew, and I will always be grateful for his support.

This thesis has comprised a tremendous amount of testing and re-testing. Dr. Bruck, Li-Jen Chang, Brian Russ, Brian Porter, and Kelsey Cellon have all combined to spend many hours helping me with what seemed like an impossible amount of lab work. Without these people, I would have needed much longer than two years to graduate. They have all shown great dedication and attention to detail in helping me, and I thank all of them for taking the time to help.

Most importantly, I want to thank my family. You are the most important people in my life, and I will always love you. Mom, Dad, Kim, Heather, and everyone else, this work is dedicated to you.

Contents

Table of Figures

Chapter 1 - Introduction

1.1 Background

1.1.1 Motivation for Miniaturized Unmanned Air Vehicles

In recent years, unmanned aerial vehicles (UAVs) have become an increasingly attractive option in a variety of applications. Larger UAVs have already proven their value in fields such as military, farming, border patrol, search and rescue, mapping, and scientific research, among others. An exciting result of continued research into the aerodynamics of flight at small size scales has been the steady miniaturization of unmanned aerial vehicles. Miniaturization offers exciting new possibilities that are not possible with larger aircraft. Applications that UAVs have dominated with great success for years are becoming manageable with smaller, lighter, and cheaper MAVs. For the purposes of this work, miniature air vehicles are defined as less than 100 grams of total weight. An important distinction is that miniature air vehicles are not the same as micro air vehicles, which DARPA defines as having dimensions of less than 6 inches.

In the wake of recent natural disasters including the Haitian earthquakes and hurricane Katrina, search and rescue teams are presented with challenging terrain preventing them from accessing many areas. Typically, a search and rescue team will consist of about ten people, including dogs and handlers, a paramedic, a structural engineer, and specialists using a variety of equipment to locate victims [1]. If these specialists were armed with a micro air vehicle, debris could be rapidly surveyed without requiring the team to enter a potentially hazardous area.

Figure 1: Search and Rescue team at disaster site [1]

MAVs are capable of very low altitude and low speed flight, making them ideally suited for searching areas that are difficult to observe from higher altitudes, or may be dangerous to access with a helicopter.

Another major area of interest is indoor flight, which would be useful for both search and rescue and military reconnaissance applications. Indoor flight would provide search and rescue teams with a valuable tool for evaluating buildings with reduced risk. While a building may still be standing after a disaster, its weakened structural integrity may present danger to rescuers, so a lightweight and slow MAV could provide a look inside and a mobile platform for a variety of sensors used to search, including microphones and cameras. Similarly, military MAVs could inspect a potentially dangerous building from the inside without requiring soldiers to enter and place themselves in harm's way, and with very light weight, one soldier would be able to carry a MAV.

Resource-intensive missions could be completed in less time with the help of MAVs, where a large number of MAVs scan a target area, thus allowing resources to be directed to the most urgently needed areas. Due to the low altitude and speed of MAV flight, the

information collected by each MAV would be at a very short distance to the target area. With low cost and ease of portability and deployment, it would be simple for a team to deploy multiple MAVs and collect data rapidly.

With one man portability, disposability from a cost perspective, rapid deployment times, and greater availability to a wide range of consumers in commercial, military, and private markets, miniaturized UAVs clearly have unique benefits. As research grows in relevant fields, MAVs continue to improve their usefulness in many areas.

1.1.2 Advantages and Disadvantages of Flapping Wing Flight

Currently, there are three primary techniques for MAV flight - fixed wing, rotary wing, and flapping wing. Each offers performance advantages and disadvantages, depending on the mission requirements. At present, flapping wing MAVs are lacking in performance relative to the other two technologies. However, biological inspiration suggests that flapping wing flight offers unique performance benefits.

Fixed wing MAVs present a challenging problem associated with miniaturization. In Figure 2, two MAVs are shown that are used in development of an aerodynamic simulation model to investigate some of the special effects that take over at small size scales. As the wings are reduced in size, a transition to low Reynolds number aerodynamics occurs, resulting in decreased aerofoil performance [2]. Due to the scaling effects, fixed wing MAVs require high forward speeds to generate the lift necessary for flight. Therefore, it is difficult to perform the intricate maneuvers needed for successful indoor flight. Furthermore, fixed wing MAVs are not well suited to short take-offs and landings, obstacle avoidance, or other behaviors dependent on low flight speeds.

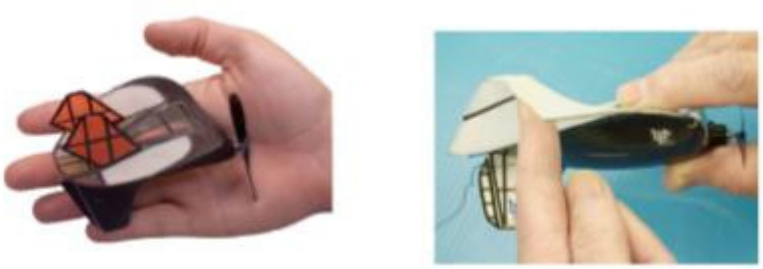

Figure 2: University of Florida fixed wing MAV prototypes [3]

A rotary wing is more capable of performing complex maneuvers, such as vertical take-off and landing, well controlled hover, zero-radius turns, and obstacle avoidance. Unfortunately, rotary wing MAVs suffer from similar disadvantages relating to aerofoil breakdown at low Reynolds numbers. In Figure 3, Seiko Epson Corporation's FR-II MAV is shown, weighing 12.3 grams and capable of a 3 minute flight time. As size is decreased, the lifting capacity of a rotor is significantly degraded [4]. Due to the rapid movement of the rotor blades, there is a distinct noise generated in flight that is easily detected, thus preventing stealthy operation. In addition, a rotary wing could be potentially hazardous to nearby people, with rotor blades spinning at great speeds, capable of inflicting serious injury.

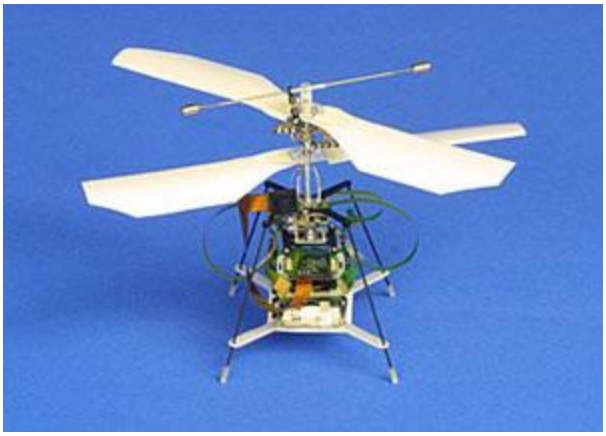

Figure 3: Seiko Epson Corporation FR-II MAV [5]

A flapping wing MAV offers the potential of combining many of the beneficial properties of the other two styles of flight, while minimizing the negative properties. Observation of flying animals suggests that extremely complex and precise maneuvers are possible with flapping wings, even at very small sizes. Animal-inspired flight provides the following advantages over traditional forms of UAV propulsion. Animals are capable of extremely agile flight maneuvers that would translate to useful behaviors such as perching, hovering, navigating tight spaces, and maintaining stability in the presence of strong variable disturbances. Animals are capable of tailoring their flight characteristics to changing aerodynamic demands. This is achieved through variation in angle of attack, wingtip trace pattern, wing area, and complex adjustments to feather orientation. Depending on the particular size, some animals can sustain flight with very low energy consumption, allowing for extended flight duration and excellent glide properties. Because of the wide range of abilities animals demonstrate, a flapping wing MAV offers promise of great versatility in flight. If an MAV were to harness flight techniques exhibited by flying animals, a variety of new missions would be possible that are unavailable at present. Behaviors such as hovering, low speed flight, short take off and landing, and efficient gliding would make flapping wing MAVs a useful compromise between fixed wing and rotary wing MAVs. A key benefit of flapping wings is the favorable scaling relative to fixed wings and rotorcraft. With increased flapping frequency, flight is a possibility even with very small wings. One of the smallest flapping wing MAVs at present is the Harvard Microrobotic Fly, weighing 60mg with a 3cm wingspan, shown in Figure 4.

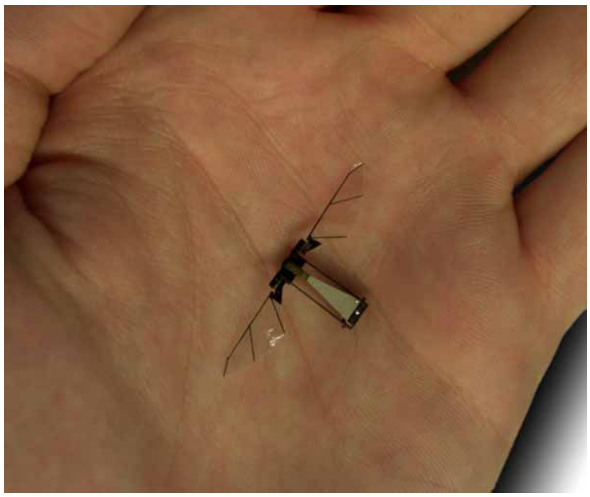

Figure 4: Harvard Microrobotic Fly [6]

An important benefit of wing flapping is that the wings can operate at a significantly lower frequency than a propeller or a rotor, so the noise would be difficult to detect, resulting in very stealthy operation. Visually, a flapping wing MAV would offer a significant stealth advantage relative to the other two styles of flight, since it could easily be decorated to resemble an animal of a similar size. Flapping wing MAVs could even provide a persistent surveillance solution with perching behavior.

1.2 Motivation

The motivation for this work can be organized into the areas of wing design, mechanism design, and modeling.

1.2.1 Wing Design

One of the main challenges in designing a flying flapping wing MAV is the design of the wings. As the wings flap, thrust is generated, propelling MAV through the air. Aerodynamic loading causes significant deformation of the wings, resulting in a large lifting surface. With good wing design, the balance of lift and thrust will contribute to flight performance in multiple ways, including maneuverability, controllability, climbing

rate, payload capacity, and flight longevity. Therefore the wing design is a key factor determining the overall MAV performance. Due to the small size of MAV wings, it is challenging to apply conventional aerodynamic theories to the design of flapping wings for a number of reasons. As wings are scaled down, low Reynolds number aerodynamic effects become more significant. Additionally, the large deformations of the wings can be difficult to accurately predict. With these two effects together, simulation becomes very difficult with acceptable accuracy. Therefore, we will present a test method for determining the lift and thrust performance for a wing design and use this method to select a design with satisfactory results, while simultaneously observing the underlying reasons for differing wing performance.

1.2.2 Mechanism Design

The design of a successful MAV must balance a number of performance metrics that will contribute to the overall suitability of the system. The flapping mechanism must efficiently transmit the power, while keeping weight to a minimum. In addition, the mechanism should be strong enough to withstand adverse weather conditions, large payloads, and crashes. While the mechanical function is important, other considerations also exist, including the cost and the complexity of construction and assembly.

It is important to consider the manufacturing process of the MAV mechanism for a variety of reasons. At present, MAVs tend to be produced one at a time, with very labor intensive assembly processes. Due to a focus on the functional requirements of the MAV, part counts tend to be very large, resulting in greater manufacturing costs. This is a significant challenge for consumers that would like to have rapid storage and field deployment abilities. Since MAVs are expected to operate in hazardous environments in

many cases, it would be beneficial to have a system that is easy to repair and maintain. In addition, if the assembly process can be partially or fully incorporated into the manufacturing process, mass production will be faster and cheaper.

If the overall cost of the MAV can be reduced sufficiently, then consumers will see MAVs and disposable from a cost perspective. This is an attractive feature for military and search and rescue teams, where hazardous missions will likely result in many losses. Without the need to recover the MAVs used in these types of missions, efficiency will be increased, allowing the focus to remain on more important mission aspects, instead of equipment recovery.

The flapping mechanism of the MAV is a key mechanical component of the overall system, and is largely responsible for flight characteristics. The main function of the drive mechanism is to reduce motor's rotary motion and convert it into flapping motion of the wings. In other words, the drive mechanism transmits the energy from the motor to the wings. The efficiency of this power transmission is of major concern. Any power losses will result in reduced performance of the MAV and increased power requirements for the motor. Low-friction bearings cannot be used due to weight considerations. The concept of compliant drive mechanisms is promising for minimization of power losses in the transmission. Additionally, compliant joints can often replace rigid body joints, leading to reduced number of parts in the assembly. However, interconnection of the materials poses several challenges in the considered scale, as current methods for interlocking chemically incompatible materials cannot be directly scaled down for the miniature flapping wing drive application. Therefore a method to create robust miniature

hinges will have to be developed to allow for full utilization of compliant mechanisms advantages in power transmission efficiency.

Limited payload capabilities of the current flapping wing MAV designs contributes to insufficient functionality and operational range for practical applications. Reduced weight of the MAV drive mechanism can contribute to increased payload carrying capability, which can be used for carrying more auxiliaries or batteries. Reduction of weight however cannot compromise the structural strength of the mechanism under operation loads. Therefore a detailed analysis of various forces acting on the structure has to be performed to optimize the drive mechanism design; namely minimize the weight and retain structural strength.

1.2.3 Modeling

A useful tool in designing an efficient flapping mechanism is a kinematics and dynamics model. This model should use measured forces as inputs, and output useful information such as motor torque, loading on mechanism parts, and time history of forces. In conjunction with physical force measurement, models are used to gain a better understanding of how to move from desired performance metrics to required physical MAV parameters.

Proper design of the MAV flapping mechanism requires a detailed understanding of the forces generated by the wing flapping motion. The forces the wings are producing can be measured using physical measurement techniques, but kinematic and dynamic models are required to understand how the forces propagate through the links and joints in the mechanism. By computing the forces throughout the mechanism as a function of time, many useful performance metrics can be observed and optimized with less reliance on

exhaustive physical testing. In addition, models can be used to optimize the performance of the mechanism in terms of weight and strength, thus maximizing payload capacity and prolonging flight endurance. With modeling tools, the process of design optimization is accelerated significantly, leading to better performance of the flapping mechanism.

Using an iterative cycle of modeling tools and physical test results it is possible to verify that the models are accurately predicting the behavior of the mechanism. The central component of this iterative cycle is the dynamic simulation model, which uses measured lift and thrust forces as inputs, and predicts how all the mechanism components are loaded as outputs. The mechanism components are then examined with a finite element solver to determine the factor of safety. As the analysis is conducted, areas of the mechanism are identified that require changes. After a few iterations, the mechanism is made increasingly efficient and lightweight, while satisfying the various constraints on strength, manufacturability, and kinematics.

1.3 Thesis Goal and Scope

The goals and scope of this thesis can be organized into the topics described in sections 1.2.1-1.2.3. First, the causes for variation in wing performance will be investigated using experimental measurement techniques. By combining physical force measurement techniques with the high speed photography, the properties of stronger and weaker performing wings will be compared to determine how factors like stiffness, mass distribution, and construction techniques contribute to the overall performance capabilities. Based on the results of these findings, a set of rules for good wing design will be described. These rules will allow future designers to build wings that provide the maximum amount of lift and thrust possible, while keeping weight to a minimum, so that

useful flight properties, including payload capacity and endurance, will be improved. Second, a technique for the mechanism design will be presented. This is a multi-faceted problem, and it is decomposed into multiple steps. The first step is the shape synthesis of the mechanism. This includes establishing the geometry of the mechanism rigid links and miniature compliant joints that will provide the desired range of motion for the wings, while accommodating the motor and gears, as well as the manufacturability constraints. Next step in the mechanism design process is to develop a parametric model of the mechanism and perform the design optimization, varying its dimensions to minimize the part volume, while meeting the required factor of safety. Finite element modeling is used to evaluate the designs using boundary conditions resulting from experimentally measured lift and thrust values. The last step is the determination of a suitable method of molding the multi-material compliant mechanism design generated by the optimization.

Once the wings, mechanism, and modeling work are completed, a fully functional flapping wing MAV is developed that meets the following goals:

1. The MAV will be low cost, due to incorporation of manufacturing automation that results in reduction of assembly steps.

2. The payload capacity of the MAV will offer significant improvements over previous versions, allowing for a wider mission scope due to enhanced sensor-carrying abilities. Alternatively, the endurance will be enhanced when a lighter payload is carried, resulting in a more versatile MAV.

3. The MAV will be robust and capable of withstanding multiple crashes without sustaining excessive damage. In the event of damage, the MAV will be easily repaired.

4. The MAV will be capable of a manual hand launch or an automated launch from ground vehicles.

1.4 Organization

Chapter 2 presents a literature survey of the relevant MAV designs and the technologies that are relevant to this thesis. The survey is divided into sections describing control technologies, flapping mechanisms, and wing designs. These three systems are largely responsible for the flight performance of most MAVs, so evaluation of existing technologies in these areas should provide insight into future possibilities for advances. To conclude the literature survey, areas of interest for future research will be identified.

Chapter 3 contains a complete description of the wing design problem. Included in the chapter is a discussion of the measurement techniques for lift and thrust forces generated by the wings flapping, with details about the equipment and settings used. Also included are the results of the force measurement for a variety of different wing styles. Wing compliance testing is performed at the centroid of each wing to provide a measure of the stiffness properties. High speed photography results are presented to provide a basis of understanding for how wing parameters impact the forces produced. A model is presented for predicting the performance of flapping wings as a function of various wing parameters like compliance, size, and flapping rate and angle. Finally, the results of the wing design study are used to select a set of wings for the MAV that maximize performance gains while keeping weight minimized.

Chapter 4 contains a description of the Jumbo Bird flapping wing MAV. The discussion will focus on the mechanical and electronic components selected for the operation of the MAV. A detailed description of each component and its important characteristics will be

presented. The interaction of each part of the MAV will be explained as it pertains to the overall operation of flight and control systems.

Chapter 5 contains a discussion of the distributed compliance flapping mechanism design. This design makes use of a flexible frame that stores and releases energy during the wing flapping motion. A detailed discussion of this mechanism design will be presented. First, the functional requirements and desired mechanical performance metrics will be established. Next, the shape synthesis of the mechanism will be presented, which will elaborate on various geometric and kinematic details of the design. The design of the mechanism shape, incorporation of flexible links, and geometric parameters will all be described in detail. Testing and modeling results will be presented to evaluate its operational performance. Using experimentally measured input forces, a dynamic and kinematic model is used to propagate the forces throughout the various links and joints within the mechanism. The results of this model are used in a finite element analysis study with the goals of weight minimization while maintaining the desired factor of safety. With an iterative cycle of improvement, the lightest acceptable design is reached so that payload of the MAV can be maximized and the functional constraints can be satisfied.

Chapter 6 contains a discussion of a localized compliance flapping mechanism design that makes use of multi-material compliant joints. First, the functional requirements will be established, with a variety of desired mechanical performance metrics. Next, the shape synthesis of the mechanism will be detailed, with consideration to both the functionality and the manufacturability of the mechanism. Since the mechanism is a multi-material injection molded part, the shape synthesis presents a multi-faceted

problem. The design of the mechanism shape, incorporation of flexible links, and geometric parameters will all be described in detail. A variety of testing and modeling results will be presented for this mechanism design, to evaluate its performance during operation. Dynamic and kinematic modeling is used to propagate the measured lift and thrust forces throughout the links and joints the mechanism. The results of this model are used in a finite element solver to minimize weight while maintaining the desired factor of safety. In addition, some discussion is presented regarding the manufacture of this mechanism, as injection molding offers unique challenges and benefits for mass production.

Chapter 2 - Literature Review

2.1 Introduction

To provide some perspective on the current state of the art in flapping wing MAVs, it is useful to examine the existing work that has already been accomplished by a variety of research groups, private builders, and companies. The goal of this review is to develop a general classification of flapping-wing vehicles based on a survey of published designs to aid a designer in determining which aspects of proven designs may be useful in a given application. For each category, advantages and disadvantages will be discussed. The discussion presented will be limited to miniature-sized flapping wing air vehicles, defined as 10-100 grams total weight. The discussion will be focused primarily on MAVs which have performed at least one successful test flight, and only those designs that are published in the literature or are commercially available are discussed. The criteria for selection of the design examples include availability of detailed mechanical design information, knowledge of intended application, and validation of design functionality through a controlled, flying prototype.

This review is intended to provide a representation of the field of current technology, rather than providing a comprehensive listing of all possible designs. This sampling of current technologies will familiarize a newcomer to the field with existing designs and their distinguishing features, as well as providing a basic understanding of the functionality of flapping wing MAVs. A comparison of a variety of MAV technology will help the designer to understand the strengths and weaknesses for various designs. By studying existing vehicles, future designers will be able to create new designs by adopting features from past and current successful solutions. This review also

summarizes the design challenges associated with the further advancement of the field and deploying flapping wing vehicles in practical applications.

Based on the survey conducted, the general categories of comparison for the flapping wing vehicles were determined to be: (1) directional control scheme, (2) wing design, and (3) mechanism design. Generally, these are the three systems that are most important in determination of a given MAV's flight envelope.

2.2 Directional Control Scheme

Successful flight of most MAVs requires the use of a tail for stabilization and/or control purposes. Wing flapping generally produces large oscillatory forces that can disturb the balance of a MAV, so the tail helps to keep the vehicle flying in a relatively straight path. Depending on the sophistication of the tail design, certain improvements to the flight envelope of the MAV are possible. The tail can provide multiple degrees of freedom for control of the vehicle, through the use of a variety of control surface schemes. The control styles that will be discussed include static or non-controlled tail, rudder style, and some other non-traditional layouts. Most examples draw inspiration from typical aircraft configurations, with the use of various styles of rudders and elevators. One example discussed accomplishes its control with independent wing control, something that insects typically exhibit in flight.

2.2.1 Static Tail

Static tail MAVs are generally the simplest yet least controllable, and are exhibited in a variety of research examples, as well as in the toy market. Researchers at the University of Delaware have created a static-tailed MAV, Figure 5, with the purpose of improving

the energy efficiency of the flapping mechanism [7]. The MAV was able to successfully complete a flight under its own power.

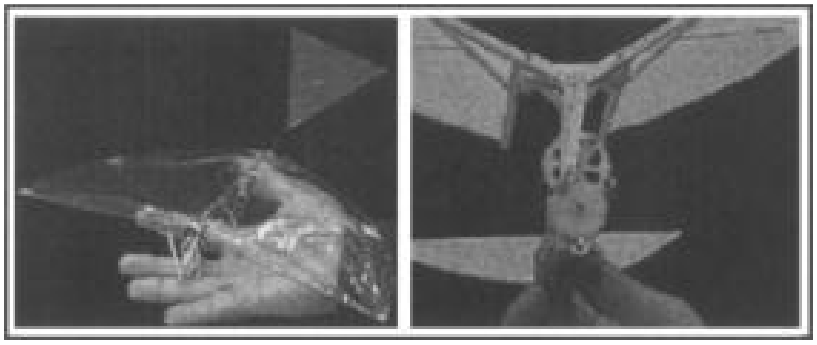

Figure 5: University of Delaware ornithopter [7]

Another example is the Microbat, Figure 6, developed as a joint venture by California Institute of Technology, University of California, Los Angeles, and AeroVironment, Inc. Microbat was meant to be a study on producing wings using MEMS technology that would be very repeatable and sturdy while leveraging unsteady aerodynamics for better flight properties. The Microbat was the world's first electrically powered flying ornithopter (bird-like air vehicle), with the first prototype flying in October 1998 [8]. The earliest version (Figure 6 left) of this ornithopter used a V-shaped tail for stabilization, but had no control actuators. In early testing, the Microbat only had enough power to complete flights of nine seconds, so control actuators were too heavy to include. Later models eventually had larger power capacity due to a change from capacitors to batteries (Figure 6 center) and included control systems mounted in the tail (Figure 6 right), this version will be discussed in section 2.2.2 in more detail.

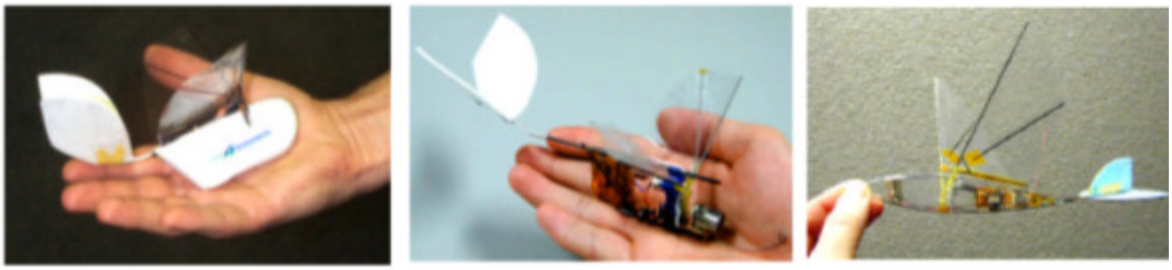

a) super capacitor-powered prototype b) battery-powered prototype c) battery-powered prototype with a radio control system

Figure 6: Microbat prototypes [8]

In addition to the research models discussed, the toy market has created a MAV that falls into the static tail category. The I-fly Vamp and Wasp are cosmetically different but function in the same manner. These MAVs are advertised as the world's smallest flying bats, with weights of 13 grams each [9]. The Vamp and Wasp operate using two flapping wings as the source of lift, thrust, and control. By varying the angle of the entire flapping mechanism relative to the body of the MAV, the wing geometry is altered during the flap cycle. The angle of the net lift and thrust vector is skewed, resulting in turning with minor loss of altitude. This is a departure from the typical control scheme at this size scale, where the tail is angled to induce yaw, while maintaining constant wing geometry. The flapping rate is proportionally controlled by radio, as well as the angle of the flapping wings, thus providing two degrees of freedom from the wings and none from the tail. The tail is not involved in the control of the MAV, but provides stability in flight. These toys are not very complex, however they provide a good example of an alternative form of steering.

2.2.2 Rudder Tail

Rudder tails can be thought of as the traditional form of steering control for a flying vehicle, since they use the same principle of operation as most airplanes. A single fin

rotates to the left or right, creating a yaw force on the MAV and causing a turn. In all the cases discussed, the tail also provides the stabilizing force of a static tail, with the added element of control surface actuation. The first example to be discussed is the Microbat, in its later versions. As development continued, the power source changed from supercapacitors to a three gram nickel cadmium rechargeable battery. Currently the best flight endurance recorded for the Microbat is forty-two seconds. With the extra power capacity came reductions in mechanism weight, thus allowing for some weight to be devoted to a radio control and actuation system. The newest version of the Microbat is equipped with 0.1 gram shape memory alloy wires embedded inside the tail to provide separate elevator and rudder control, in a layout similar to most aircraft.

The University of Maryland Small Bird, **Error! Reference source not found.**, was designed and constructed in the Advanced Manufacturing Laboratory at University of Maryland [10]. This MAV sought to achieve similar performance gains as the University of Delaware model by incorporating compliance as a characteristic of the flapping mechanism. Altitude control is provided with variation in wing flapping rate, but steering is done with the tail surface, mounted at the rear of the MAV.

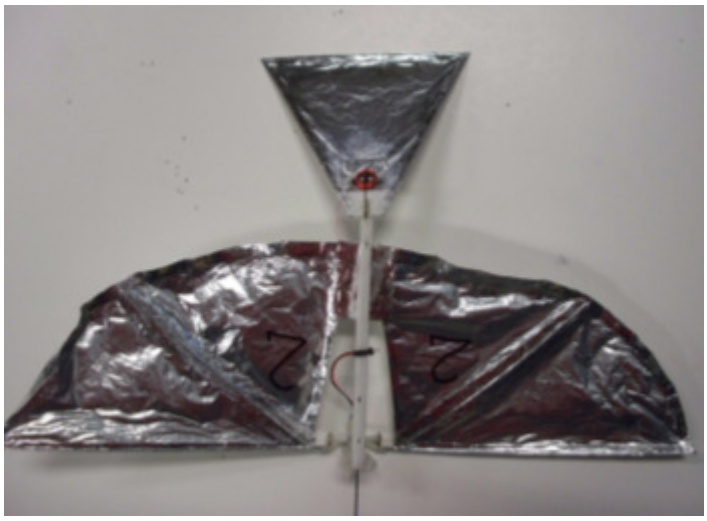

Figure 7: University of Maryland Small Bird [10]

The tail is actuated in a rudder-style motion using a lightweight magnetic actuator. A pair of magnets is mounted inside a wire coil, and by sticking the magnets to the tail surface and applying a voltage to the wire coil, electromagnetic force is used to rotate the tail left and right. In continuation of this project, the same group also created a Big Bird, Figure 8, a larger and improved version of the Small Bird.

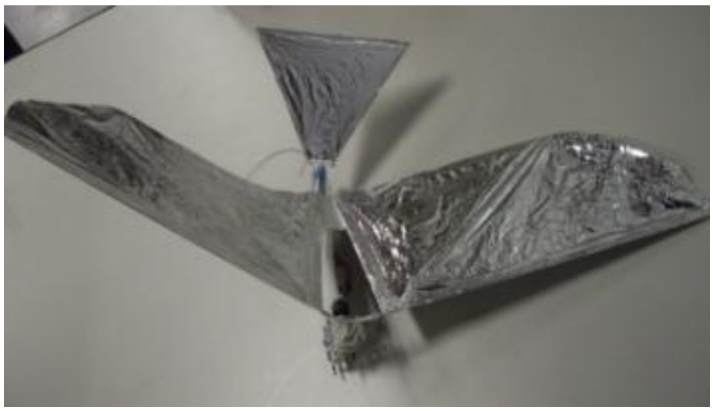

Figure 8: University of Maryland Big Bird [11]

Due to increased size and weight, this version uses a servo for tail actuation. By mounting the tail assembly at a large angle of attack and using the servo to create

rotation, a yaw force turns the MAV. In both the Small Bird and Big Bird, the tail creates a torque that keeps the nose of the bird up and allows for more stable flight.

The toy and hobby market has produced some very successful MAVs that fall into this category of tail style. I-fly sells a line of MAVs called the Wingsmaster Ornithopters that use 2 sets of clapping wings like a dragonfly for flight with a tail rudder actuated with a servo for steering control. Another entry from the toy market is Wowwee's Flytech Dragonfly MAV. This model also makes use of a pair of wings that clap together, however it uses a non-traditional tail setup. Instead of the usual method of using an actuated control surface to provide yaw, the Flytech Dragonfly draws its inspiration from a helicopter tail rotor. A small motor is mounted in the tail that is capable of variable speed rotation in both directions. This provides a thrust force that yaws the MAV left and right to provide steering. The hobbyist market has spawned some extremely lightweight MAVs, with one of the lightest in the world coming from the Osaka Slow Fliers Club in Japan. The MAV shown in Figure 9 weighs a total of just 1.54 grams and has a rudder capable of steering left and right. Such a diminutive MAV presents major design challenges due to the reduced effectiveness of traditional aerodynamics with very small wings. Therefore, the MAV flies very rapidly to maintain sufficient airflow for flight. The rudder is based on the coil and magnet actuator technology also used in the University of Maryland Small Bird, due to its ability to be constructed at a very light weight.

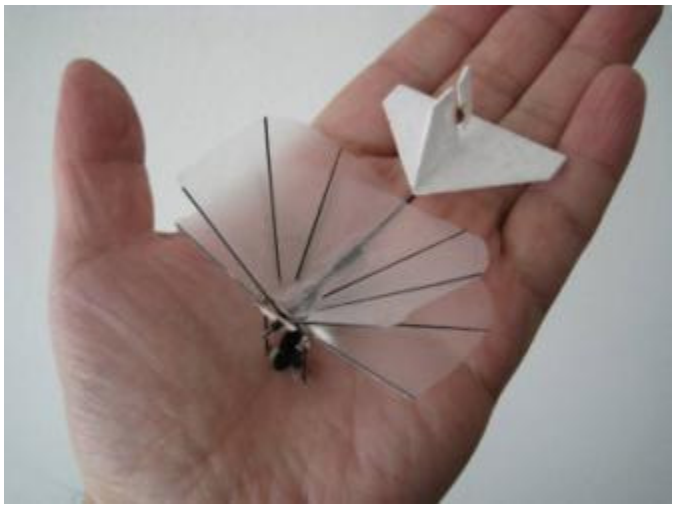

Figure 9: Osaka Slow Fliers Club MAV [12]

The Technical University of Delft in the Netherlands has created a miniaturized version of its Delfly MAV, called the Delfly Micro, Figure 10. The tail design for the Delfly Micro also uses a magnetic coil rudder actuator, for reduced weight. This MAV has the very noteworthy feature of vision-based stabilization. By mounting a camera onboard, the optical flow is used to determine the attitude of the MAV, and apply corrective control inputs to the tail and wings to improve stability during flight. This allows the Delfly Micro to be more controllable than most fliers at this size, where steering becomes difficult for a human operator due to rapid changes in flight characteristics.

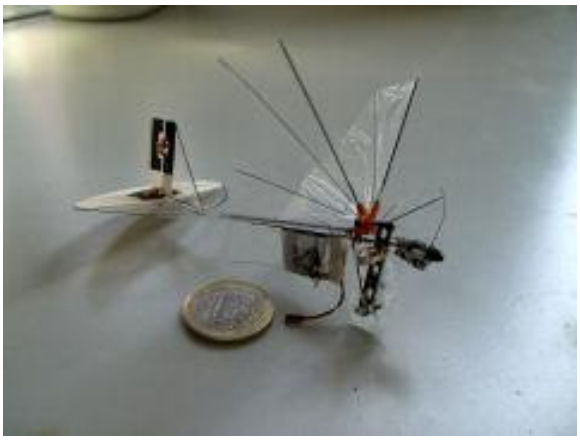

Figure 10: Delfly Micro [13]

It is worth noting the reason for this choice of actuation being so popular at small size scales. Since the control surface is very small and lightweight, the load is generally not so large that a servomotor is required for steering, which would be a much heavier option.

The Naval Postgraduate School has created a non-traditional MAV shown in Figure 11 that also uses the magnetic coil actuator to steer a tail rudder [14] The NPS MAV uses a flying wing body with the rudder mounted towards the rear in the center of the MAV. Steering control is separate from altitude control, which is accomplished with variation in flapping speed. This flier has the unique benefit of being practically impervious to stall, since its flapping wings draw air in with a suction effect. Control is improved through this phenomenon and this makes the NPS flier one of the most maneuverable MAVs in this category.

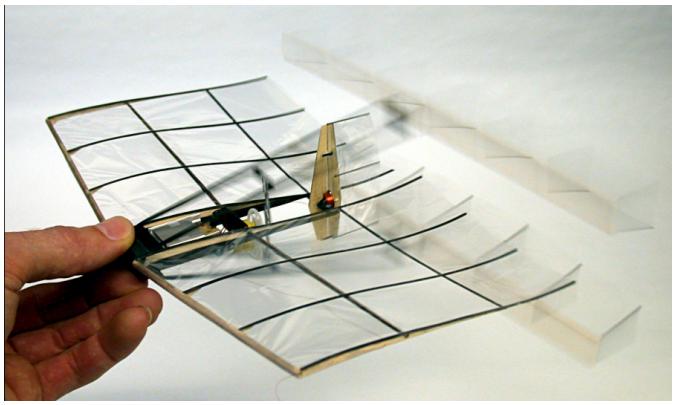

Figure 11: NPS Flier [9]

2.2.3 Ruddervator Tails

The ruddervator tails category refers to a control layout that is not readily classified with the more traditional schemes. This configuration uses surfaces called ruddervators, more commonly known as a v-tail. The general idea is that instead of using a vertical rudder arranged perpendicular to a left and right elevator fin, as with most aircraft, two fins are arranged at an intermediary angle between vertical and horizontal. By mixing the two control surfaces, it is possible to achieve both the rudder and elevator degrees of freedom. There are two MAVs discussed here that make use of this configuration.

The original Delfly, shown in Figure 12, uses ruddervators angled downward so that the mechanism will be protected during landing. The original Delfly is similar to the Micro version in that it uses camera vision-based stabilization to maintain stability in flight. This is similar to fly-by-wire technology that many modern aircraft use, which allows for stable flight in aircraft that are inherently unstable. With small magnetic actuators, the ruddervators can be coordinated to both move in the same direction for elevator commands, or they can move in opposite directions for steering commands. Any combination of the two commands allows for a full flight envelope, just as a MAV with a separate elevator and rudder could achieve.

Figure 12: Delfly [15]

2.2.4 Independent Wing Control

An alternative to using the tail for control is to alter the phase of the wings to achieve force imbalance. The result is turning is achieved, without the aid of a separate devoted control surface for that degree of freedom. Such examples are very rare in the field of miniature air vehicles, due to the typically rapid flapping rates required to sustain flight. This creates a complicated control problem that requires a non-traditional flapping mechanism. One example that achieves the force balance needed for steering but not successful MAV flight is shown in Figure 13 [16].

The four bar linkage mechanism is flapped with two unimorph actuators, Figure 14. Such a configuration avoids the weight penalty associated with an electric motor.

Figure 13: Unimorph actuated independently controlled wings [16]

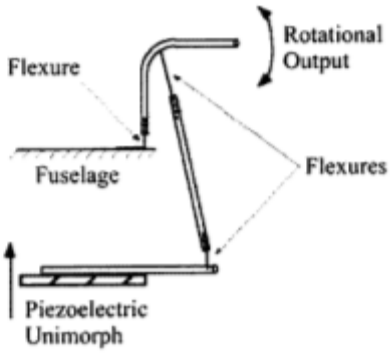

Figure 14: Functional schematic for four-bar unimorph actuation [16]

By using actuators with slightly different resonant frequencies, it is possible to create asymmetry in the flapping for steering purposes. While this MAV has not successfully completed a flight, the technology employed shows great promise for future designs. Independent wing control coupled with fast flapping rates is a key step towards realizing the same level of maneuverability that is present in flying animals, and if successfully implemented in a flying prototype this would be a noteworthy advancement of the MAV field.

2.3 Wing Designs

2.3.1 Flapping Wings

The category of flapping wing locomotion is the most well known, and is often seen as the traditional method of flapping flight. Flapping wings are used by a wide variety of animals including birds, bats, and a variety of insects. The general principle of operation is that two wings are flapped to produce both lift and thrust, thus overcoming gravity and drag to provide sustained flight. Generally, flapping fliers can most easily be distinguished based on their respective size scale and flight speed or the Reynolds number experienced in flight, and therefore flight style. By observing nature, one can see the difference in flight style between a large soaring bird such as an albatross, and a hummingbird, which must flap its wings very rapidly to stay aloft. A similar relationship holds for man-made flapping wing fliers. At larger size scales, higher Reynolds numbers are encountered and therefore slower flapping and soaring are the most effective modes of flight. Fliers in the centimeter scale however, experience very different aerodynamic effects, with less favorable lift to drag ratios. The general trend is that as the flier decreases in size, the wings must flap faster to produce the necessary lift and thrust to support flight. This creates a unique challenge for miniature MAV designers, because traditional aerodynamics break down with such small wings. However an interesting trade-off is that with higher rates of flapping comes the opportunity to realize greater control resolution, and some impressive acrobatic maneuvers become possible. In this section, we will discuss a number of successful flapping wing miniature fliers, both commercially available, as well as research platforms.

One of the design goals of the Microbat was to create wings using MEMS technology. Several MEMS wings were constructed, with variation in parameters such as chord and spar width, membrane thickness, number of spars, and sweep angles. Wing materials chosen were titanium-alloy metal (Ti-6Al-4V) as the structure, and poly-monochloro-para-xylelene (parylene-C) as the membrane. The wings were designed to make use of unsteady-aerodynamics to achieve a high lift coefficient, relative to a fixed wing of similar size. One of the key benefits of MEMS-based wings is that the wings can be created exactly the same every time, using a template style of construction. With such lightweight MAVs, the small variations present in hand-made parts translate to large differences in performance from one version to another. The Microbat has a very short wingspan, with the current version measuring 9 inches from wingtip to wingtip.

Another MAV using MEMS technology to produce wings is shown in Figure 15. By creating one wing with a PVDF skin as a smart wing, it acts as a real time lift sensor. Comparison of its results to a load cell mounted to the MAV shows that it is a viable means of determining performance in flight [17]. Such a feedback system is a key difference separating man-made MAVs from flying animals, and incorporation of this style of distributed sensing technology gives great promise for the future of MAVs.

Wings do not necessarily have to be constructed with MEMS technology at this size scale. They can be constructed by hand using traditional materials as well. The University of Maryland Small Bird and Big Bird and the University of Delaware ornithopter all use flapping wings constructed in a similar manner. The wings use lightweight and stiff rods to provide structure, much like a bird's skeleton. The rods serve to strengthen the wings and help them to achieve an airfoil shape during flapping.

The wing surface is made of a thin mylar film, stretched over the stiffeners. As the wings flap, the configuration of the stiffeners combined with aerodynamic loading causes the wings to create a rounded airfoil shape, providing lift. Since these wings are handmade, construction repeatability becomes an issue due to the small difference between sets of wings created.

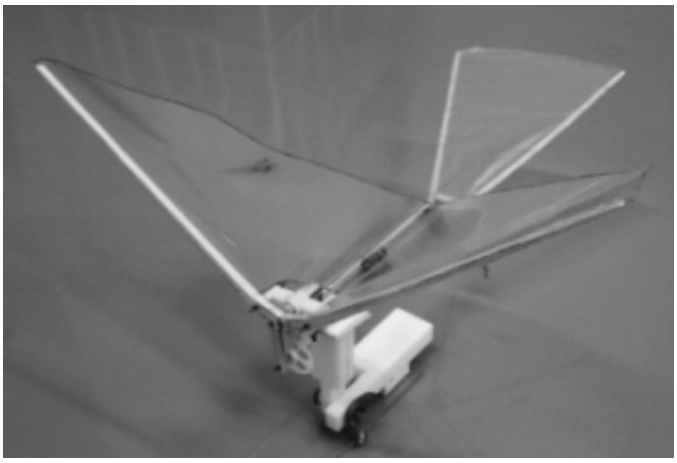

Figure 15: MEMS wings with PVDF sensing capability [18]

The I-fly Vamp and Wasp also use a thin foil skin stretched over front and rear wing spars to provide stiffness. The front spars of the wings are mounted into the flapping mechanism, providing the power for flight. The rear section of the wings is mounted into a surface that can be tilted left and right along the body of the MAV. By shifting the angle of the entire flapping plane of the wings, steering is achieved. Due to the economical nature of the flier, the MAV is somewhat underpowered, so steering results in altitude losses. However, if a more advanced MAV were to incorporate skewing wings into a system that also has a rudder, redundant control would be possible, thus safeguarding against system failures. For this reason the research community could draw inspiration from the toy market for a technology that can improve the robustness of their MAVs.

2.3.2 Four Clapping Wings

This category includes any MAV that uses one or two pairs of wings flapping opposite each other, such that the vertical inertial oscillations present in a two-winged flier are cancelled out. This style of flight offers the key benefit of greater stability, which could allow for more delicate sensors and payloads to be carried successfully.

In this category, there are a variety of examples that use generally the same principle of operation. The Osaka Slow Fliers Club 1.5g ornithopter is one of the lightest that has completed a successful flight. The toy market has contributed models such as the Wowwee Flytech Dragonfly, and Wingsmaster Ornithopters all use a pair of wings constructed of thin film with stiffener ribs, flapping in opposing phase. The Delfly, Delfly II, and Delfly Micro all use a similar style of wings, with the added benefit of their vision-stabilization system. This makes these MAVs more suited to outdoor flights, and capable of more advanced maneuvers. The Delfly II is the most capable of the three, with the ability to fly forward, hover, and even fly backward at low speed.

The Naval Postgraduate School MAV is an unusual entry into this class, however due to the manner of its wing flapping, it has been classified as a clapping wing MAV. The NPS MAV uses a flying wing fuselage shape with a pair of wings that flap in a vertical plane mounted to the rear. These wings flap in counterphase, thus thrusting the wing through the air and providing lift. The design and operation of this MAV is unlike any of the others discussed, however the performance of this MAV offers some interesting performance tradeoffs. The speed is controlled by trimming the pitch of the flapping wings, pre-flight, and the altitude is controlled by varying the flapping rate. This is an unusual configuration for an MAV, however the maneuverability is very good. The key

benefit of this style of flight is related to the energy expenditure during flight. In many two-winged MAVs, the wings flap and the body will oscillate opposite the wings' motion. This means that valuable battery power is being wasted performing the work of accelerating a massive body up and down. Or in four-winged MAVs, the wings are mounted to a body that functionally does not contribute to the flight capability, it just provides a structural support for flight systems. In the NPS flier, all energy expended by the motor is directed into the flapping wings that drive a wing into the air. Therefore, the entirety of the MAV is being used for the beneficial purposes of thrust and lift generation. A new concept for clapping wings is the use of 3-way clap and fling, to augment lift. Clap and fling has been shown to produce extra lift in the literature [19-24] [25], however, the idea of 3-way clap and fling is relatively new. The WSU MAV exploits the effect at the left and right sides where the wing pairs meet, as well at the top of the MAV where the opposing wing pairs meet, Figure 16, thus improving lift.

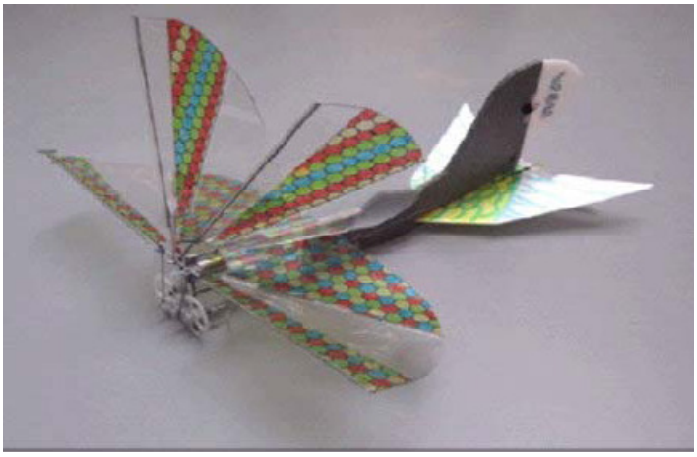

Figure 16: WSU MAV [26]

In a similar manner as the Delfly II, the MAV shown in Figure 17 uses passive stability to achieve hovering flight.

This MAV is designed to mimic insect-style flight, with a Reynolds number of about 8000. It maintains its stability in much the same manner as a damped pendulum that returns to rest when disturbed, by creating a balance of forces that tends to keep the MAV upright and centered. The sails act as dampers to prevent unstable or oscillatory motions from taking over during flight.

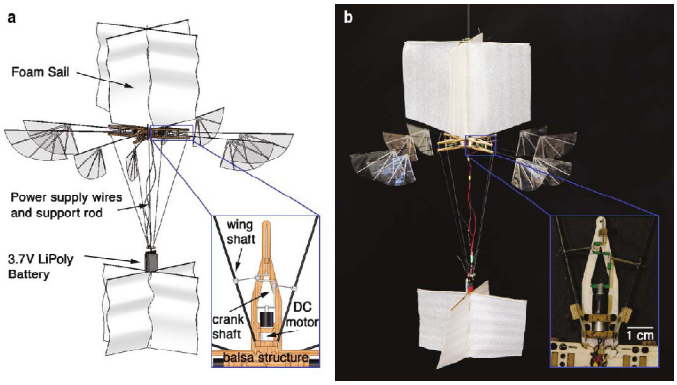

Figure 17: Passively stable hovering MAV [27]

2.3.3 Folding Wings

Observation of larger birds in nature reveals that wing flapping is tailored to the requirements and conditions faced at the time. When a bird is taking off, the wings are flapped differently than during cruising flight. Since the bird does not have the airstream flowing over their wings from the static position, lift must be somehow augmented, since aerodynamic lift is lacking in this condition. Therefore, birds will flap their wings downward, fold them in towards their body, during the upward flap, then re-extend their wings during the downward flap. This results in maximum wing area during the down flap, which is producing helpful upward lift. During the upflap, the area is minimized, thus reducing the magnitude of harmful negative lift. By using this style of flapping, the bird is able to get airborne, then transition to standard flight. For a MAV to recreate this style of flapping, passive wing folding is an attractive option due to the excessive weight

of actuators that would be needed. In [28] the authors describe a successfully flying MAV that uses wings with one-way compliance to accomplish the desired folding effect, Figure 18.

Figure 18: Wings with one-way compliance

The result is that the wings can lift the same amount of weight, but with slower forward velocity. Thus, a behavior much like the bird during takeoff is accomplished with folding wings. In [29, 30], the authors attempt a similar style of wings, resulting in augmented lift production in non-moving air. However, flight was not achieved probably due to the extreme amount of folding used by the wings, thus disturbing the balance of forces in flight. The MAV used in this particular experiment is too large to be considered a miniature air vehicle, however the results are similar.

2.4 Mechanism designs

There are four primary classifications of mechanisms used by the MAVs discussed: (1) double pushrod, (2) double crank, (3) single pushrod, and (3) side-mounted crank. Each of these four mechanisms presents a tradeoff of multiple important performance attributes. Some of the considerations for selecting a mechanism layout include the particular geometry and weight constraints for the MAV, as well as the required forces to

be transmitted and the rate of flapping. Other concerns include the manufacturability of the selected design, especially with very small and light MAVs. As the size of mechanisms grows ever-smaller, the human limitation becomes a factor in the construction of more complex mechanism layouts. Due to the reduced stability of MAV platforms, a durable mechanism is desired, due to a variety of damaging factors including dirt contamination, crashes, assembly stresses, and the fatigue effects of high flapping rates.

2.4.1 Front Mounted Double Pushrod

The first style of mechanism discussed is a front-mounted double pushrod mechanism, shown in Figure 19 [8].

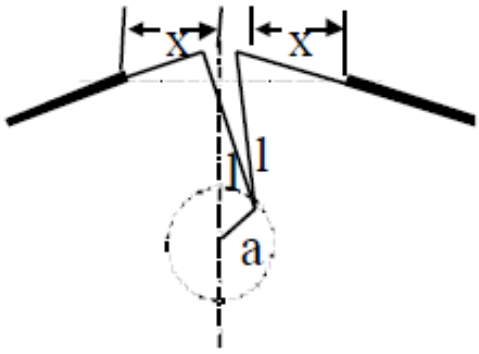

Figure 19: Double pushrod flapping mechanism [8]

This mechanism uses a motor connected to a system of gears that increase flapping force while reducing flapping rate. Attached to the slowest moving and therefore highest torque gear are a pair of pushrods of length l. These pushrods connect to each flapping spar, thus driving the wing motion up and down through pinned connections. Due to the pinned connections, the vertical translation is the only component of motion that is transferred from the drive gear. Since each wing spar has its fulcrum located at a fixed distance x from the central axis of the mechanism, and the pushrods are of fixed length l,

a problem arises. The two pushrods are never exactly in the same vertical location, except for the apex and the nadir of the flapping motion. This creates a phase lag between the two wings, resulting in slightly asymmetric flapping of the wings. At the miniature size scale, this is an undesirable situation, where control is already difficult due to the low inertia of the fliers relative to their large wing and fin surface area. This style of mechanism is used in the Microbat, Figure 20, the Chung Hua University MAV, Figure 21, and the University of Delaware ornithopter, Figure 5 on the right.

Despite its inherent limitations, this configuration is popular due to its simple construction, light weight, and ease of part replacement. If the MAV is very small and has a sufficiently high flapping rate, it is possible that the asymmetry of the wings can be masked during the overall flap motion. If the throttle is reduced however, the MAV will begin to exhibit noticeable oscillations and be more difficult to control.

Figure 20: Double pushrod from microbat [8]

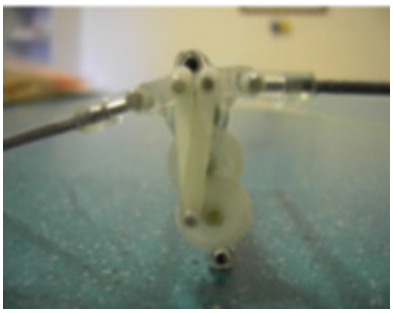

Figure 21: Chung Hua University MAV double pushrod mechanism [31]

2.4.2 Front Mounted Double Crank

A variation of the double pushrod design is the double crank. This design is similar in functionality, except that the two pushrods no longer share a common mounting point on the crank. The Delfly uses this style mechanism, shown in Figure 22.

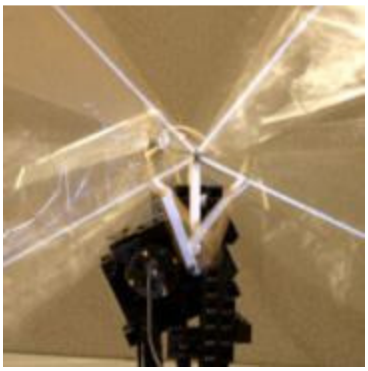

Figure 22: Delfly I front mounted double crank

The benefit of this change is that the asymmetry in wing flapping can be reduced, thus improving the stability of the MAV. Unfortunately, the wing flapping cannot be made perfectly symmetric with this configuration.

2.4.3 Front Mounted Single Pushrod

The single pushrod mechanism drives the two wings' motion together with a common pushrod, mounted to the crank in a central pinned connection, shown in Figure 23.

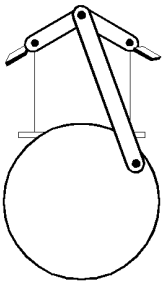

Figure 23: Single crank functional schematic [32]

The key difference between the single crank as compared to the double crank is the wing flapping can be made always symmetric, thus improving the low-speed stability of the MAV. A performance tradeoff with this mechanism is that the stresses will be much higher in the single pushrod, since it must drive both wings at the same time, in phase. In addition, the stress on the electronics components including the motor and electronic speed controller will be greater, since the wing flapping is exactly in phase. With the double crank, the wing flapping was slightly out of phase, thus distributing the load of a single flap cycle over a larger time period. While the overall work required is equivalent, the spike in loading is more focused in the single crank mechanism. It is possible to adapt the single crank mechanism to have a phase lag as with the double crank mechanism, by incorporating sliding hinges to support each wing spar [32]. As the wings flap, the hinges that provide a fulcrum for the wings are free to move so that the motion is not jammed up at any point during the flapping motion.

As a method of reducing the loading spike, a compliant frame can be used. The general principle of operation is that by incorporating elastic links into the mechanism, energy spring energy can be stored and released during the flap cycle. By designing the geometry and stiffness of the system to optimize the energy storage and release, the loading range, i.e. the difference between the largest and smallest load can be reduced. Reduction in the loading range has been shown to improve the efficiency of the mechanism, thus prolonging battery life and improving the reliability of the electronics components [7] [10]. This style of mechanism is used in newer versions of the University of Maryland Small Bird and Big Bird, Figure 24.

Figure 24: UMD single crank mechanism

Due to the layout of the mechanism, it is possible for both of the compliant links in the mechanism to deflect simultaneously in the same direction, a degree of freedom that can be thought of as 'sway'. Causes for the sway effect include driving wings that are too large for the mechanism, driving wings too rapidly, or large wind gusting or other external loads of the mechanism that remove it from its design range. This effect serves to reduce the distance from the pushrod to the pinned connection that drives the wings up and down, thus altering the designed-in flapping range and causing undesired dynamic effects. For these reasons, it is important to ensure the single pushrod is staying within its designed limits. This behavior can be alleviated with the addition of a pin and slider joint in the center of the mechanism, resulting in always symmetric deflections by the compliant links

Figure 25: Parallel single cranks [26]

One variation on the single crank mechanism concept is shown in Figure 25. With a pair of front-mounted single cranks, some of the problems of this mechanism style are solved. The mechanism is set up to flap the wings in phase, with a pair of equally sized cranking gears attached to the drive motor. Assembly is made easier with the use of multi jet modeling rapid prototyping machines. The gears are deposited with a removable wax that is dissolved during post processing, so that the mechanism is assembled automatically.

2.4.4 Side Mounted Crank

Some of the MAVs discussed use another style of single crank mechanism, the sideways pushrod layout. In this configuration, the axis of gear rotation is shifted 90 degrees to be perpendicular to the direction of flight and coincident with the MAV elevation axis. There is one pushrod used to drive each wing in this mechanism layout. Each pushrod is attached to the slowest-moving gear, with one on both the left and right side of the MAV that moves vertically with the gear using a pinned connection. The vertical movement of the pushrods is transmitted to the wing spars at a mounting point, thus driving the wings

up and down. In the Delfly II, Figure 26, Delfly Micro, Figure 27, and Osaka Slow Flier's Club MAV, Figure 28, a sideways pushrod mechanism is used.

Figure 26: Delfly II side mounted pushrod mechanism

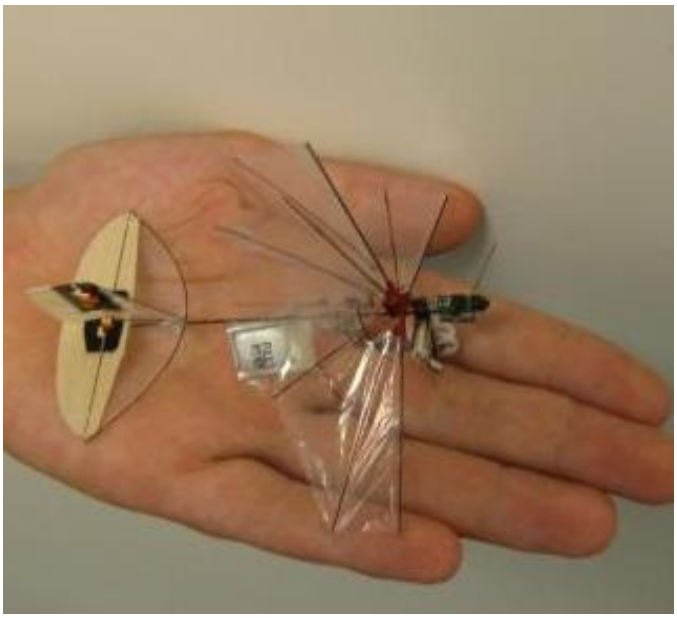

Figure 27: Delfly Micro side mounted pushrod mechanism

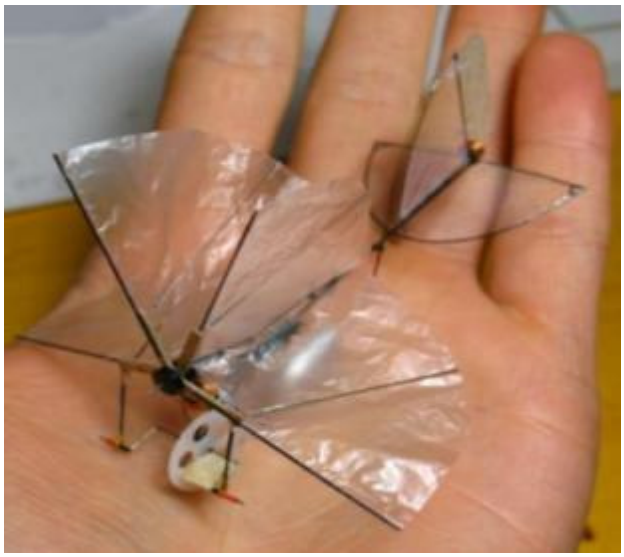

Figure 28: OSFC side mounted pushrod mechanism

The benefit of this type of layout is a reduction in rolling vibrations transmitted to the airframe. The tradeoff is that vibrations are transmitted into the elevation axis of the MAV instead. However, this is a more manageable behavior for maintaining directional control, since the MAV tends to move the same direction it has been pointed. With throttle modulation, it is possible to correct for the elevation vibrations. For lighter MAVs or MAVs with a large surface area to weight ratio, this benefit is helpful in maintaining stability and controllability during flights. A difficulty with the sideways layout is that the construction is more complex than the other two layouts. The pushrods must be able to access the wing and the crank mounting locations without interference from any other structural components on the MAV. It is also important to consider the level of exposure to crash damage when using this style. Since the pushrods are exposed on both sides of the MAV, it must be shielded from crash damage in a variety of different directions. If a pushrod were bent in a crash, it would probably need replacement since small difference between the two sides of the mechanism could cause large stresses to

result at rapid flapping rates. If the manufacturing and durability limitations can be overcome, the symmetric flapping, light weight, and compact size make this mechanism a good layout for very small MAVs.

2.5 Summary

This review has presented a sampling of miniature air vehicles. These MAVs have been classified by the tail, wing, and mechanism functionality. Each MAV has been discussed in detail, and the advantages and disadvantages of each example have been explored. Furthermore, the overall advantages and disadvantages of each general classification have been explored, to determine any general trends that arise. In table 1, values are presented for some of the MAVs discussed to provide a comparison.

The primary conclusions of this review are to identify the progress made so far, and to determine the areas in which further research are needed to advance the state of the art. Flapping wing flight can be used by unmanned aerial vehicles to complete a variety of mission objectives that fixed or rotor wing fliers are unsuited for, but there are a number of practical drawbacks to using ornithopter style flight at such a small size scale which must be overcome to continue the advancement of the field.

Some areas where future research could help advance the state of the art in MAVs include autonomous flight, including take-off, landing, and perching. In addition, greater sensor carrying abilities would contribute to the goal of autonomous missions. Another area requiring advances is sophisticated wing control. Animals posess many more degrees of freedom than MAVs, a major reason for their advantage in maneuverability, endurance, and effectiveness in adverse weather conditions.

The current field of miniature ornithopters displays impressive depth as well as breadth, and has definitely made significant progress since the Microbat first flew in 1998. With the current rate of progress by research groups as well as the ever-increasing level of accessibility to a variety of private groups and consumers, the future of small ornithopters should continue to be an exciting field. As research continues in the key areas of research that are lacking, small ornithopters will be adopted by many more consumers as a viable flight platform for carrying out missions, as well as by private consumers for entertainment.

Table 1: PHYSICAL DATA [33-40]

Category	Name	DOF	Weight (g)	Span (in)	Length (in)
Clapping Wing MAVs	**Wright State University**	2	12.56	7.9	9
	I-Fly I-bird/fairy/wings (wingsmaster ornithopters)	2	12	10.5	8.25
	Delfly I	3	30	19.69	20
	Delfly II (hover)	3	16.07	11.02	11
	Delfly II (forward)				
	Delfly Micro	3	3.07	3.94	4
	NPS Flier Dr. Jones	2	12.4	10.6	7.09
	OSFC Flier	2	1.47	2.36	2.76
	Flytech Dragonfly	2	28.35	12.3	16.5
Flapping Wing MAVs	**I-Fly Vamp/Wasp**	2	13	10.5	8.5
	Microbat (UF/DARPA)	2	12.5	9.06	6
	UMD small bird	2	16.3	13.5	8
	UMD big bird	2	47	22.5	10.5
Animals	**Northern Oriole**	many	35	10.5	7
	Ruby-Throated Hummingbird	many	3	4	3.5
	Northern Cardinal	many	45	11	8.5
	Canary	many	23	6.5	5

2.6 Future Flapping Wing Research Directions

At present, flapping wing MAVs have achieved an impressive level of sophistication, and through the persistent efforts of various researchers and private builders during the last decade, marked progress has been made in several important areas. While flapping wing MAVs offer great promise for future missions, at present certain areas in the field require advancement. With improvements in these key areas, flapping wing MAVs will become as widespread as larger-sized UAVs, which are used in a variety of applications. Most importantly, MAVs will offer a new level of availability to consumers that cannot access conventional UAVs due to cost or size constraints.

An important limitation of small sized flapping MAVs is the lack of sophisticated control over multiple wing degrees of freedom. Flapping-wing fliers generally strive to achieve a biologically-inspired subset of degrees of freedom and wing dynamics, but they tend to only partially reproduce the aerodynamic performance of their organic counterparts. With increased control over the entire wing surface, much more acrobatic and efficient flight will be enabled, instantly improving the scope of objectives available to a mission planner. Some of the key underdeveloped areas in wing control include lightweight active and passive wing morphing capability, active wingtip dynamic control, control over many degrees of freedom in the wing, and ability to independently control each wing throughout the flap cycle. All these factors require improvement in the miniature size regime, where there is precious little payload available for complex or bulky active control systems. New technologies under development that show promise include distributed sensing and actuation, which would approximate the functions of a nervous

system and muscles. Such departures from more traditional technology may hold the key to improving this area of small ornithopter technology.

An area that presents a unique challenge is the creation of miniature ornithopter systems equipped with autopilots. Achieving autonomous flight becomes increasingly difficult as size is reduced, for a variety of reasons. The light weight and small size of miniature ornithopters means they are vulnerable to any sudden change in surroundings, such as wind gusting, and will be highly disturbed relative to a larger and more stable flight system, which has the benefit of added mass, and therefore resistance to wind gusting. Furthermore, the small size of miniature ornithopters means that any control input will translate into very large directional changes that take place rapidly, just as a hummingbird or a bumble bee is able to dart quickly from place to place. Therefore, any effective autopilot would have to be very fast in terms of processing speed, and also have high resolution sensor inputs and control outputs to provide a sufficient degree of control. This is a much more difficult task in urban or indoor environments, when the margin for error is extremely small and the difference between a successful flight path and a crash is measured in inches. The high flapping rate and corresponding inertial loading of the wings will transmit a fairly violent pitching force to the internal gyroscopic sensors of a typical autopilot, greatly complicating the process of developing a suitable controller. In order to control the elevator for example, the autopilot will need to be able to cope with the large vertical excursions that the body will experience, and still be able to determine the altitude of the flier successfully and apply control inputs. Birds, insects, and other small fliers employ independent wing control as a method of dealing with such large disturbances, so a similar approach in ornithopters may be an effective means of rejecting

large disturbances. However, such a system has very strict weight constraints, and must achieve the proper balance between weight and control sophistication. The small size of the miniature ornithopter platform necessitates that the autopilot used is extremely lightweight, and does not cause undue interference with the flight dynamics or weight distribution. At present, the lightest commercially available autopilot weighs roughly 17 grams, which is a fairly heavy payload for miniature MAVs. Further miniaturization and refinement of autopilot technology should allow even lighter versions, while maintaining full functionality.

In order to maximize the versatility of miniature ornithopters, a multi-mode locomotion system should be developed. With the ability to land, perch, walk, and even take off and land under its own power, the ornithopter can become an even more versatile platform. For example if power was running low, an ornithopter could perch on the top of a tree and recharge its battery using an onboard solar cell. Alternatively, if an ornithopter were tracking a target that became stationary, it could land and await further movement, thus conserving precious battery life. Most importantly, if an ornithopter could take off and land on its own, it would be separated from the necessity of a human operator nearby to launch and recover the system manually. This has tremendous implications for a large portion of potential consumers who would value such autonomous capability. Especially in the military, any system that is self-operating is a great addition because it allows the human operator to simply monitor progress instead of actively controlling the ornithopter at all times.

More research needs to be performed to better understand the properties of flight at the miniature size scale, where unsteady aerodynamics becomes increasingly important.

Small fliers tend to flap their wings very rapidly, which creates difficulty in measurement of forces. Therefore, a number of researchers have created tests where wings are aerodynamically scaled, such that the wings are larger or flap in a more viscous fluid [19, 22, 41]. Such devices have given researchers great insight, experimental data, and analytical and computational models about small wing aerodynamics [20, 21] [42]. Researchers have also created tests where a wing is un-scaled that have shown promise, however creating a prototype that can fly using such a wingbeat has proven very difficult, due to the prohibitive weight of the mechanisms used [16, 43-45]. This style of flight, typically exhibited by insects and small birds such as the hummingbird, involves a very complex wing beat. The wing flaps in more of a horizontal plane, as opposed to the more traditional vertical stroke plane seen by larger fliers. At the end of the downbeat, the wing pronates, meaning the trailing edge flips forward. At the end of the upbeat, the wing supinates, or flips back to its original orientation. The wing is rotated in this manner because there is an unsteady wake structure that is formed, and the rotation of the wing serves to capture this vortex and has been shown to greatly augment lift [22]. By altering the timing of the pronation and supination of the wings independently or in unison, natural fliers achieve directional control and improved lift and thrust, respectively. Due to the difficulty of faithfully recreating this style of flight, man-made fliers tend to lag behind their natural sources of inspiration in terms of payload capacity, maneuverability, and most importantly, flight endurance. This is because man-made fliers at best use a crude approximation of such complex flap patterns, which is less effective at generating lift and thrust, per unit energy used in the system.

The dynamics of the wing flapping require improvements, but hardware advances in the areas of battery energy density, small electric motor efficiency, and power transmission efficiency are also required to improve the duration of ornithopter missions at the miniature scale. Alternatively, new research into actuation modes other than electric motors may allow for lighter MAVs. By making batteries with higher energy density, and optimizing energy usage through the use of elastic energy storage and release, flight endurance can be further improved [10, 46]. If new progress is made in these areas, an entirely new class of flapping fliers can be created that will possess useful and practical flight endurance. Eventually, if ornithopters can be created that can remain aloft for extended periods of time, then miniature ornithopter systems will be capable of longer range and longer duration missions with less downtime.

Chapter 3 – Wing Design and Selection

3.1 Introduction

Compliant wings play an important role in the successful flight of flapping wing MAVs. During the wing flapping motion, the interaction of aerodynamic and inertial loading will cause deformation of the wings. The camber and mid-chord velocities will be significantly changed during the flapping cycle with the amount depending on the configuration of the primary and secondary spars. This is a primary underlying cause for successful flight of flapping wings. A major goal of this thesis is to characterize compliant wings that effectively produce lift and thrust. However, existing computational and analytical models do not fully account for the interaction of wing compliance on force production. Therefore, modeling will not be sufficient to describe the performance properties of a given wing; additional physically-based tests will be needed. Dynamic lift and thrust measurement will provide useful insight for both the design of optimized wings as well as developing models that account for the compliance of wings. Lift and thrust measurement of a dynamic system such as a flapping wing MAV will require some specialized equipment and setup to deal with the unique loads that will be produced during the flapping motion. The results of lift and thrust testing will be compared to establish any trends that explain performance differences. High speed photography of each wing during the flapping motion is used for additional insight. While it is difficult to accurately model the deflections experienced by a compliant wing during flapping, it is much simpler to observe the deflections, compare with the forces produced, and draw conclusions based on real-world test results. Each wing will be modeled to determine its center of mass, then the high speed photographic analysis will

focus on tracking this point, as well as the deflections of the wing spars and membrane. Analysis of these results will help to explain the measured force production values from the load cell equipment. Finally, the forces measured will be compared to flight testing results for each wing style including payload capacity and top speed to provide a foundation for validation of measured and observed results.

3.2 Force Measurement

3.2.1 Design Criteria

Due to limitations in computational models, designers must turn to direct measurement of wing forces to provide insight for the design of compliant flapping wings. By measuring the dynamic response of the wings during flapping, the effects of varying design parameters can be investigated. Two key observations can be made from the dynamic response of the wings. First, the average lift and thrust output can be measured and compared to different wing configurations to understand what styles of wings are more effective. Second, the time-varying force profile can be examined to gain understanding into why particular wing designs prove more effective than others. Since the wings flapping are compliant, there are multiple dynamic effects present other than simply the primary flapping frequency. In the design and selection of force measurement equipment, these effects must be considered, to ensure that the forces measured are not a misrepresentation of reality. With a combination of hardware vibration isolation devices and software post-processing of data, it is possible to observe the lift and thrust forces that drive the flight of the flapping wing MAV.

3.2.2 Equipment Setup

The first and most important component of the force measurement system is the transducer. This component will convert the loads generated by the wing flapping into a voltage signal for subsequent recording and processing. The key concerns in the selection of the force transducer will be the response characteristics and the natural frequencies of the system. In slower applications such as tensile testing, the dynamic response is not important due to gradual loading and unloading of the transducer. However, this particular application results in many excitation frequencies transmitting through the MAV. If a natural frequency of the force transducer is excited, the response characteristics will be highly contaminated by resonant effects from the measurement equipment, thus hiding the true forces output by the MAV.

The transducer selected for measurement of forces is an Omega Engineering, Inc. LCFD-1KG miniature load cell, Figure 29.

Figure 29: Omega Engineering, Inc. LCFD-1KG miniature load cell [47]

The LCFD-1KG has a 1000 gram capacity with precision of 1.5 grams. This model was selected because of its high frequency resonant characteristics, minimal contamination from off-axis loads, and robust overloading tolerances.

The LCFD-1KG load cell is mounted using a threaded connection to the RAB1S linear air bearing system that minimizes friction and stiction caused by off-axis loads, Figure 30. The inner slider bar is precisely machined to a tolerance of 0.0005” and slides along

a single axis inside the outer housing. Pressurized air is supplied to the outer housing, preventing the inner slider bar from encountering friction due to the cushion of air. By aligning the axis of motion for the air bearing with the axis of the load cell, the desired forces are strongly isolated from any external signals that could cause disturbance to the true measurement values.

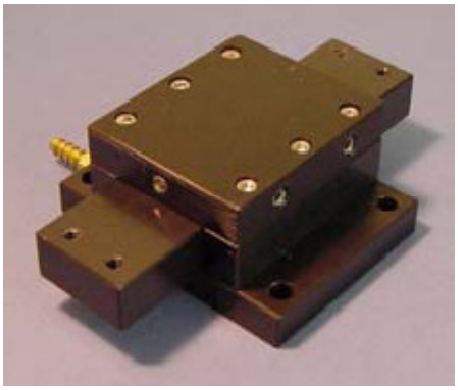

Figure 30: Nelson Air Corporation RAB1S linear air bearing [48]

A Newport Optics SA breadboard provided a secure mounting surface for the assembly of the air bearing and load cell, Figure 31. This breadboard is constructed of solid aluminum and has considerable mass to provide a stable platform for the components.

Figure 31: Newport Corporation SA2 aluminum optics breadboard

The SA2 breadboard is equipped with four hemispheric Edmund Optics Sorbothane® Mounts, Figure 32. These mounts are made of a polymer material that provides 57% absorption of energy and 70% specific damping [48]. Each mount is located at a corner of the breadboard, providing additional isolation from contaminating noise signals that may arise due to environmental disturbances, or the breadboard interacting with the surface it is resting on.

Figure 32: Edmund Optics Sorbothane® polymer mounts

The final component required for collection of lift and thrust forces is a clamping fixture that securely mounts the MAV to the load cell and air bearing assembly. Due to the load cell and air bearing operating along only a single axis, it was necessary to create a fixture that can be reconfigured for both lift and thrust measurement. The clamp is shown with the MAV mounted in thrust measurement mode, Figure 33. In this configuration, it is possible to adjust the height of each of the three mounting posts to ensure the angle of attack is properly setup. The plate at the front of the clamp has a pattern of mounting holes that match with the carbon fiber rods protruding from the front of the MAV, thus providing a secure grip. The three clips spaced along the length of the body can be

secured using the friction of the foam body, or tightened with a nut and bolt to provide a solid connection. For lift measurement, the orientation of the MAV is altered so that a moving airstream can be used and lift forces can be measured, Figure 34.

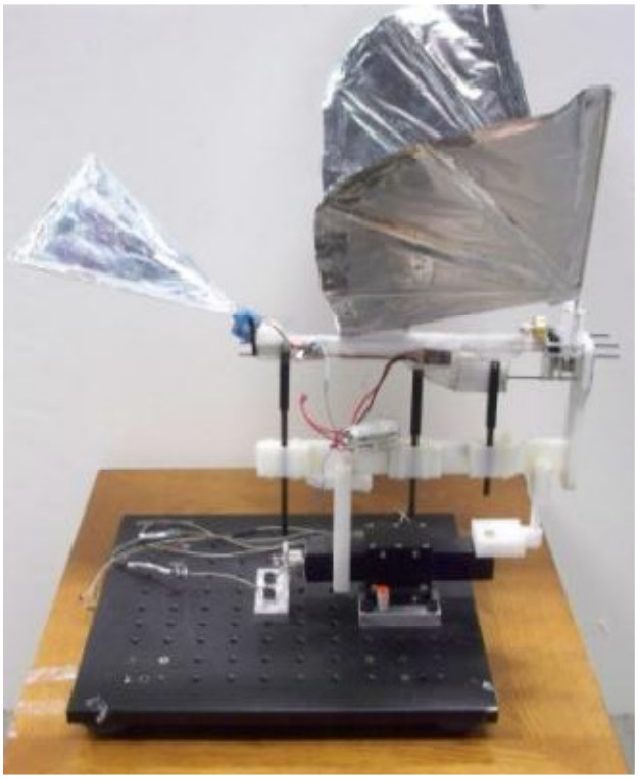

Figure 33: MAV force measurement equipment configured for thrust measurement

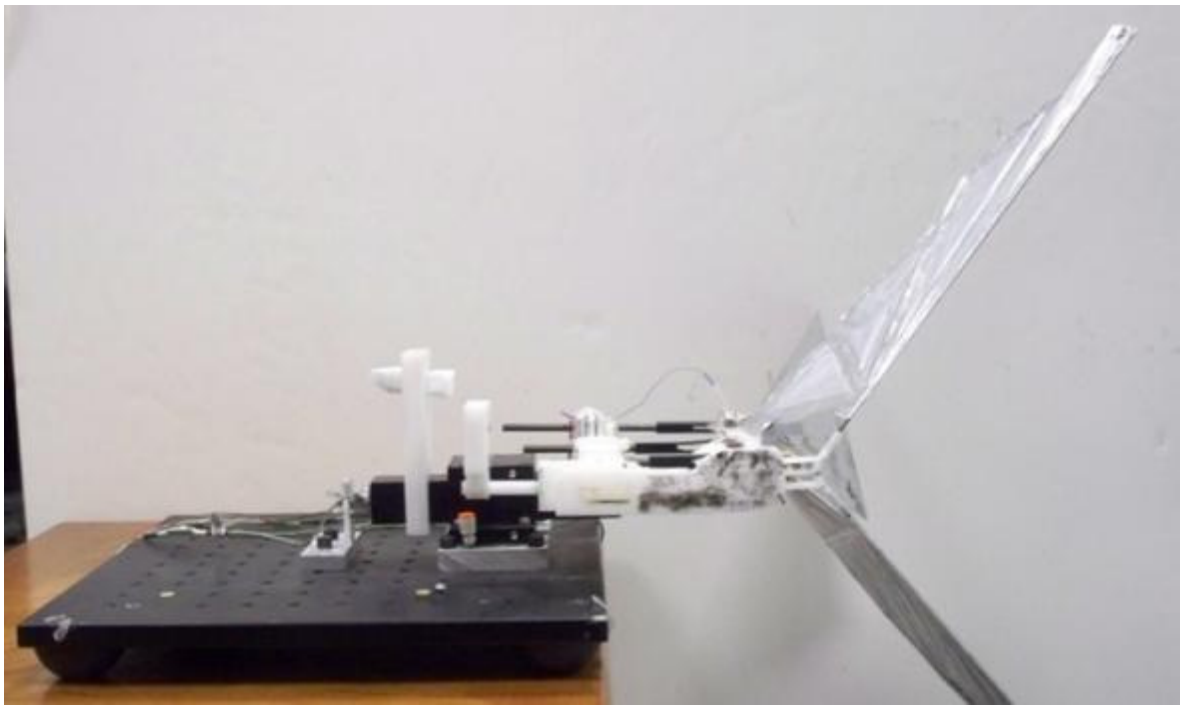

Figure 34: MAV force measurement equipment configured for lift testing

With all the necessary components assembled for the force measurement system, the next step in preparation for testing was to calibrate the load cell to known force values. For the purposes of this calibration, a rudimentary force generator was created, Figure 35. An eccentric object of known mass was rotated with a small electric motor at a known radius of eccentricity, such that it would generate centripetal forces of a known value. By mounting this force generating device to the end of the air bearing and load cell assembly, the forces were transmitted to be collected and scaled to the appropriate values, Figure 36. The plot shows that the load cell is functional with small errors up to frequencies exceeding 20 Hz, well beyond the maximum flapping frequency of 6.1 Hz. Therefore, the load cell is properly scaled to measure the forces generated during wing flapping.

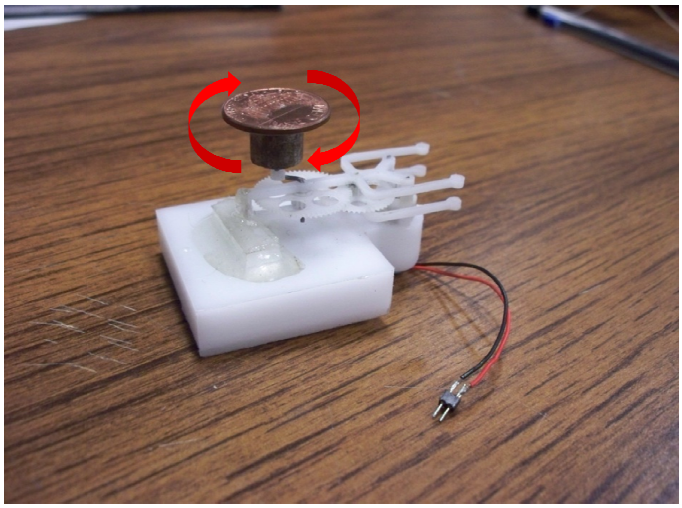

Figure 35: Eccentric rotating mass used for calibration of load cell

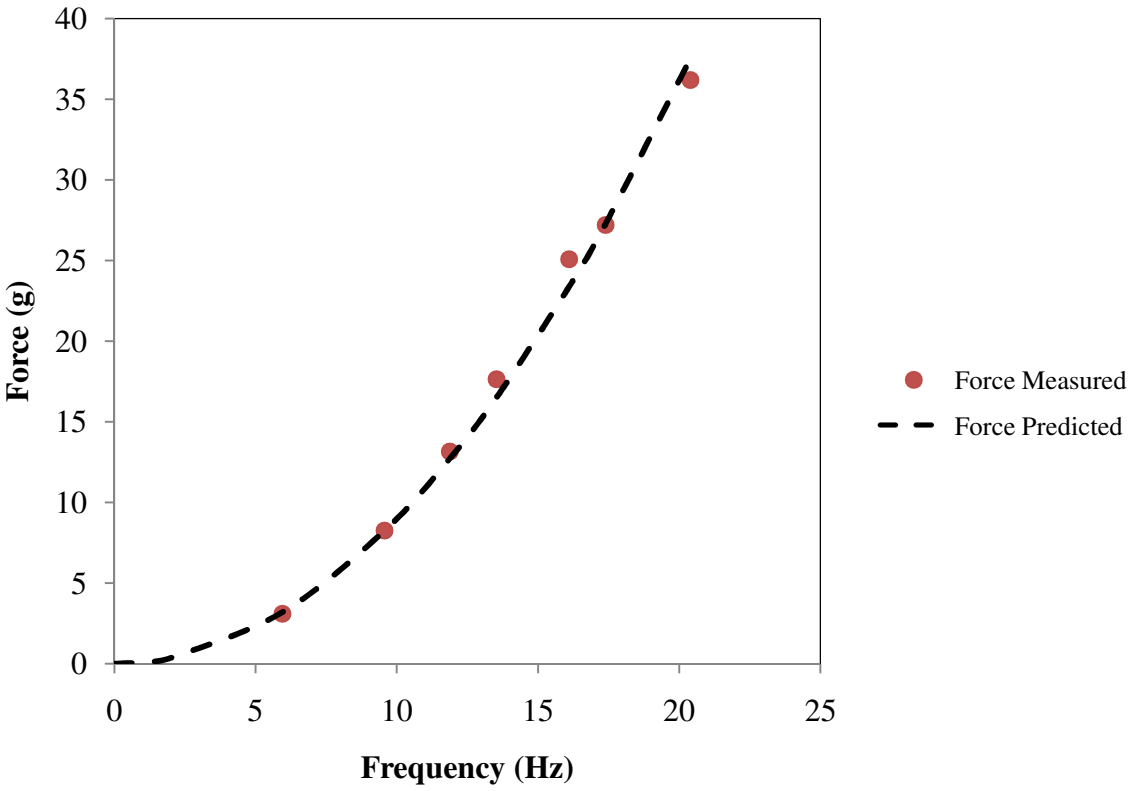

Figure 36: Correlation of measured load cell forces and theoretically predicted forces

While the equipment described so far is acceptable for measurement of static forces (non-moving airstream), additional equipment is required to perform lift testing. The reason for this is the coupling of lift and thrust forces. As the wings of the MAV flap, thrust forces are produced. The primary reason for this thrust production is the flexibility of the wings. As the leading edge spar is flapped between the minimum and maximum angles, the trailing edge of the wing lags behind. The result is the wing is moving up and down at a large angle of attack, thus directing airflow toward the rear of the wings. Without some amount of flexibility in the wings, no thrust would be produced. A flat plate wing moving up and down would only produce drag forces along the flapping axis. Therefore, a crucial element of the wings performance is the flexibility that results in shape change during the flapping motion. In flight, the wings flapping are generating thrust forces that propel the MAV forward through the air. The wings take an aerofoil shape during the flapping motion due to their compliance, and when this aerofoil is placed in a moving airstream, the resulting lift is what allows for flight, thus thrust and lift are coupled. If the lift production of wings were tested in a non-moving airstream, the measured forces will average out to very near zero, due to exact cancellation of upstroke and downstroke inertial and aerodynamic forces, therefore, it was necessary to generate a moving airstream.

The wind tunnel is a common method of creating a moving airstream for the purposes of evaluating aerodynamic performance. Typically, wind tunnels must be carefully designed to obey certain rules that dictate its length to diameter ratio, test section properties, and other parameters with the goal of creating a highly laminar and smooth airstream. However, due to the small size of this particular MAV and the wind

conditions it routinely encounters in flight, a more realistic depiction of flight properties can be obtained from a somewhat turbulent airstream. Keeping this in mind, a tunnel was designed for the purpose of evaluating the lift performance of this MAV as would be seen in real-world flight conditions. Basically this means the tunnel provides a moving airstream, but not all the properties of a low velocity laminar flow wind tunnel. The tunnel consists of five interlocking sections, four feet in length, for a total distance of twenty feet. The test section is square with three foot sides, providing enough room for the previously described equipment to fit inside. The tunnel is shown in Figure 37.

Figure 37: Tunnel used for lift testing of the MAV

3.3 Lift and Thrust Testing Results

Using the equipment and setup described in sections 3.2.2 and 3.2.3 a variety of lift and thrust performance tests were conducted for each wing. For thrust testing, the test was

performed with non-moving air. To investigate the effects of different testing parameters, the filtering threshold was varied to ensure no important forces were being lost during the attempt to remove noise signals. The tests were repeated multiple times to ensure random errors were not affecting the measured values between separate runs. Lift was also tested using the load cell equipment. To create conditions similar to flight, a moving airstream was used in lift tests. Finally, the stiffness of each wing was measured using a load cell at the wing centroid. The stiffness of each wing is related to the flight performance and offers insight into why some wings are stronger performing than others. In order to investigate the aerodynamic performance of each wing, the lift and thrust were evaluated at half throttle and full throttle. Generally, flights of the MAV at half throttle correspond to high altitude cruising behavior, where the benefit of greater wind velocity boosts lift output and there is less reliance on self-generated thrust to propel the wings through the air. Full throttle corresponds to take-offs, heavy payloads, and low altitude flight, where maximum force output is required to sustain flight. The results of the half throttle testing and full throttle testing are shown in Figure 38 and Figure 39, respectively.

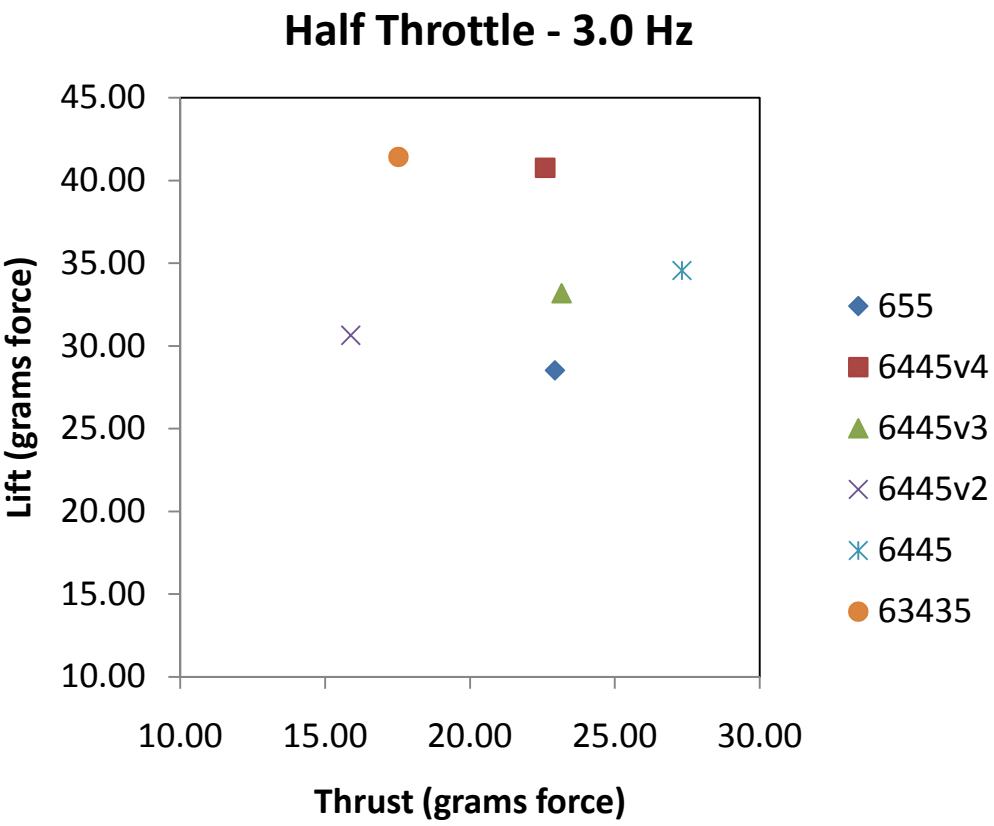

Figure 38: Lift and thrust performance results

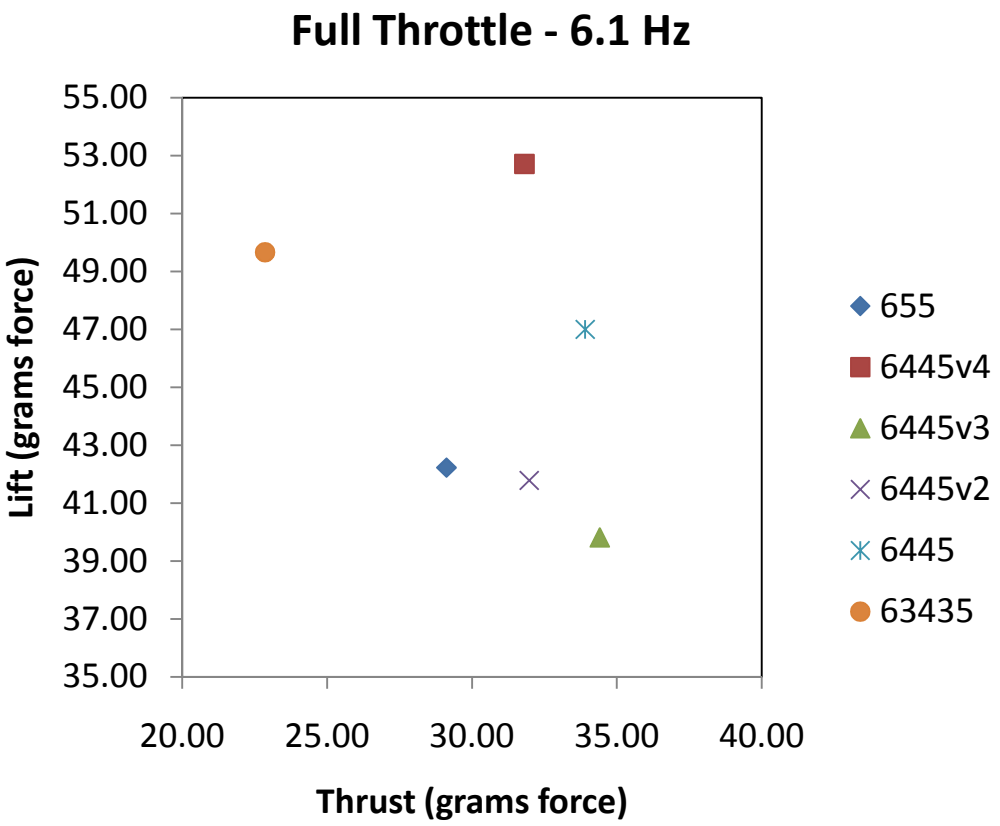

Figure 39: Lift and thrust performance results

3.4 Data Post-processing

The flapping wing MAV is a dynamic system with a primary frequency located at the flapping rate of 6.1 Hz. However, the measurement equipment that the MAV is mounted on is also a dynamic system, and has its own response characteristics. Depending on the excitation signal the MAV is generating, a resonant frequency of the measurement equipment could be excited during testing. During the earlier stages of equipment selection, multiple s-beam cantilever designs were evaluated to establish the proximity of their respective resonance frequencies to the flapping rate of the MAV. Each of the s-beam style load cells showed resonant frequencies in their dynamic responses that

overlapped with the wing flapping frequencies, thus preventing successful deconvolution of the flapping from the response of the measurement equipment.

The LCFD-1KG is stiffer than the s-beam load cells evaluated, thus moving its resonant response to a higher frequency. By using a fast fourier transform of data collected during an actual test, it was possible to observe and separate the signals from the MAV and the load cell, Figure 40. There is a noticeable peak in the frequency content centered around 340 Hz, corresponding to the resonant dynamic response of the load cell and air bearing system. There is also a secondary noise peak centered around 115 Hz, corresponding to the resonant response of the clamp and fixture parts. Using a simple low pass filter, this undesired frequency content is removed from the data collected, leaving behind the wing forces only.

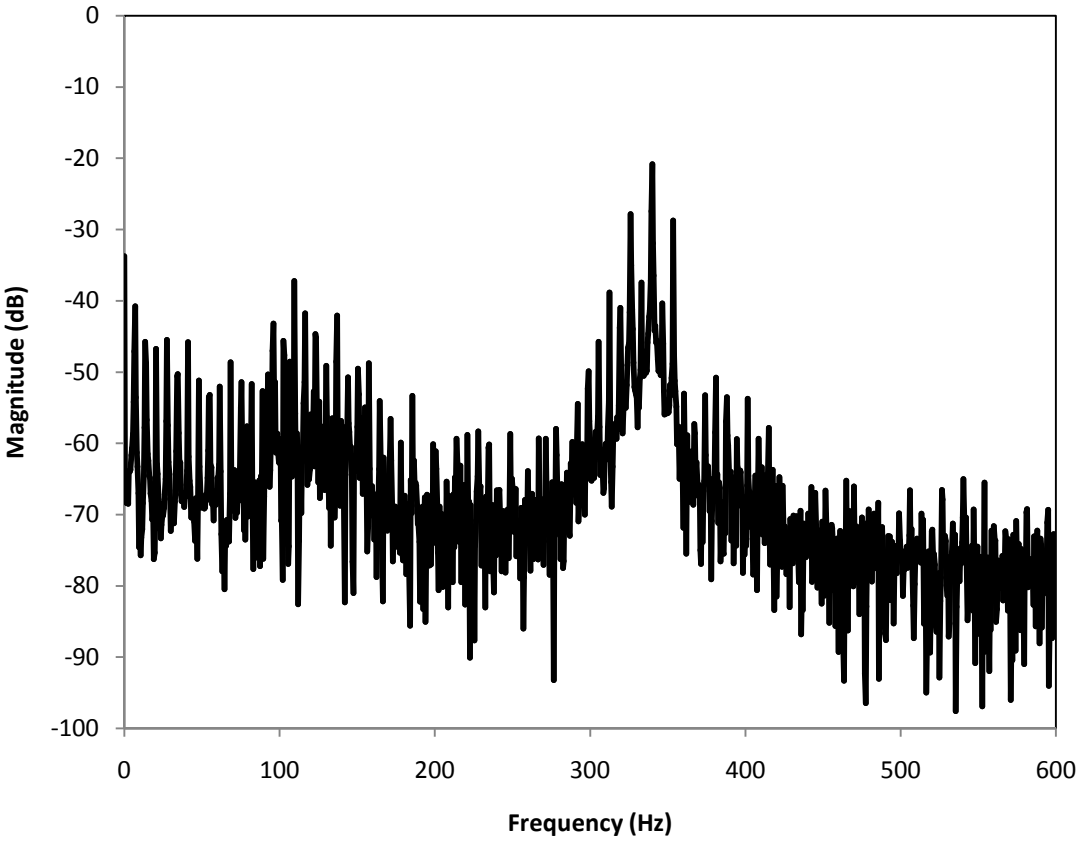

Figure 40: Fast Fourier Transform of data collected using LCFD-1KG load cell

An important consideration when applying filtering to the data collected was the effect on the force magnitude. With excessive filtering, the true value of thrust or lift output could be diminished due to improper removal of a real signal, rather than just dropping noise out of the signal. Therefore, a variety of filtering thresholds were evaluated to determine the effect on the average force magnitude. Any value that was more than twice the maximum flapping rate of 6.1 Hz caused no difference in the measured force values. Figure 41 shows two flap cycles with changing filter thresholds, however there is no effect on the average force value of 29.1 grams for all three filter values. Similar testing was performed between the limits of 10 Hz and 1000 Hz to ensure the results were consistent and only noise was being removed from the signals measured.

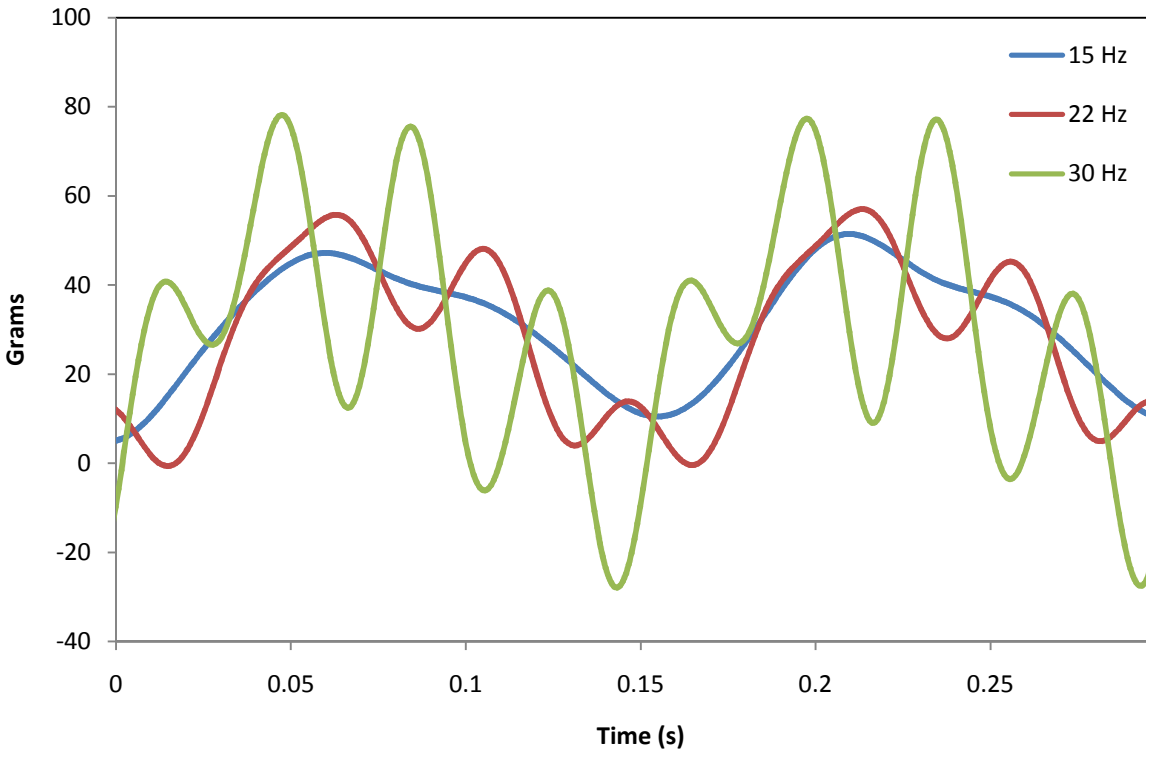

Figure 41: Effects of varying low pass filter cut-off frequencies

3.5 Wing Construction

In the design and construction of any MAV, one of the most crucial components governing overall performance is the wings. Especially in a flapping-wing MAV, the wings are paramount to flight performance aspects including endurance, speed, maneuverability, climbing, gliding, and many other useful behaviors. The wings are the source of lift and thrust, and must therefore be capable of supporting the weight of the MAV plus any desired payloads.

The wings produce lift and thrust primarily due to their ability to change shape during the flapping motion. As the wing is accelerated, aerodynamic loading causes the wing to deform. The result is a fairly large camber change of the wing that results in the normally flat plate shape changing to an airfoil shape. The aerodynamic loading also produces

large angles of attack that create thrust. When these two effects are combined, the airfoil wings are placed in a moving airstream, thus creating a flight sustaining lift force.

In the construction of the wings, there were two materials used. Carbon fiber rods provided a lightweight and stiff structure of spars, similar to the skeletal structure of a flying animal. Thin mylar foil approximately 0.002 inches thick was then attached to the carbon fiber structure to provide the lifting surface. By using a special metalized form of mylar foil, it was possible to use heat to stick the foil to itself, allowing for the wings to be constructed without adhesives or tapes that would have added extra weight.

The wings constructed were designed to investigate the effects of a variety of spar patterns. In the design of the wings, there were two main topics of interest to be studied. First, wings were created to study the effect of localizing stiffness at different locations moving from the leading edge to the trailing edge of the wing. Second, wings were created to study the effect of focusing stiffness at fewer points or distributing stiffness along the entire wing surface. By creating a set of wings that fills these two solution spaces with some candidate wings, testing results could then offer insight into how these factors impact the lift and thrust performance.

The general approach to the layout of spars is shown in Figure 42, with the leading edge at the top of the figure. Each set of wings was constructed with the same mylar foil pattern, resulting in equal surface area for all wings. The span L was set to 13 inches for every set of wing, the chord H was set to 6 inches, and the overall surface area for each wing was 68 square inches.

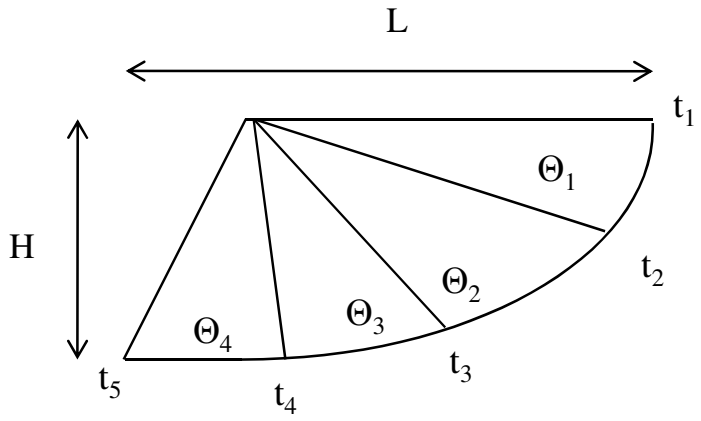

Figure 42: Wing configuration template

By varying both the thickness values and the angles of each spar, various styles of wings were investigated. A summary of each wing prototype constructed is shown in Table 2.

Table 2: Wing prototype parameters

Wing	t_1	t_2	t_3	t_4	t_5	Θ_1	Θ_2	Θ_3	Θ_4
1(655)	0.06”	0.05”	0.05”	-	-	36	69	-	-
2(63435)	0.06”	0.03”	0.04”	0.03”	0.05”	20	19	32	34
3(6445)	0.06”	0.04”	0.04”	0.05”	-	19	51	35	-
4(6445v2)	0.06”	0.04”	0.04”	0.05”	-	34	36	35	-
5(6445v3)	0.06”	0.04”	0.04”	0.05”	-	69	17	19	-
6(6445v4)	0.06”	0.04”	0.04”	0.05”	-	17	17	71	-

As a method of easily identifying a particular set of wings, a nomenclature has been adopted that is descriptive of the wing spar configuration, shown in parentheses in column one of Table 2. For example, wing 3 is referred to as 6445 because of the thicknesses of its structural spars having values of 0.06”, 0.04”, 0.04”, and 0.05” moving from leading edge to trailing edge.

3.6 Force Measurement Verification

3.6.1 Overview

When testing the lift and thrust performance of the wings, an important consideration was the calibration of the test equipment. Some real-world test results were needed to validate the results measured using the load cell. To establish a baseline of performance, each wing was flight tested to measure its maximum payload capacity. While flying at maximum payload, the MAV was speed tested to establish a thrust performance level. With the combination of these two indisputable real world results, a basis for verification of testing using the load cell was in place.

The technique for verification is based on the proportionality of lift and thrust. As the MAV increases its velocity through an airstream, its lift should increase as the square of the velocity. Therefore, by measuring the lift and velocity encountered in the tunnel, as well as the lift and velocity of flight, a relationship should hold that is described by:

$$\frac{L_f}{V_f^2} = \frac{L_t}{V_t^2}$$

where the left side of the equation describes the lift and velocity encountered in flight, and the right side of the equation describes the lift and velocity encountered in the tunnel testing environment.

3.6.2 Flight Testing Results

Each candidate set of wings described in section 3.5 was flight tested to find its maximum payload, and corresponding velocity at maximum payload. The results of flight testing were then compared to recorded values from the load cell to investigate the correlation of measured values. In general, the flight testing agreed closely with the measured values.

The first step in this process was to perform payload testing to verify wind tunnel measured values. First, the wind velocity was measured in the tunnel, and found to be an average of 10.5 ft/s. The value is expressed as an average due to the semi-turbulent nature of the airstream, therefore this value is indicative of a typical velocity encountered in the tunnel. This is a slightly lower value than the flight velocity of the MAV exhibited during flight tests, resulting in a somewhat diminished lift value, based on the discussion of lift and thrust coupling in section 3.2.2. A comparison of lift values is shown in Figure 43.

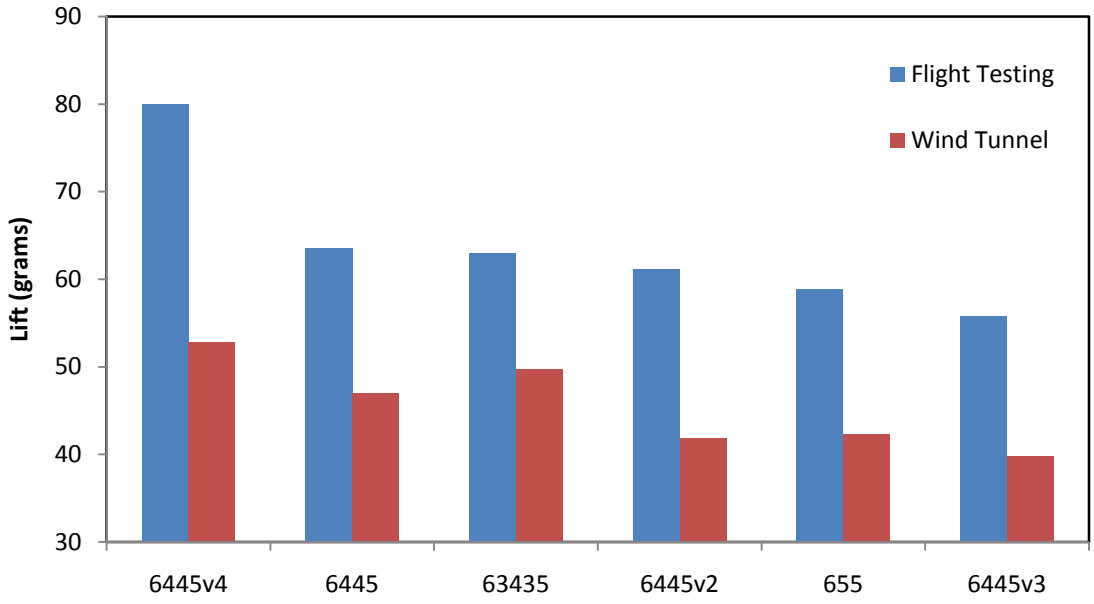

Figure 43: Comparison of tunnel measured and actual lift values

The next step in the validation process was to compute the ratio of lift to squared velocity for both the flight tests and tunnel results, as a means of comparison. If these values are well-aligned, then the tunnel will have proven its worth as a useful tool for the evaluation of flapping-wing aerodynamics. Results of this comparison are summarized in Table 3.

Table 3: Comparison of lift to squared velocity ratios for flight testing and tunnel testing

Wing	Velocity (ft/s)	Flight Payload (g)	Wind Tunnel Lift (g)	Wind Tunnel L/v^2	Flight L/v^2	Tunnel/Flight Error
1(655)	12.04	58.8	42.2	0.381	0.406	6.1%
2(63435)	12.49	62	49.7	0.448	0.397	-12.8%
3(6445)	12.49	62.9	47.0	0.424	0.403	-5.2%
4(6445v2)	12.13	61.1	41.8	0.377	0.416	9.3%
5(6445v3)	12.04	55.8	39.8	0.359	0.385	6.7%
6(6445v4)	13.24	79.9	52.7	0.476	0.456	-4.4%

Due to the usage of hand-built wings, there exists some variability in the errors computed in Table 3. Mainly, this effect is attributed to a skewing of the thrust vector for some of the wings. Put simply, this means the wings are not perfectly in trim, so the tail must be used to correct the flight direction. This in turn impacts the drag of the MAV during flight testing, resulting in the errors shown. The results shown here highlight one of the fundamental weaknesses of manually assembled parts, the lack of precise repeatability leads to randomness in flight performance.

3.7 Wing Compliance Measurement

3.7.1 Overview

As a means of explaining the lift and thrust performance of the wings, compliance measurement was performed at the centroid of each wing. The measured compliance is one of multiple factors that determine wing lift and thrust performance, due to the dependence of force output on the deformation of the wings. Without any deformation, the wing would exhibit a nearly zero angle of attack, and thrust output would drop to zero. In addition, the camber of the wing would remain constant, resulting in a nearly zero average coefficient of lift for the wing. By measuring the compliance of each wing

and comparing these results to the lift and thrust, certain conclusions can be made about how and why compliance is affecting force output.

3.7.2 Testing Procedure

Evaluation of wing compliance involves a relatively simple procedure of applying a controlled deflection, and measuring the loading response. By deflecting the wing at a slow and controlled rate, the loading response will provide information about how the spars and mylar foil combine to resist this motion, and add together to produce an overall global behavior. Hence, two main pieces of equipment were required to conduct this test. First, a displacement control apparatus, capable of computer-controlled motion, and second, a load cell to measure the wing response forces. Included with the load cell were some data collection and filtering devices, used to record and condition the measurements from the load cell. This setup is shown in Figure 44.

Figure 44: Wing compliance measurement equipment

As described in Section 3.5 Wing Construction, the arrangement of wing spars is different for each set of wings evaluated. This raised the question of where on the wing surface to conduct a compliance measurement. If the same point were tested on every wing, comparisons would be invalidated by local stiffness effects superseding the global stiffness values that are desired. Therefore, each wing was modeled using the appropriate geometric layout, as well as measured densities for the film and spars. The center of mass for each wing was then located, and marked on the wing surface. By testing each wing at its center of mass, a more fair comparison can be made between each set of wings, resulting in more meaningful conclusions from the data collected.

The tests were conducted as follows. First, the load cell was clamped into the controlled displacement arm. Second, the wing was mounted below the load cell with the calculated wing centroid positioned directly below the load cell. The load cell was then used as an

end effecter to cause gradual displacement of the wing centroid, until a sufficient amount of data was collected to observe the displacement-stiffness relationship. By repeating the test multiple times, the data was verified and ready for post processing.

3.7.3 Stiffness Results

Each wing was tested using the procedure described, and the data from the displacement equipment and load cell were synchronized. For comparison, all the collected data points have been plotted together in Figure 45. There are a number of conclusions that can be drawn from the data presented. The obvious comparison is in the relative stiffness of each wing, ranging from a minimum of 0.507 grams/mm to a maximum of 1.569 grams/mm. When comparing these stiffness values, it is important to keep in mind the measurement was taken at the centroid of the wing, which is located at approximately one-third of the total wingspan length.

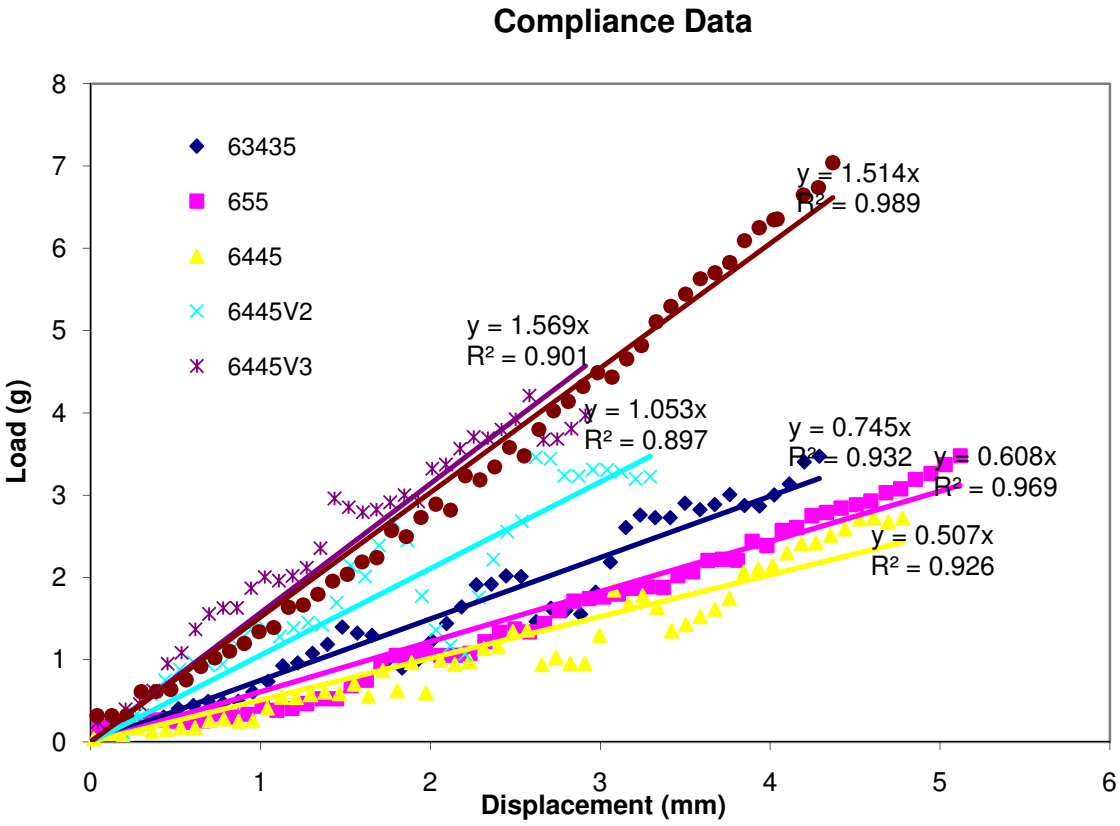

Figure 45: Centroid stiffness-displacement measurements

3.8 High Speed Photography Analysis

To properly explain the performance of a given set of wings, three main factors are required. First, the amount of deflection present in the wing must be quantified. This is important because the formation of a large pocket in the wing surface during flapping will capture more air, resulting in a greater amount of thrust output. Second, the spanwise point of maximum deflection must be determined. This point helps to explain the direction of thrust production. If a given set of wings produces a large amount of thrust, but directs most of it laterally, then this is basically lost work. Thrust must be directed parallel to the flight direction for the maximum benefit. The third piece of information required is the angle at which the wing assumes its peak deflection. If a

given set of wings is achieving its maximum deflection earlier in the wing motion, then it will be spending a larger portion of the total available flapping range producing larger forces.

Evaluation of each wing was performed by clamping the MAV and filming the deflections of the wings during maximum throttle flapping. The peak deflection of the centroid was plotted for each wing, during both the downward flapping motion and upward flapping motion. In addition, the angle that the main wing spar was at when this deflection was reached was plotted. The results are shown in Figure 46 and Figure 47. For the downward flapping direction, the motion starts at 52.5°, so the closer to this value that the peak deflection is occurring, the better. Similarly, during the upflap, the motion is starting at -12.5°, so the closer to this value the peak deflection is occurring, the better. In general, it is desirable for the wing to reach its maximum deflection as rapidly as possible, because then a larger portion of the flapping motion is providing the largest possible thrust forces. The data is reflective of this point, as in both cases, the wings that start deflecting earlier in the flapping cycle tend to have greater thrust output. In addition, the wings that deflect by a larger amount tend to have greater thrust output. These two trends provide important design insight for the creation of an effective set of wings.

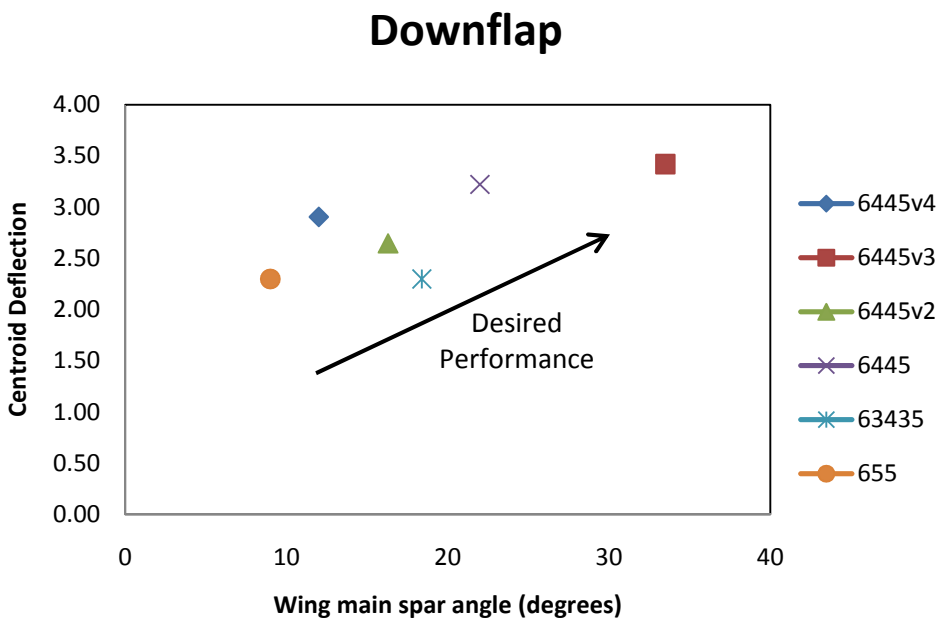

Figure 46: Angle during downflap that maximum deflection is reached

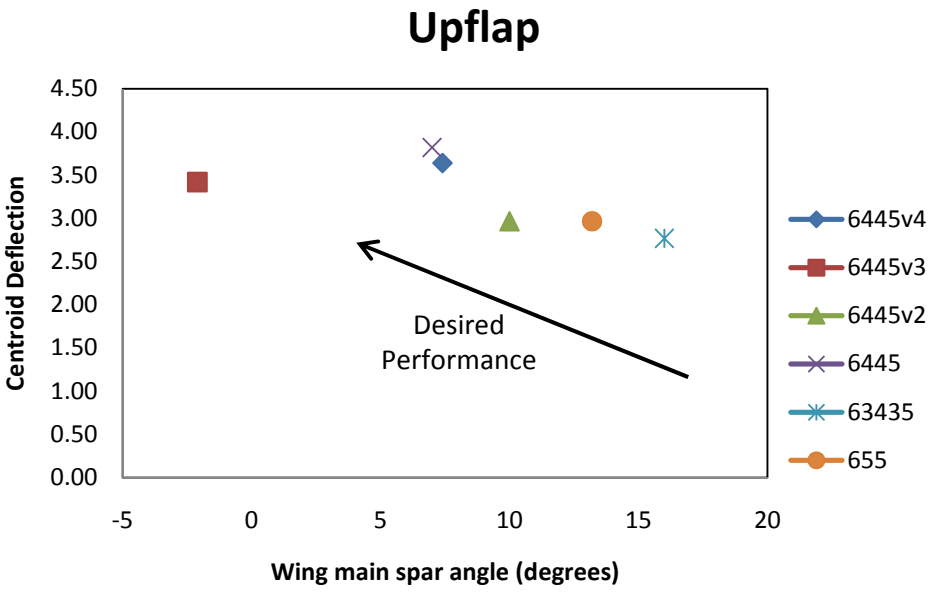

Figure 47: Angle during upflap that maximum deflection is reached

The centroid provides a measure of two of the three factors impacting wing performance, the amount of thrust and the portion of the flapping cycle during which this thrust is exerted. However, the direction of thrust output is another key piece of information needed to explain how a given wing performs. For each wing, some spanwise point farther out on the wing than the centroid reached a maximum deflection value. This value was plotted for each wing, as well as its location along the wingspan in Figure 48. The combination of the two values provides useful insight into both the magnitude and orientation of thrust output. In the plot, the desired point of maximum performance is up and to the left. The reasons for this are simple, as the deflection is increased, a greater volume of air is thrust from the wings. As the spanwise point of peak deflection is moved inward along the wing span, the thrust produced is directed closer to parallel to the flight direction. These results are reflected in the data, where the highest performing wings are up and to the left, while moving to the right skews thrust away from the flight path, and moving down reduces thrust magnitude.

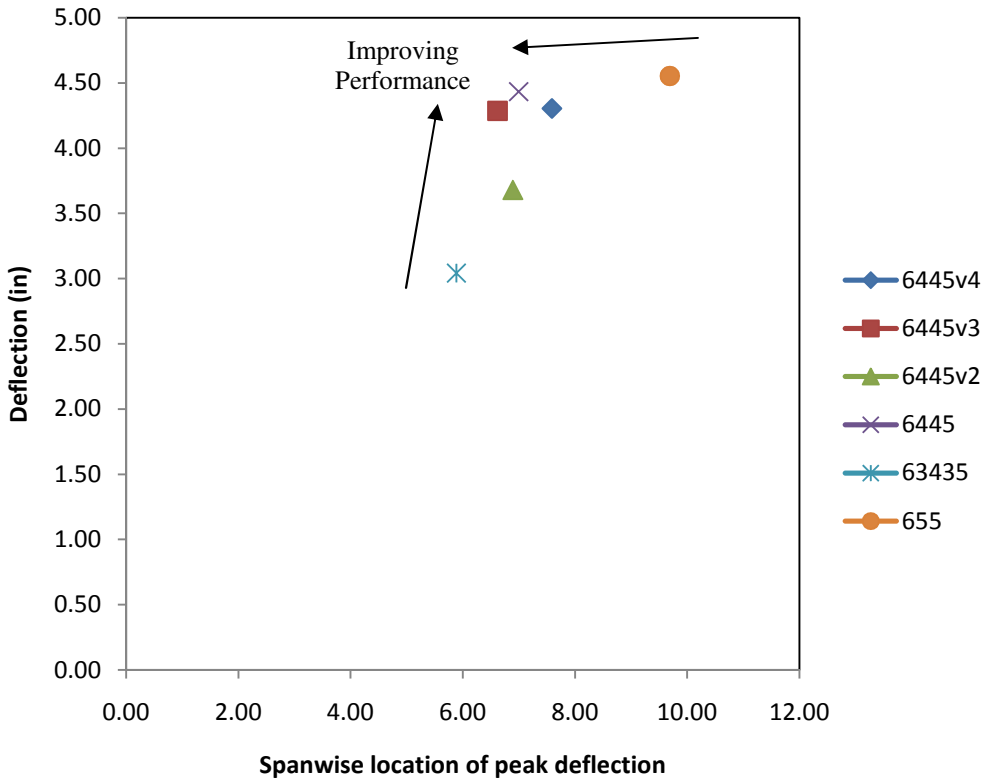

Figure 48: Peak deflection properties from high speed photography

3.9 Summary

This chapter has presented an approach to the design and selection of flapping wings for a MAV. The approach consists of a combination of lift and thrust testing using both moving and non-moving airstreams, flight testing for payload and velocity, and stiffness analysis of wings, using both direct and indirect measurement techniques. The results of this chapter suggest certain rules of good design to be followed such that a wing will produce larger lift and thrust forces.

Thrust forces are primarily attributed to the formation of a large pocket in the wing, due to compliance allowing a camber change to occur as aerodynamic loading is applied. The distribution of compliance in the wing is an important determining factor for thrust performance. The compliance distribution must be such that the peak deflection occurs

inboard along the wing span, resulting in thrust directed parallel to the flight path. With a combination of large wing deflections and properly distributed compliance, a given set of wings will be able to produce larger locomotive forces.

Lift forces are primarily attributed to two factors. First, the shape created by the wings during flapping must have a large coefficient of lift. This is achieved with a lift producing airfoil shape, and with a smooth surface, resulting in reduced flow separation. The second important factor is the thrust production of a given wing. Lift is coupled with thrust because as the airflow velocity is increased, there is a corresponding increase in lift due to greater flow velocity over an airfoil.

While the techniques in this chapter do not directly specify how to construct a successful wing, there is still value to the general approach. By following the steps presented, a designer can iteratively build wings, evaluate them, and make improvements that are justified with test results.

Chapter 4 – 'Jumbo Bird' Flapping Wing MAV

4.1 Introduction

Flapping wing MAVs requires at present have a seriously limited mission scope. Due to strict weight limitations, it is difficult to carry sensors, autopilots, extra batteries, and other useful mission payloads on miniaturized air vehicles. Therefore, fundamental advances are required in the following areas to allow for successful field deployment of flapping wing MAVs in a variety of applications:

1. ***Reduction in Drive Mechanism Weight***: Current flapping wing MAV designs have very limited payload capabilities. This seriously limits the number of on-board sensors and the flight time. A main contributor to the weight controlled by the designer is the drive mechanism that converts motor's rotary motion into the flapping motion of the wings. Usage of polymer as the structural material reduces the weight of the drive mechanism. This will allow for MAVs to carry more auxiliaries. Reduction in the weight will also enable the use of larger batteries and hence increase the overall mission time. However, we have to ensure that the reduction in weight will not compromise the structural strength of the mechanism under operation loads. By performing detailed analysis of various forces acting on the structure, the shape of the drive mechanism was optimized to minimize the weight and retain structural strength.
2. ***High Power Transmission Efficiency***: In order for a flapping wing MAV to work, the rotary motion of the motor needs to be converted into flapping wing motions. Moreover, the motor speed needs to be reduced to match the desired wing flapping frequency. Power transmission from the motor to the wings is accomplished by the

drive mechanism. The efficiency of the power transmission is a major concern. Due to weight considerations, low-friction bearings cannot be used in this application. Losing too much power in the transmission will reduce the operational range and also require use of a bigger motor. Hence, we are interested in exploring new concepts such as compliant drive mechanisms to minimize the power loss in the transmission without increasing the mechanism weight.

3. ***Low Cost***: Currently, the distributed compliance flapping mechanism used in our MAV is produced using CNC machining and manual assembly. Unfortunately, CNC machining is not a scalable process and is not feasible for low cost production of MAVs. In order to make flapping wing MAVs attractive in search, rescue, and recovery efforts, they should be disposable from the cost point of view. The distributed compliance mechanism discussed in this section is manufactured using CNC machining and manual assembly. Hence, the next step beyond this mechanism will be to apply successful design traits to a new mechanism that is manufactured using a scalable process that can bring cost and assembly time down.

4.2 Electronic Components Required for MAV Functionality

To drive the flapping mechanism and provide basic flight functionality, a variety of electronics components are necessary. These components have been selected to compliment the flapping mechanism while keeping weight to a minimum. Without these components, throttle and steering control would not be possible.

The desire to keep the weight as light as possible led us to use the lightest functional electronic components available on the market. We chose a brushless DC motor as the

source of the rotary motion, due to high thrust output of 210 grams, good efficiency, and acceptable weight, Figure 49.

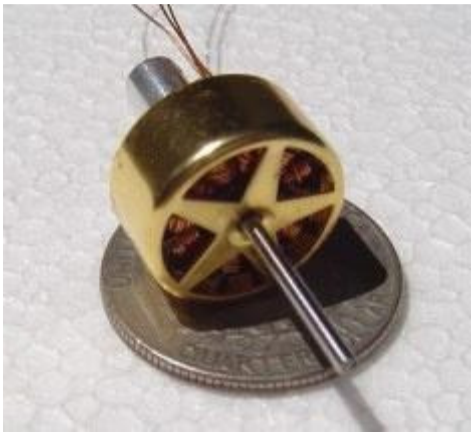

Figure 49: LRK 13/6/11Y brushless DC motor [49]

This brushless motor requires an electronic speed controller for operation, so we selected a lightweight brushless speed controller rated for up to six amps of current draw, Figure 50. This component is required to convert throttle signals into the coordinated electrical pulses that drive the brushless motor. While the motor is only supposed to draw three amps, smaller speed controllers were erratic in operation for two main reasons. First, flapping wings present an unusually irregular loading pattern as compared to a propeller. Second, the flapping wing MAV moves through the air relatively slowly compared to a fixed-wing aircraft, resulting in less air cooling and increased risk of overheating.

Figure 50: Feigao 6A brushless electronic speed controller

We then picked the lightest matching remote control receiver, a Microinvent Minor, Figure 51. This receiver weighs 0.75 grams and provides four-channel radio control. One channel each is devoted to throttle and steering, leaving two extra channels for auxiliary functions in future missions.

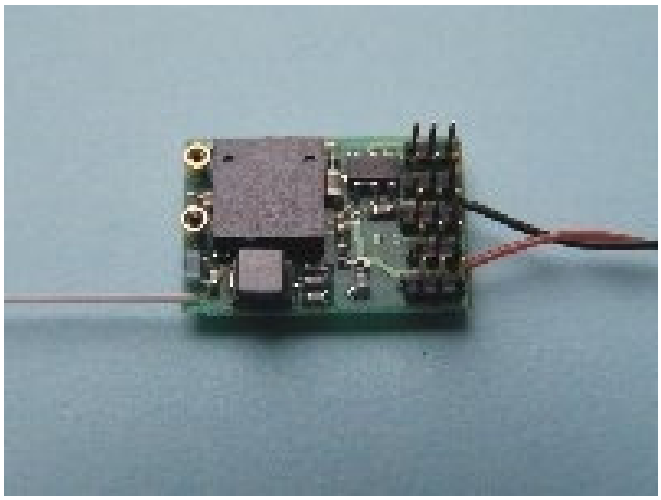

Figure 51: Microinvent Minor radio receiver [50]

For steering of the MAV, the lightest available servo was used to deflect a tail surface constructed in the same style as the wings, Figure 52. The tail provides functionality much like a rudder, where drag is uneven left to right, resulting in steering. While lighter actuators such as magnetic coils are available, the size of the MAV was too large for this to be feasible. Due to the rate of flapping having a strong impact on climb rate, an elevator was tested and deemed unnecessary and too heavy to be practical in this MAV.

Figure 52: Blue Arrow S0251 servo used for tail rudder actuation [51]

For power, lithium polymer battery cells were used, with three cells connected in series to provide 11.1 volts. The batteries come in a variety of capacities, thus providing a tradeoff to the pilot depending on the desired mission. If it is desirable to carry a very heavy payload, small capacity batteries can be used to provide shorter flights with greater lifting capacity. For typical flights, three 250 mAh capacity cells were used, with minimal packaging and lightweight wires used for interconnections to keep weight to a minimum, Figure 53. The battery is a key contributor to overall MAV weight, with a typical pack weighing about 20 grams.

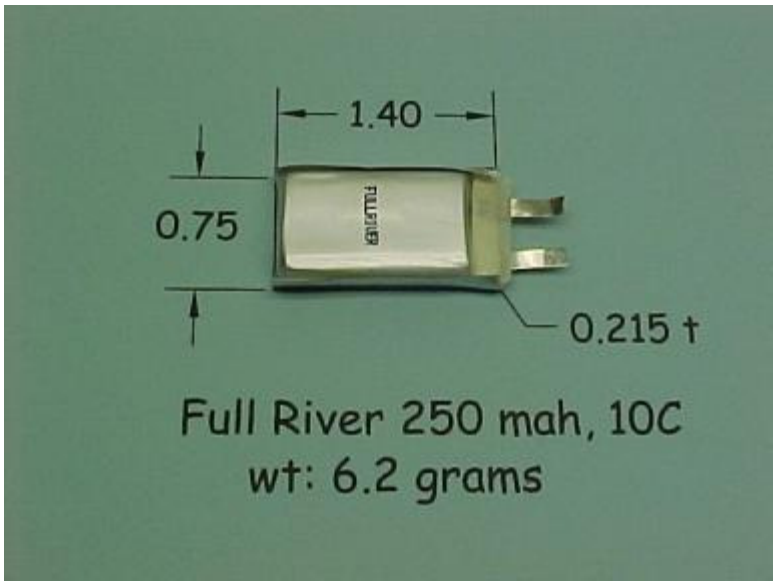

Figure 53: Lithium polymer battery cell [51]

4.3 Functional Decomposition

Each of the parts identified in section 4.2 is part of the overall MAV system, described in Figure 54. All the parts in the system combine to provide two primary functions, control over wing flapping motion, and control over a tail rudder. Achieving these two functions requires the transfer of power, control signals, and motion through multiple components. First, power is sourced from the lithium polymer battery pack, which provides 11.1 Volts to the system, nominally. This voltage is first sent to the electronic speed controller. The electronic speed controller contains on-board circuitry called a battery eliminator circuit (BEC). The function of this BEC is to step down the voltage to 5 Volts, so that other components in the system can be run without the need for a separate low voltage battery, thus providing weight savings. The low voltage is used to power the radio receiver, which is set to receive signals on channel 12 (72.030 MHz). An equal setting on the radio transmitter ensures that the control signals commanded by the pilot are received

without interference. The receiver is used to distribute the pilot's command signals to the two actuators in the system, one for steering, and one for driving the wings. The steering signals turn a servo that holds the tail, resulting in rudder-like steering. The throttle commands require further processing, and are sent to the electronic speed controller. The throttle commands are received and converted into a series of precisely timed pulses that drive the brushless electric drive motor at the desired speed. This rotary motion is then converted to wing flapping action by the flapping mechanism, completing the system.

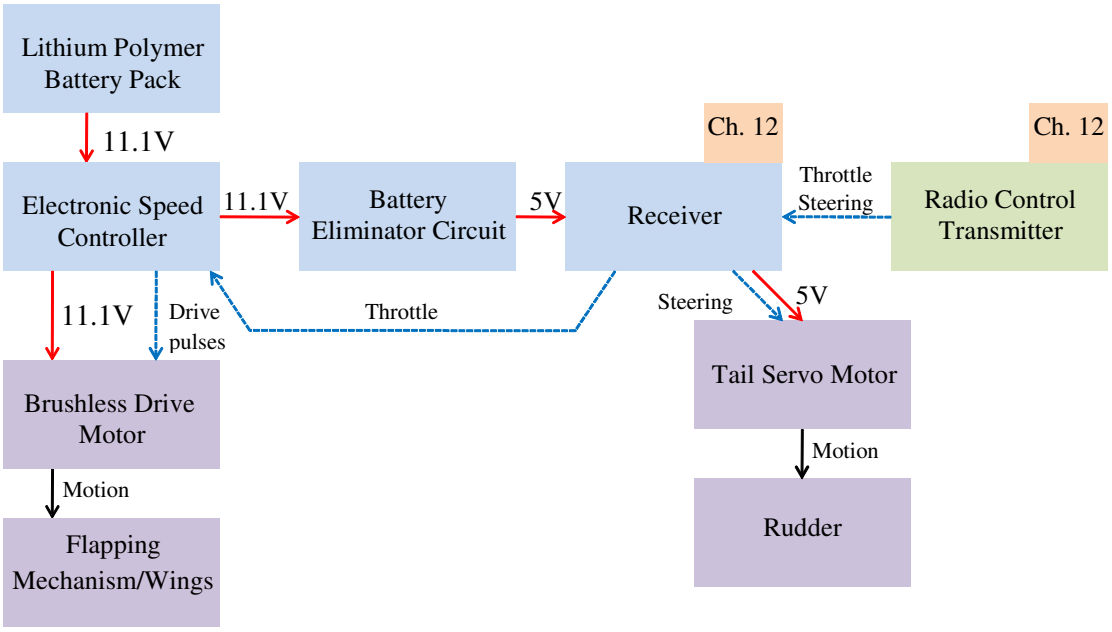

Figure 54: Functional decomposition of MAV system

While selecting the components to be used in the MAV, a strong emphasis was placed on weight minimization. Therefore, the components used are highly miniaturized, and represent some of the lightest available over the counter products. The weights for each component are listed in . A weight is not included for the flapping mechanism, because this will be discussed in greater detail in chapters 5 and 6. The 6445v4 wings selected

were used for all subsequent testing in Chapter 5 and Chapter 6, due to their strong performance in the evaluation presented in Chapter 3.

Table 4: MAV component weights

Component	Weight (g)
11.1V 250mAh lithium polymer battery pack	21.0
Electronic speed controller	4.5
Radio receiver	1.4
Tail servo motor	4.6
Rudder	1.6
Brushless electric drive motor	7.5
6445v4 Wings	7.1
Body (Foam, carbon fiber)	3.0
Wires and connectors	3.9

Chapter 5 – Distributed Compliance Flapping Mechanism

5.1 Introduction

A crucial component of the Jumbo Bird flapping wing MAV is the drive mechanism used to convert rotary motor output into wing flapping motion. This chapter describes an approach for determining the drive mechanism shape and size that meets both the design and functional requirements. This problem has many facets that need to be simultaneously considered. The primary objective is to minimize the weight of the drive mechanism. The secondary objective is to select the structure shape that will provide maximum performance benefits. The structure shape and size need to ensure that the forces acting on the structure do not induce excessive stresses. Furthermore, structure shape and size need to allow for unpredictable forces seen during wind gusting, crashes, and other events. In this section, a detailed approach is presented for decomposing this challenging problem into more manageable steps. First, a quasi-static kinematic and dynamic model of the flapping mechanism will be presented that determines the distribution of forces present in the mechanism during the flapping motion. This model uses physically measured real-world forces created by the wings flapping as inputs, for improved accuracy of the modeling. The outputs of the model will be used in Finite Element Analysis (FEA) of the mechanism. By using these tools, the mechanism will be improved until it reaches the specified design and functional requirements. The design generated by this approach was used to successfully realize a flapping wing MAV that has completed many test flights under a variety of conditions.

5.2 Motivation for Distributed Compliance Design

This section describes the design and construction of a flapping mechanism that incorporates distributed compliance to provide efficient power transmission. Compliance is used in the mechanism as a technique for reducing power input requirements, thereby contributing to the goal of an efficient mechanism.

Using a motor and drive mechanism necessitates that the motor provide enough force to both accelerate and decelerate massive wings. This constant usage of power to reverse the direction of the wing flapping results in reduced efficiency relative to a propeller or rotor driven design, where the motor is constantly driving the wings (propeller) in a useful direction, rather than fighting to overcome inertia it previously generated. A method of recovering this wasted energy is to use a compliant flapping mechanism. A compliant mechanism is a flexible structure that elastically deforms to produce desired force or displacement. Compliant mechanisms serve two important functions. First, they transmit and transform motions, forces, and energy, resulting in the wing flapping motions. Second, compliant mechanisms store elastic strain energy as their flexible members are deformed. Such a design can be seen as analogous to a hybrid drive vehicle where the braking energy that would otherwise be lost as heat is partially recovered and re-used at a later time.

Compliant mechanisms offer several benefits over mechanisms with rigid links and articulated joints. Some of these benefits include reduction in backlash, friction, and wear between moving parts. This can result in reduced noise and vibration during operation. Compliant members provide energy storage when deflected. This energy storage is the key to efficiency improvements over traditional rigid mechanisms. By coordinating the deflections of the mechanism with the motion of the wings flapping, the

energy storage can be exploited to reduce inertial losses due to acceleration and deceleration of the wings. The result of compliant mechanisms used in this fashion is a reduction in the range between minimum and maximum loading, and a corresponding decrease in power consumption of the electronics components in the MAV [7].

The flapping mechanism described in the following section makes use of distributed compliance in its structure, meaning that the links in the mechanism are flexible, and the revolute joints that connect flexible and rigid links are free to move. Both a dynamics and a finite element analysis will be presented to determine the stresses and strains in the mechanism. In addition, high speed video results will show strengths and weaknesses of this mechanism design when used in the 'Jumbo Bird' flapping wing MAV.

5.3 Functional Concept

In this section the main requirements for the mechanism are outlined, a mechanism concept is described, and the main steps in the approach for converting the concept into a detailed design are explained.

Based on the weight, size, and functionality constraints, a compliant mechanism was found to be a suitable design for the purposes of the MAV. The compliant mechanism provides minimized friction losses, energy recovery, and ease of manufacture due to part consolidation. Figure 55 shows the schematic diagram of the mechanism concept. Flexural members were incorporated into the mechanism to provide for compliance in the structure to facilitate motion.

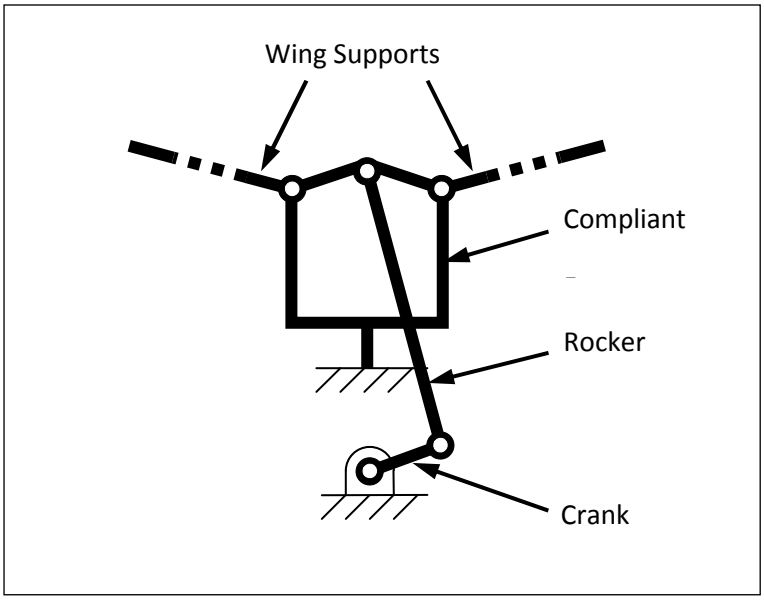

Figure 55: Schematic diagram of the compliant mechanism for flapping wing action

It was determined during flight testing that strong flight performance is highly dependent on total weight, therefore, the goal for the mechanism weight was less than 5 grams. By minimizing the mechanism weight, there is increased available capacity for batteries and payload. Also, more agile flight is possible, including better climbing, maneuverability, and softer landings with reduced risk of damage. The desire to minimize the mechanism weight led to the use of a polymer for the structural material. DuPont Delrin® acetal polyoxymethylene (POM) was used due to its light weight, acceptable strength, and suitability for CNC milling operations. The material properties of Delrin are listed in Table 5: DuPont Delrin® acetal polyoxymethylene material properties [52].

Table 5: DuPont Delrin® acetal polyoxymethylene material properties [52]

Measure	Value	Units
Ult. Tensile Strength	75.8	MPa
Elongation at Break	30	%
Flexural Modulus	3.10	Gpa
Tensile Modulus	3.10	Gpa

While one of the goals of this mechanism was to use a scalable manufacturing process such as injection molding, this would have been very time consuming during the earlier development stages. Therefore, in the interest of speeding the process of building concepts and making changes quickly and easily, CNC milling was chosen as the manufacturing process for this mechanism. This resulted in quicker manufacturing times due to the possibility of rapid machining of plastic relative to aluminum for injection molds. Especially in the earlier stages of development, the choice to use milling proved to be beneficial due to the many changes that were made as new problems were discovered during testing. In later stages, a transition to injection molding was planned, and will be discussed later in chapter 4 with a new mechanism concept.

A crucial functional requirement for the MAV drive-mechanism is that the flapping action of both wings should be synchronized. Based on previously conducted exploratory tests of a flying prototype, the desired range of flapping was found to be 65°. Importance of synchronization is emphasized, because it not only ensures the required flapping action for a successful flight of the MAV, but also contributes to the overall stability of the mechanism. Preliminary tests indicated that with the wing area of 8.8E-02 m^2, the flapping frequency needed to be at least 3 Hz to sustain flight.

The main functional requirements for the drive mechanism were as follows:

- Flap wings at more than 3 Hz
- Achieve flapping range between –12.5° and +52.5°
- Transmit motor torque of 1.85 Nm
- Support wings of total area of 8.8 E-02 m^2

5.4 Mechanism Shape Synthesis

The first step in the design approach for this flapping mechanism is to establish detailed part shapes and dimensions using the concept illustrated in Figure 55. To accomplish this goal, the shape synthesis of the mechanism followed a three step approach. First, the basic shape of the mechanism was established by detailing the design concept with functionality constraints and manufacturing constraints. Second, the constrained dimensions of the mechanism were determined by analyzing the mating components and motion requirements. Third, parametric optimization and finite element analysis (FEA) were used to determine the values of other critical unconstrained dimensions. This approach is summarized in Figure 56.

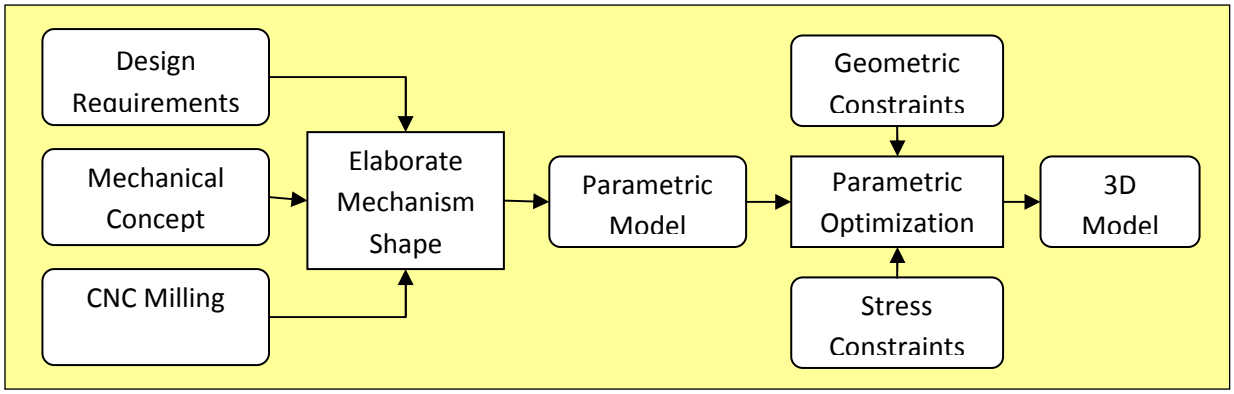

Figure 56: Shape synthesis from the mechanism conceptual design to the detailed part design

5.5 Elaboration of Design Concept

To obtain the desired flapping wing action from the rotary input of the motor shaft, a crank-rocker mechanism was designed based on the concept in Figure 55. The motion of this flapping mechanism is powered by the crank at the bottom, which is driven by a set of gears that transmits the rotation of the motor. By selecting a set of gears that is properly matched to the motor speed, the desired flapping rate is achieved. In order to reduce the rotational velocity of the motor to match the flapping frequency requirement,

the mechanism uses a three-stage set of gears that provide a 55.4:1 reduction, resulting in a maximum flapping rate of 6.1 Hz, based on the peak rotational velocity of the motor. The gears were selected such that the necessary flapping rate was well within the throttle range of the motor, while also providing the ability to drive the wings faster so that demanding flights were possible, including heavy payloads, bad weather, and other scenarios. As the crank turns, the rocker is pulled up and down, with each side of the rocker using a pinned connection to allow for free rotation. As the rocker moves up and down, the vertical arms of the compliant frame will be stretched inward and outward. Note that the compliant frame must be able to move in this manner, because without this flexure, the mechanism would be locked in place. By altering the dimensions of the wing supports, the amount of flexure in the compliant frame can be controlled, as well as the flapping range of the wings. The wings are driven by hollowing out the wing supports and inserting the leading edge spars of the wings. The rear of the wings is then fixed to the body of the MAV, and as the mechanism drives the wing supports, the wings are flapped.

Several prototypes of the design concept illustrated in Figure 55 were constructed to investigate the effects of various disturbance forces on the flapping action. Experimental results showed that disturbance forces cause unintended motion out of plane, resulting in excessive stresses on the gears and wing supports, as well as improper flapping motion. To remedy this problem, a bi-planar support design was used to help constrain the flapping motion to a single plane. The structure that holds the flexural members in plane is shown highlighted red in Figure 57.

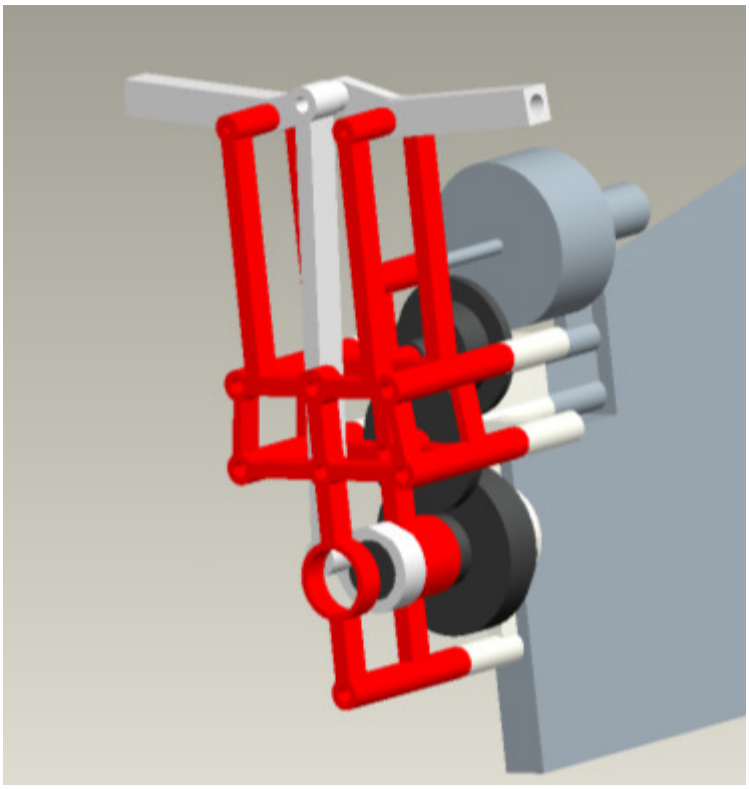

Figure 57: Bi-planar support structure

Once the basic shape of the mechanism was established using the functionality constraints, the next step was to determine the dimensions in the mechanism. The overall length and width of the mechanism were found to be 57 mm and 14.6 mm by combining the motor size with the dimensions of the gears selected, such that a protective housing could shield these components from impact damage in a compact package. To achieve the desired flapping range of 65°, the length of the crank and the rocker were set to 4.1 mm and 44.2 mm, respectively. Finally, to shift the flapping range to the desired minimum and maximum values, the wing supports were designed with a 15° inclination at the hinge point, resulting in +55° to -15° flapping motion. The key dimensions of the mechanism are shown in Figure 58. With the shape of the mechanism established, the next important step was to determine the stresses and strains present in the flexural beams

at the top of the frame using a combination of kinematic and dynamic modeling along with FEA.

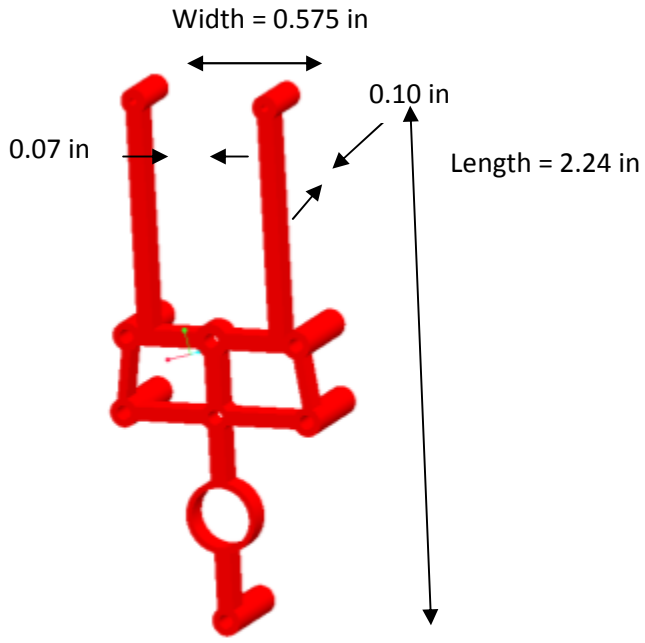

Figure 58: Dimensions of the mechanism body

5.6 Estimation of Forces for Optimization of Mechanism Dimensions

After elaborating the mechanism shape and determining the constrained dimensions, the next step was to estimate forces acting on the mechanism during the flapping motion. These forces were used in determining the stresses of the flexural frame that arise during the wing flapping motion, and are important for determining the factor of safety. The mechanism flapping motion is a dynamic problem, however due to the maximum flapping frequency of 6.1 Hz combined with the relatively small masses of the moving parts, the inertial forces were neglected. In this analysis, the motion cycle was divided into multiple time frames and static equilibrium analysis was performed at each time step.

As a technique for modeling the flexural frame in the mechanism, a pseudo-rigid body planar mechanism was used, Figure 59. In this model, the motor output shaft and pinion are located at point C, the gears are located at points D, E, and F, and the pushrod is driven by the crank at point F. This means the compliant members flexibility was modeled using stiff links with torsion springs at the anchoring joints. Motion was generated using a constant rotary input that would drive the mechanism at the proper maximum flapping rate of 6.1 Hz. The wing force inputs were modeled normal to the wing spars, with sinusoidal profiles and magnitudes equal to the maximum wing forces measured. Since these inputs were used in an effort to determine unconstrained mechanism dimensions, the forces modeled were chosen with the goal of creating the worst case scenario of loading, so that the mechanism would be robust.

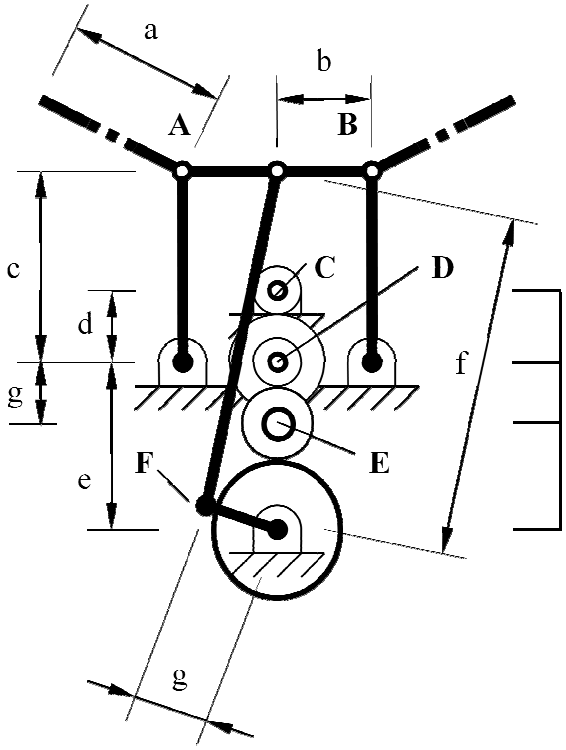

Dimensions:

a	13.00	in
b	0.297	in
c	0.981	in
d	0.331	in
e	0.736	in
f	1.738	in
g	0.319	in

Gear Reductions:

i_1	0.244	-
i_2	0.227	-
i_3	0.325	-

Figure 59: Kinematic representation of the model

A key parameter of the pseudo-rigid model was the two torsion springs that anchor the bottom of the flexural frame. By tuning the stiffness and damping of the torsion springs, the behavior of the actual mechanism was approximated as closely as possible. To determine the appropriate stiffness value for the torsion springs, Equation 1 was used.

$$k_{rot} = \frac{3EI}{l}$$

Equation 1: Bending stiffness of a beam

where:

k_{rot} – Rotational Stiffness
E – Young's Modulus
I – Moment of Inertia
l – Beam Length

The mechanism was modeled using MSC Adams/View R3 Software, using the model inputs listed in Figure 59. A reaction force distribution analysis was performed by running a static equilibrium simulation for a full flapping cycle. The goal was to investigate the entire flapping cycle and find the worst-case combined loading scenario, such that the highest von Mises stress would be present on the mechanism. Therefore, the reaction forces and deflections were recorded at critical points A through F shown in Figure 59 with a resolution of 4.0E-4 seconds. The times with the highest loading intensities and deflections were chosen as the most likely for worst-case loading. These loading scenarios were then used as inputs in finite element analyses, using the Mechanica module of Pro/Engineer Wildfire 4.0 software. The goal of the FEA was to input the modeled force distribution seen by the mechanism and find the resultant displacement and von Mises stress induced on the mechanism structure. By carefully selecting the loading cases output by ADAMS/View to be investigated, the number of

finite element analyses was reduced significantly. This approach can be generalized to any time-dependent loading applied to a designed part to establish dimensions that will lead to a desired factor of safety.

A sensitivity analysis was performed to determine the effect of varying torsion spring damping values on the sought reaction forces. The effects of varying the torsion springs' damping coefficient is shown in Figure 60. The pseudo-rigid modeling technique was unstable without some damping force included, so this was a necessary part of the model.

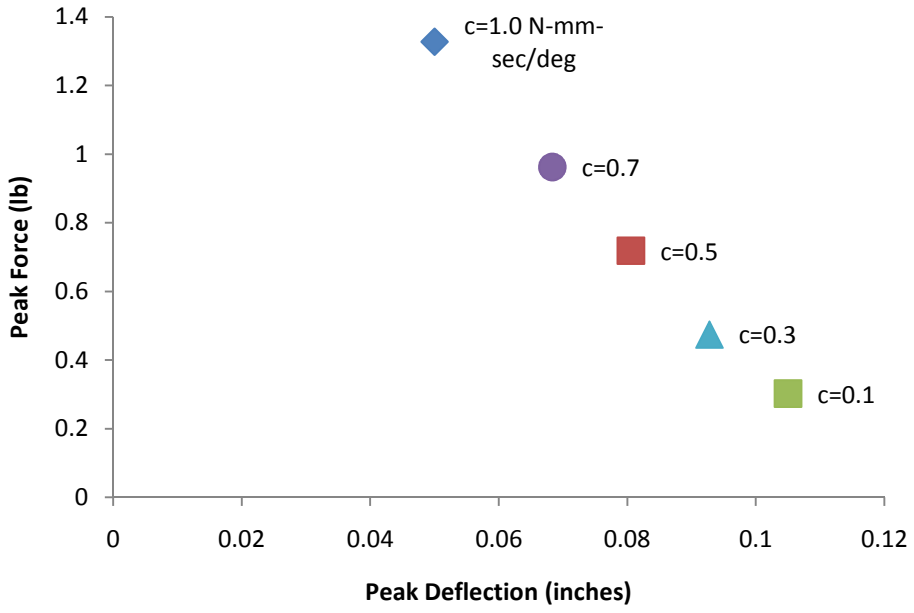

Figure 60: Effect of damping coefficient on compliant frame.

By filming the motion of the mechanism with a high speed camera, the actual deflections were recorded during flapping, and by adjusting the damping value, a similar amount of deflection could be achieved in the model. For the model, a damping value of c=0.5 N-mm-sec/deg was chosen to match the filmed deflections as closely as possible. In making this selection, the primary goal was to achieve a similar peak deflection magnitude between the model and the filmed results, rather than trying to match the

entire time-dependent profile. Due to the complexity of the motion filmed and the many factors impacting the model, capturing both the magnitude and time-profile becomes extremely challenging. A comparison of modeled deflections and actual deflections is shown in Figure 61.

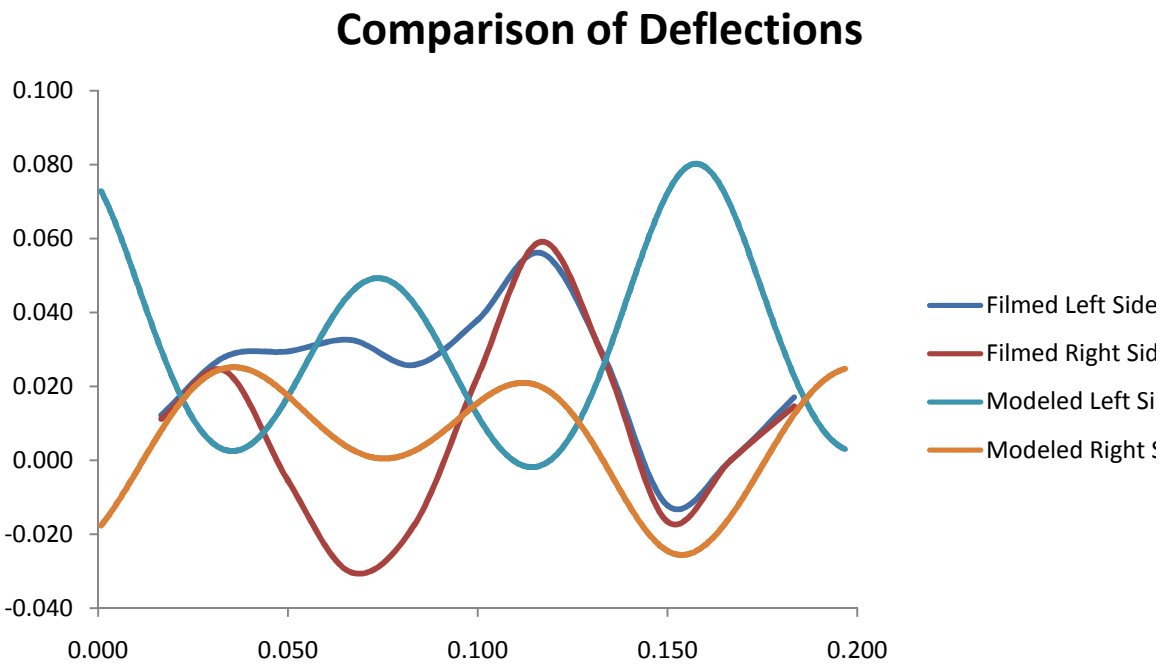

Figure 61: Comparison of actual and predicted deformations of compliant frame

This comparison reveals a key limitation of this mechanism design. Due to the lack of a horizontal constraint at the connection point where the rocker drives the wing supports (in between points A and B in Figure 59), there is an unintended extra degree of freedom that can be described as sway. High speed video analysis revealed this effect to be present in the mechanism during higher flapping rates, Figure 62. This effect is very difficult to exactly capture using the pseudo-rigid body model that has only linear stiffness and damping coefficients, therefore, it was important to use good engineering judgment when setting the stiffness and damping coefficients, and when interpreting the

results from the modeling. The filmed peak deflection magnitude of the compliant frame ranged from +0.06 inches to -0.02 inches. By comparison, the prediction of the deflection magnitude ranged from +0.08 inches to -0.025 inches, therefore, the model used was a conservative estimate.

Figure 62: Asymmetric deflection of the flexural frame

5.7 Summary

This chapter has presented a mechanism that converts the rotary motion of a motor into flapping action. The flapping mechanism is designed to take advantage of a distributed compliance strategy for efficiency improvements. The mechanism weighs a total of 6.4 grams, with the distribution of weights listed in Table 6.

Table 6: Distributed compliance flapping mechanism weight breakdown

Part	Weight (g)
Compliant frame (3 parts)	2.9
Pushrod/crank	0.4
Motor mount	0.5
Wing support arms	0.5
Carbon fiber rods (structural support)	0.5
Pins for revolute joints	0.6
Gears	2.0

Flight testing has shown this mechanism to be an effective design in a variety of metrics. The evaluations of Chapter 3 were all performed using this mechanism, due to its excellent reliability. In addition, a variety of tests were performed to determine the limits of functionality for this mechanism. Successful outdoor flight testing in wind speeds of up to 15 mph and endurance tests as long as 20 minutes were successfully completed without any damage to the flapping mechanism. The maximum payload test of 79.9 grams total weight was also completed with this mechanism. During the course of many flight tests, this mechanism showed good robustness, and was able to withstand repeated crashes without sustaining damage in most cases.

Chapter 6 – A New Localized Compliance MAV Flapping Mechanism

6.1 Introduction

In Chapter 5, a flapping mechanism was presented that sought to address three major challenges the MAVs are currently facing. The challenges were to design a mechanism that was highly efficient in force and motion transfer, while maintaining light weight, and to manufacture this mechanism at low cost with a scalable technique. The mechanism design approached these challenges by making use of distributed compliance in its flexible frame, thus reducing the inertial losses associated with cyclic acceleration of massive wings. Another approach to this problem is to use localized compliance in the flapping mechanism. This strategy uses rigid links that are connected with compliant joints, resulting in similar functional benefits.

As with the distributed compliance mechanism of Chapter 5, this chapter describes an approach for determining the drive mechanism shape and size that meets both the design and functional requirements. The primary objective is to minimize the weight of the drive mechanism. The secondary objective is to select a shape for the structure and the compliant joints that will correct the performance problems exhibited by the previous design, while obeying various injection molding rules. The design of the flexible joints will be particularly important, due to the small size and large loads to be carried. Consideration will be given to the interlocking techniques that will ensure good resistance to failures of the material interface. A brief discussion of injection molding concerns relevant to the production of the flexible joints and rigid structure will also be covered.

A detailed force analysis will be presented for the localized compliance mechanism. As with Chapter 4, a quasi-static kinematic and dynamic model of the flapping mechanism will be presented that propagates the wing forces throughout the mechanism. The outputs of the model will then be used in finite element analysis (FEA) of the mechanism.

The design generated by this approach was used to successfully realize a flapping wing MAV that has successfully completed many test flights.

6.2 Motivation for Localized Compliance Design

The motivation for a localized compliance design is to offer a new approach to the same problem that is presented in Chapter 5. However, changing to a localized compliance strategy presents a performance tradeoff. While the design of Chapter 5 was largely successful, testing revealed some important issues. A reduction in performance was observable in the form of decreased flapping range, out of plane compliance, and an unintended extra degree of freedom. By using more rigid materials in the construction of the links in a localized compliance mechanism, some of this out of plane motion can be more easily eliminated. Since the distributed compliance mechanism was produced mainly with CNC milling, there was a large part count, geometric complexity, and heavy reliance on time-consuming manual assembly operations. However, with a new scalable manufacturing technique, the benefits of large batch production can be harnessed to drive down the cost and time of producing the localized compliance flapping mechanism. This in turn should improve the viability of the MAV to its consumers by offering expendability. It is important to emphasize that a localized compliance strategy is not definitively better or worse than a distributed compliance strategy, merely it offers a new approach to the same problem. A key drawback of the localized compliance mechanism

is the design of the joints. By attempting to focus all the stored energy into such a small volume of material, the stresses and displacements become highly concentrated. Complicating this matter is the difficulty of creating multi-material joints at such a small size. Without careful design decisions, this can result in significant reductions in reliability of the MAV.

The mechanism design of this chapter seeks to learn lessons from the previous mechanism design. This mechanism will correct the factors contributing to functionality weaknesses identified during the testing of the previous mechanism. In addition, the manufacturing process will be faster and cheaper due to adoption of classical injection molding, as well as some innovative molding techniques. As these challenges are remedied, attention will still be given to the new challenges that arise due to a change in layout and manufacturing technique. A goal of the localized compliance mechanism design will be to synthesize the lessons learned from the distributed compliance mechanism with emerging manufacturing techniques, resulting in a design that meets all of the requirements from the areas of functionality, size and weight, and manufacturability.

6.3 Functional Concept

In this section the main requirements for the mechanism are outlined, a mechanism concept is described, and the main steps in the approach for converting the concept into a detailed design are explained.

This mechanism seeks to use compliance as a functional characteristic, due to the multiple performance benefits offered. Compliant mechanisms provide minimized friction losses, energy recovery, and ease of manufacture due to part consolidation. The

key difference will be the localization of compliance to the joints. As with the distributed compliance mechanism, the main functional requirements for the drive mechanism are summarized as follows:

- Synchronized flapping of left and right wings
- Flapping frequency between 4 and 6 Hz
- Flapping range between –12.5° and +52.5°
- Support wings of total area of 8.8 E-02 m^2

Figure 63 shows the functional concept of the localized compliance MAV flapping mechanism.

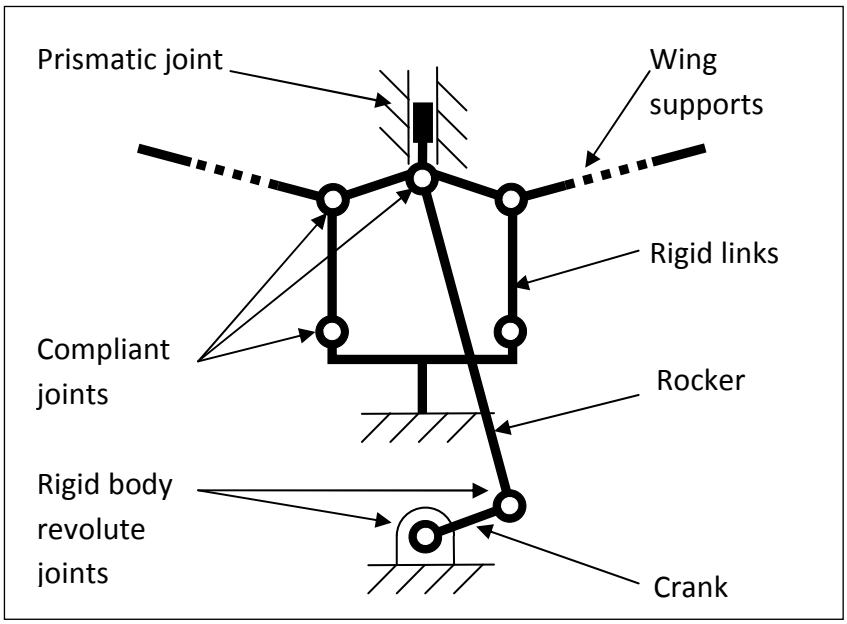

Figure 63: Schematic diagram of localized compliance mechanism for flapping wing action

In the design of the flapping mechanism described in Chapter 5, there were a variety of benefits obtained from the usage of compliance as a functional characteristic. These benefits enabled the mechanism to perform efficiently while maintaining light weight. The compliance strategy in the mechanism was to distribute the compliance spatially, thereby creating a flexible frame to absorb, store, and release energy elastically. One of

the main problems with the distributed compliance flapping mechanism was the appearance of the 'sway' degree of freedom, described in Section 5.6. The problem with the compliant frame was that the structural strength suffers from an inability to deal with large loads imposed by the wings. This manifested as excessive deformation of undesired areas of the mechanism, resulting in diminished flapping performance. Especially when flying outdoors, powerful flapping that covers the full angular range is required to overcome aerodynamic loads and drive the MAV through the air. In an effort to improve the flapping mechanism, an extra constraint has been added. By pinning the central connection point to a prismatic joint, undesired lateral motions were eliminated from the mechanism. This change offered multiple performance benefits, including improved synchronization of wing flapping, larger angular range of flapping, and more powerful flapping.

Polymers were selected for both the rigid and compliant materials in this mechanism, due to multiple performance benefits. Relative to metals, they offer reduced weight, cost, and require fewer post-processing operations. Considering the many polymer grades available to choose from, the complexity of the mechanism shape, and the need for a scalable manufacturing process, multi-material injection molding (MMM) was selected for production [53]. The rigid material selected for construction of the non-compliant links was a 15% glass fiber filled polyacrylate (PA6,6F). The properties of this material are summarized in Table 7. For the flexible hinges, a material that is capable of a large amount of deflection was desired. Therefore, low density polyethylene was chosen. The material properties for LDPE are summarized in Table 8. An important property of these

two materials is the respective melt temperatures. The difference in processing temperatures allows multi-material molding to be used as the manufacturing technique.

Table 7: Material properties of 15% glass fiber filled polyacrylate [from manufacturer's datasheets]

Measure	Value	Units
Ultimate Tensile Strength	110	MPa
% Elongation at Break	1.9	%
Flexural Modulus	22.2	GPa
Tensile Modulus	5.5	GPa
Minimum Melt Temperature	260	°C

Table 8: Material properties of low density polyethylene (LDPE) [from manufacturer's datasheets]

Measure	Value	Units
Ultimate Tensile Strength	9.7	MPa
% Elongation at Break	130	%
Flexural Modulus	0.226	GPa
Tensile Modulus	0.237	GPa
Minimum Melt Temperature	190	°C

6.4 Shape Synthesis

6.4.1 Elaboration of Mechanism Shape

The first step in moving beyond the functional concept was to perform the shape synthesis of the MAV drive mechanism. This included the development of the basic mechanism geometry from the functional schematic in Figure 63. In addition, development of interlocking features on miniature compliant joints was considered. The shape synthesis of the mechanism was performed using the following three step approach. First, to generate a basic shape of the mechanism, the design concept was detailed by adding functionality and manufacturability constraints. Second, the constrained dimensions of the mechanism were determined by analyzing mating components and motion requirements. Third, the miniature compliant joint geometry was investigated to determine how to achieve a successful connection between

chemically incompatible polymers in a multi-material structure. This approach is summarized in Figure 64.

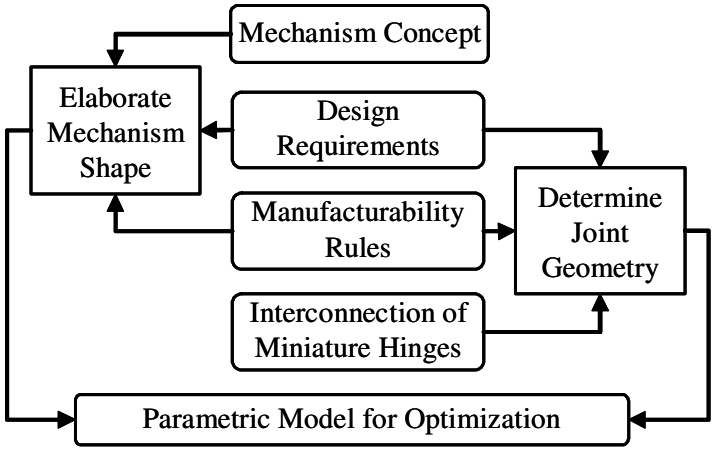

Figure 64: Shape synthesis for parametric model

To achieve flapping wing motion from the rotary input of the motor, a crank-rocker mechanism was designed based on the concept illustrated in Figure 63. The motor's rotational velocity was transferred to the crank through a gearbox to obtain the required flapping frequency. The crank was connected to a rocker, which displaced the symmetrically placed wing arms. These arms were pivoted on supporting members, which allowed for the displacement of the pivoting point by utilization of a lumped compliance. To ensure symmetry in the flapping motion, a prismatic joint was introduced at the point where rocker transferred the energy to the wing arms. This was crucial to the forces produced by the wings of the MAV. Experimental results showed that disturbance forces can cause significant out of plane motion of the rocker and the wing arms. To eliminate these issues, an additional frame physically constrains the rocker motion to a single plane, and an undercut feature on the back of the prismatic joint constrains its motion to only one degree of freedom. Figure 65 shows the developed mechanism with characteristic features highlighted.

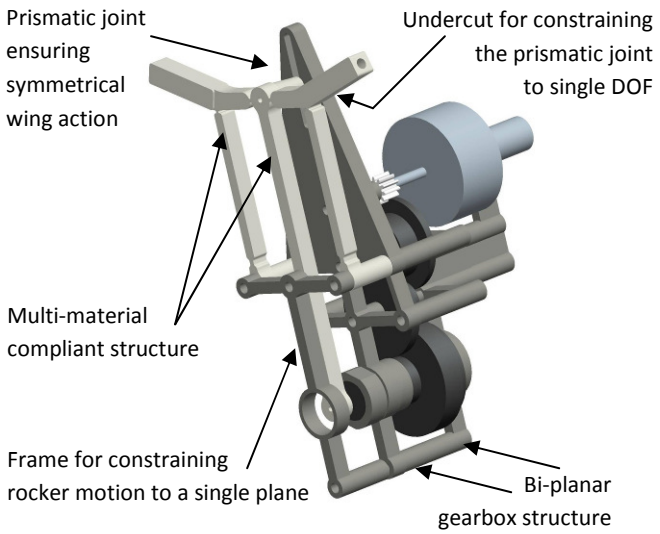

Figure 65: MAV drive mechanism design using localized compliance

After identifying the basic shape of the mechanism using the functionality and moldability constraints, the next step was to determine the dimensions of the mechanism. Considering the functional requirements and constraints on the overall size of the MAV, it was important to first identify the constrained and free dimensions of the mechanism design. The constrained dimensions were identified from the functional requirements of the MAV as follows.

The design of the mechanism required the rocker operational envelope to be placed between the wing arm supports. Therefore the minimum separation between the supporting members was constrained to 19 mm.

For the required flapping range of 65° the relative angle on the wing arms was designed to be 15° and the length of the crank and the rocker to be 4.1 mm and 45.7 mm respectively. The range of flapping motion also determined the range for the prismatic joint to be at least 12 mm to account for elastic deformations of the structure in operation due to loading. The gear axis separation and the range of motion for the prismatic joint determined the minimum length of the mechanism to be 66 mm.

Moldability constraints of the compliant mechanism frame required that the main parting direction of the mold had to be perpendicular to the frame plane. Therefore the minimum thickness of the compliant joints was set to be 0.8 mm. Figure 66 illustrates the fixed dimensions of the mechanism based on the constraints described.

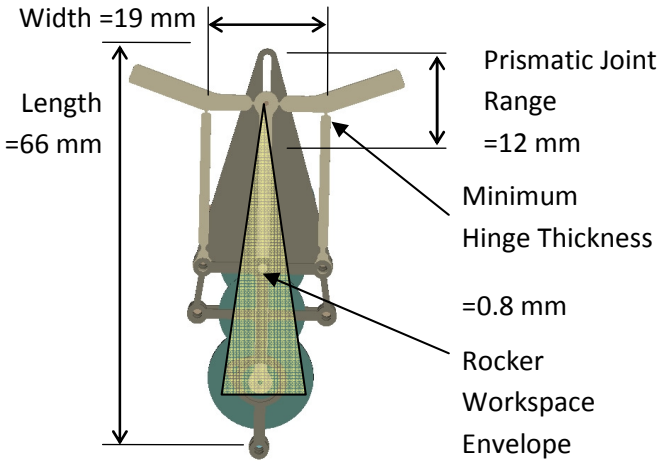

Figure 66: Constrained dimensions of the mechanism

In order to reduce the rotational velocity of the motor to match the flapping frequency requirement, a three-step gear reduction of 55.4:1 was designed. Futaba FUTM3405 spur gear set with modules 0.3 and 0.4 was used. The gearbox was designed to match the gear bearing surfaces and it utilized a bi-planar design for enhanced stability. This allowed for two-point support of the gears' axis and allowed for prevention of the crank wobbling effect induced by the large torque transmission to the rocker. To reduce friction, machine grease was applied to the bearing surfaces and the gear teeth. The bi-planar gearbox assembled with the frame constraining the rocker created a rigid tri-planar enclosure of the mechanism, preventing it from damage during MAV landing.

The mechanism utilized a multi-material compliant structure to transform the motor's rotational velocity to the flapping motion. This novel design combined seven rigid links

connected with six compliant hinges to create a functional, single-piece mechanism. The molded structure consisted of the rocker, wing arms and their supports. It also provided for the prismatic joint attachment point and proper offset with respect to the crank.

6.5 Estimation of Forces for Optimization of Mechanism Dimensions

6.5.1 Optimization Process

The next step in the approach undertaken in this design was to develop models to allow for optimization of the multi-material compliant drive mechanism of the MAV. To this end, the parametric models of the mechanism resulting from unconstrained dimensions developed in Section 6.4 were employed and the experimental data from Section 3.3 were used as the boundary conditions in a design evaluation simulation. Since the overall functionality of the MAV depends on its payload capabilities, the weight of the drive mechanism should be minimized with constraints set on load transfer capability. The design variables used included sizing of the mechanism rigid links, critical for the drive functionality, as well as sizing dimensions of the miniature compliant joint cross-section. The experimental results of lift and thrust forces generated by MAV wings were inserted into a dynamic simulation model as input boundary conditions. The simulation was then used to estimate propagation of the wing forces through the mechanism structure. The resulting reaction forces were then used as boundary conditions in the Pro/Mechanica Wildfire 4.0 FEA module to calculate stresses and strains on the structure. To minimize the weight of the mechanism without risking its failure, parts were sized to achieve the required factor of safety. The overview of the optimization process is shown in Figure 67.

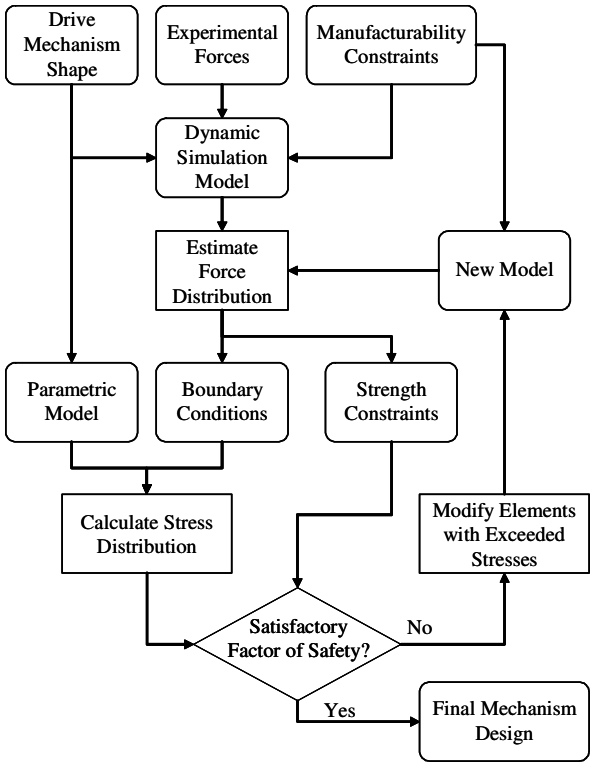

Figure 67: Optimization process flowchart

6.5.2 Kinematic Modeling Synthesis

A planar kinematic representation of the model with key dimensions is shown in Figure 68. This kinematic representation was used to create a planar dynamics model using MD ADAMS R3 software. Motion was generated using a constant speed rotary input of Ω = 338 Hz applied to the gear input, resulting in a maximum flapping rate of 6.1 Hz. Weights of the mechanism components were first included in the model; however, they were observed negligible, due to the low operating frequency of the mechanism, and a relatively low mass of the moving components. Therefore the inertial effects of the mechanism were ignored. The analysis was performed by dividing the motion cycle into multiple time frames and performing a static equilibrium analysis at each time step.

Wing lift and thrust forces from the 6445v4 wings were modeled normal to the wing spars. The planar dynamics model is shown in Figure 69.

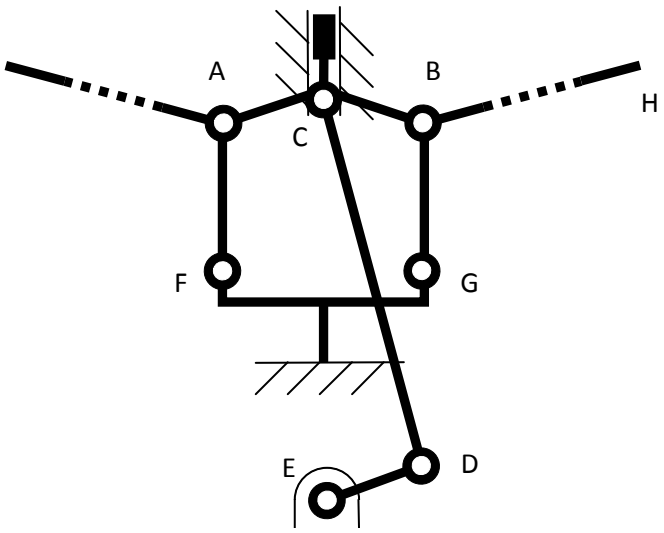

Dimensions:		
AC	9.5	mm
BD	21.5	mm
EF	22.5	mm
CF	45.0	mm
DE	4.1	mm
BH	165	mm

Figure 68: Kinematic representation of the model

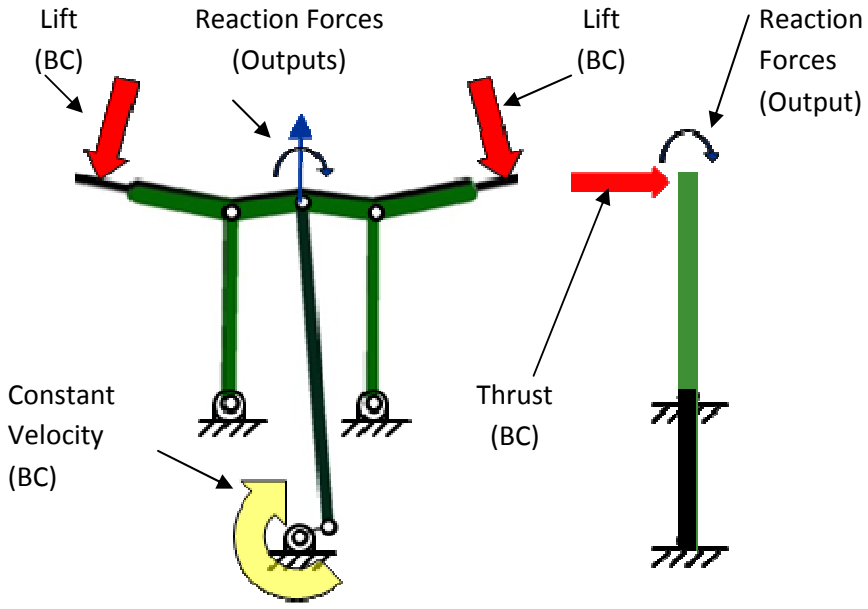

Figure 69: Model synthesis with input boundary conditions (BC) and estimated reaction forces

This was a time-dependant problem, therefore it was necessary to identify the cases where combined loading on the structure would induce the highest von Mises stresses.

The mechanism components most prone to failure were identified as the rocker element (at point C), and the wing arms (at points A and B). The most demanding hinges were present also at point C, so the reaction forces and torsions in these points were plotted in Figure 70 with a resolution of 1e-3 second. The time steps during the flapping cycle that resulted in the highest magnitude of loading were selected as the inputs for finite element analysis, so that the designed factor of safety would correspond to the worst anticipated loading scenario.

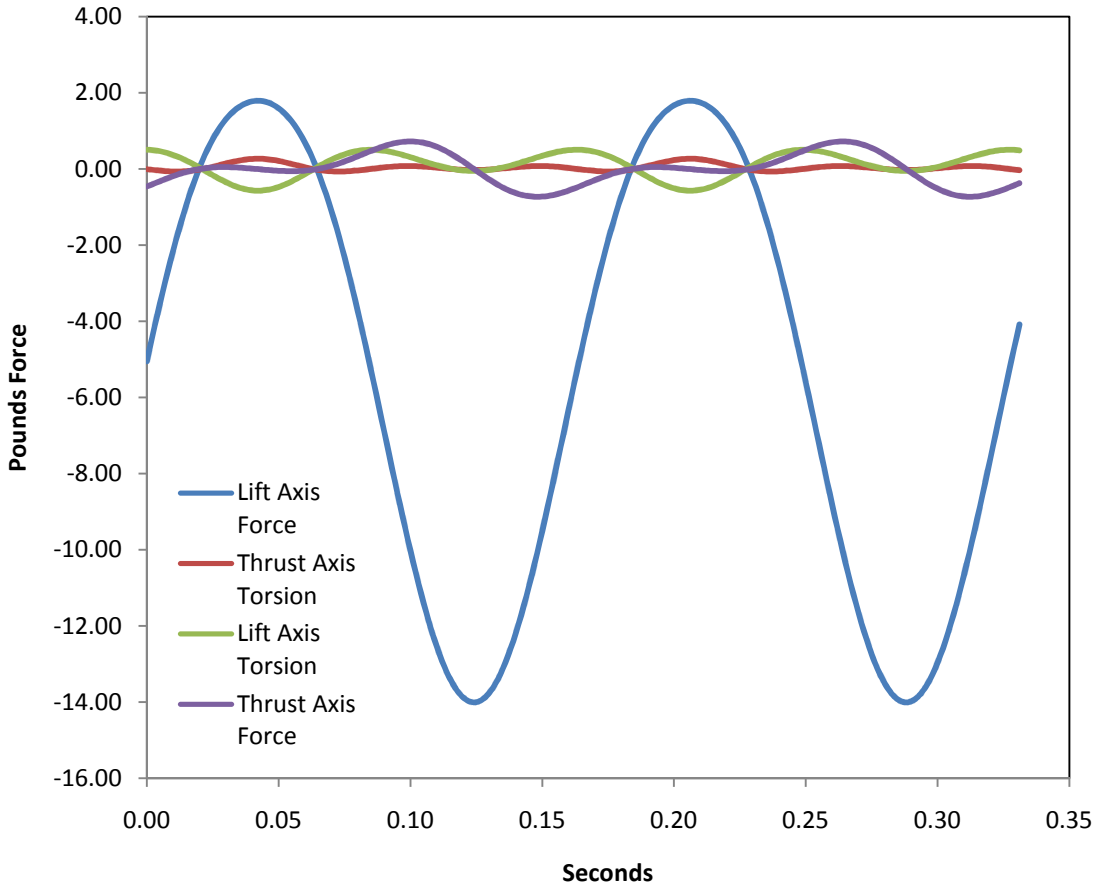

Figure 70: Reaction forces and torsions output by planar dynamics model at point C

The model created for this mechanism differs from the model used in Chapter 5 in an important way. Due to the addition of a prismatic joint, the mechanism was made fully

determinate. This means there was no longer an extra degree of freedom present, where the flexible frame was able to sway left and right. The consequences of this change are evident from the results of the modeling, manifesting in the form of more stable results.

6.5.3 Finite Element Analysis

The final step in the development of the localized compliance flapping mechanism was to use the forces calculated in the planar dynamics model in a finite element analysis. The resulting stress and strain were then used to optimize the remaining mechanism dimensions, specifically the rocker (CD) thickness, wing supports' (AC) thickness, and the compliant hinge cross-section thickness. The goal of the optimization was to minimize the weight of the mechanism, while still satisfying the manufacturability and maximum stress constraints.

The planar dynamics model was run for two full flapping cycles, and the points of the highest loading intensity were selected as candidates for FEA. An analysis of all time steps likely to produce maximum stress in the mechanism was performed, and the loading conditions found to generate maximum von Mises stress values are listed in Table 9.

Table 9: FEA load components

Component	Applied to	Unit	Value
X	A	*N*	-1.159
Y	A	*N*	-32.767
Z	A	*N*	-1.559
X	C	*N*	0.026
Y	C	*N*	62.282

These loads were applied to the corresponding points on the 3D mechanism model. Since forces resulting from the weight of motor and gears were an order of magnitude smaller than the forces resulting from the motion, these forces were excluded from the FEA. The rigid links of the mechanism were modeled using the material properties of

PA6,6F (density=1230 kg/m3, Poisson's ratio=0.3, Young's Modulus=5.5 GPa), and the compliant hinges were modeled using the material properties of LDPE (density=918 kg/m3, Poisson's ratio=0.4, Tensile Strength=9.7 MPa).

Finite element analysis was performed using the Mechanica module of Pro/Engineer Wildfire 4.0 software. The FEA of the worst case loading scenario was performed and the maximum von Mises stresses was plotted across the structure. The yield strength of the PA6,6F material (110 MPa) was then divided by the peak stress to determine the resulting FoS. The rocker and wing arms were designed to have a FoS of 2. This was identified as the average recommended value for known materials with certification under constant environmental conditions, subject to stresses that can be determined using qualified design procedures. Therefore the required cross-section dimensions of the rocker were found to be 2.1 x 2.5 mm and of the wing arms to be 2.5 x5.1 mm. Similarly, the hinge cross-section dimensions were obtained. To allow for low-energy bending, the thickness of the hinge was determined to be 1.1 mm. Considering the forces transmitted by the miniature hinges in point C, the depth of the hinge was calculated to be 6.1 mm in order to meet the FoS of 2 requirement.

6.6 Summary

This chapter presents a new mechanism that converts rotary motion into flapping action using the functional principle of localized compliance. The compliant joints are embedded within the structural material of the mechanism and provide similar benefits as the distributed compliance strategy presented in Chapter 5. The design and analysis approach presented for the localized compliance mechanism uses a combination of functional and manufacturing constraints, as well as loading boundary conditions to

optimize the dimensions of the parts in the mechanism. Kinematic modeling and finite element analysis tools are used in this optimization process to allow weight to be minimized while meeting necessary constraints.

At present, the mechanism is still in the testing phase of its development. Flight tests have been successful, however reliability remains a concern. Due to strong forces out of the flapping plane of the wing arms, unintended deflections are degrading the lifespan of the compliant joints. As these issues are identified and remedied, the reliability of this design has gradually shown improvements, and in time, this mechanism should prove a more effective solution than the mechanism of Chapter 5.

Chapter 7 – Conclusion

7.1 Contributions

The contributions of this work can be separated into three primary categories:

1) A generalized simulation and experimentation methodology has been presented and applied to the design of a flapping mechanism. This approach synthesizes experimentally measured values and kinematic, dynamic, and finite element modeling. By continually validating the results of modeling with real-world test results, model fidelity is enhanced.

2) An experiment-based methodology has been presented for the design of successful compliant flapping wings. A novel test apparatus has been presented that allows for rapid experimental evaluation of the lift and thrust output. By testing a range of wings, a variety of qualitative and quantitative design rules have been established that will allow a designer to understand the necessary properties of a wing that efficiently produces lift and thrust.

3) A successfully flying and controllable MAV has been constructed using the results of contributions 1 and 2. This MAV offers new levels of payload and endurance performance in its size scale, and provides evidence of the benefits of both the mechanism and wing design approaches.

7.2 Anticipated Benefits

The work presented in this thesis can potentially unlock a variety of new applications for flapping-wing MAVs. If designers adopt the techniques for improvement of flapping mechanisms and wings into current and new designs, the performance envelope, and therefore consumer base, will be increased. The ability to enhance the key properties of

payload and endurance offer potential for autopilot-controlled flight, GPS waypoint navigation, and a variety of autonomous flight behaviors.

With the injection molding assembly techniques presented for the localized compliance mechanism design, assembly operations would be reduced relative to a traditional MAV construction approach. With decreased reliance on manual assembly operations, cost and production rates would be improved, thus increasing the disposability of flapping wing MAVs. Many consumer groups would value this trait due to decreased reliance on a single vehicle.

The greatest anticipated benefits of this work are offered to the future designer. Hopefully, the techniques in modeling and experimentation presented in this work will inspire the designer to overcome some challenging problem, and produce the next generation of flapping-wing MAV. The hope that such an accomplishment could be made is the ultimate inspiration motivating this work.

7.3 Future Work

While this thesis has comprised a considerable step towards development of improved flapping-wing MAVs, there are many areas in which future work can offer further insight to designers. The main areas of interest for this future improvement are directly related to the work that has been completed in this thesis.

7.3.1 Improvement of Distributed Compliance Mechanism Model

The pseudo-rigid body mechanism used to model the distributed compliance in the flapping mechanism used torsion springs and dampers to anchor rigid links. While this technique offered acceptable modeling success in this work, significant room for improvement exists. The non-linear stiffness and damping effects that are present in the

real mechanism are not accurately modeled, resulting in significant disagreement in the time profile of deflection and loading. To accurately model these effects, a flapping mechanism would need to be instrumented using highly miniaturized strain gages, and a variety of dynamic characterization tests would need to be performed. With a more comprehensive understanding of the behavior of the compliant frame, the modeling fidelity would be greatly enhanced.

7.3.2 3-D Motion Tracking of Wing Deformation

In this work, the deformation of compliant wings was performed in a rudimentary way. By filming the wings motion, the deflections could be indirectly measured. However, a more thorough approach would require the wings to be equipped with motion tracking beacons and filmed using multiple camera angles. The data could then be used to construct a 3-D time dependent surface plot of each wing. With this information, a rigorous aerodynamic model could then be imposed to explain, at the lowest level, why a given wing is exhibiting certain lift and thrust performance values.

7.3.3 Improvements to Load Cell Measurement Techniques

The techniques used to measure lift and thrust forces for each set of wings were limited in reflecting the real-world results. Ideally, the wind tunnel and load cell should be reading an average lift that corresponds to a payload flight test. The reasons for these limitations were as follows: the wind tunnel did not provide a perfect laminar airflow, the flow velocity was too low, and the design of the load cell platform did not allow for adjusting the angle of attack to be used during testing. Design of a wind tunnel is a very significant task by itself, however the benefits of a proper wind tunnel would provide a greater

confidence in collected data, and therefore a sharper view of the trends that correspond to small design changes in a given wing.

7.4.4 Standardized Wing Construction Technique

A key issue in the MAV system is the hand-built nature of the wings. As with anything that is built manually, variations will exist that cause random performance anomalies. If a technique were to be devised that could create constant wing geometry and stiffness, much more useful information would be gleaned from testing. Unfortunately, some of the test results were somewhat masked by the randomness of hand-built wings, contaminating the desired measurements.

References

[1] Yim, M., Duff, D. G., and Roufas, K., 2000, "Modular Reconfigurable Robots, an Approach to Urban Search and Rescue," *Proceedings of the 1st International Workshop on Human-friendly Welfare Robotics Systems*, Taejon, Korea.

[2] Viieru, D., Albertani, R., Shyy, W., and Ifju, P., 2005, "Effect of Tip Vortex on Wing Aerodynamics of Micro Air Vehicles," *Journal of Aircraft*, Vol. **42** (6), pp. 1530-1536.

[3] Albertani, R., Stanford, B., Hubner, J. P., and Ifju, P., 2005, "Characterization of Flexible Wing Mavs: Aeroelastic and Propulsion Effects on Flying Qualities," *Proceedings of the AIAA Atmospheric Flight Mechanics Conference and Exhibit*, San Francisco, California.

[4] Tsuzuki, N., Sato, S., and Abe, T., 2007, "Design Guidelines of Rotary Wings in Hover for Insect-Scale Micro Air Vehicle Applications," *Journal of Aircraft*, Vol. **44** (1), pp. 252-263.

[5] Epson, 2004, Epson Announces Advanced Model of the World's Lightest Micro-Flying Robot, February 3, http://global.epson.com/newsroom/news_2004_08_18.htm

[6] Finio, B. M., Shang, J. K., and Wood, R. J., 2009, "Body Torque Modulation for a Microrobotic Fly," *Proceedings of the IEEE International Conference on Robotics and Automation*, Kobe, Japan, pp. 3449-3456.

[7] Madangopal, R., Khan, Z., and Agrawal, S., 2005, "Biologically Inspired Design of Small Flapping Wing Air Vehicles Using Four-Bar Mechanisms and Quasi-Steady Aerodynamics," *Journal of Mechanical Design*, Vol. **127** (4), pp. 809-817.

[8] Pornsin-Sirirak, T., Tai, Y., Ho, C., and Keennon, M., 2001, "Microbat: A Palm-Sized Electrically Powered Ornithopter," *Proceedings of the NASA/JPL Workshop on Biomorphic Robotics*, Pasadena, CA,

[9] Ltd, F. T., 2009, Wingsmaster Ornithopters, March 17, http://www.flyingtoys.com/index.php?categoryID=28

[10] Bejgerowski, W., Ananthanarayanan, A., Mueller, D., and Gupta, S., 2008, "Integrated Product and Process Design for a Flapping Wing Drive-Mechanism," *Journal of Mechanical Design, Accepted for Publication*, Vol.

[11] Mueller, T. J., 2001, "Fixed and Flapping Wing Aerodynamics for Micro Air Vehicle Applications," American Institute of Aeronautics and Astronautics, Reston, VA.

[12] Osaka Slow Fliers Club, January 4, http://blog.goo.ne.jp/flappingwing

[13] Delfly, T., 2005, Delfly, January 4, http://www.delfly.nl/?site=DI&menu=&lang=en

[14] Jones, K. D., Bradshaw, C. J., Papadopoulos, J., and Platzer, M. F., 2004, "Improved Performance and Control of Flapping-Wing Propelled Micro Air Vehicles," *Proceedings of the AIAA 42nd Aerospace Sciences Meeting and Exhibit*, Reno, Nevada,

[15] Croon, C., Ruijsink, Remes, Wagter, 2009, "Design, Aerodynamics, and Vision-Based Control of the Delfly," *International Journal of Micro Air Vehicles*, Vol. **1** (2),

[16] Cox, A., Monopoli, D., Cveticanin, D., Goldfarb, M., and Garcia, E., 2002, "The Development of Elastodynamic Components for Piezoelectrically Actuated Flapping Micro-Air Vehicles," *Journal of Intelligent Material Systems and Structures*, Vol. **13** (9), pp. 611-615.

[17] Hsu, C.-K., Ho, J.-Y., Feng, G.-H., Shih, H.-M., and Yang, L.-J., 2006, "A Flapping Mav with Pvdf-Parylene Composite Skin," *Proceedings of the Asia-Pacific Conference of Transducers and Micro-Nano Technology*,

[18] Yang, L.-J., Hsu, C.-K., Ho, J.-Y., and Feng, C.-K., 2007, "Flapping Wings with Pvdf Sensors to Modify the Aerodynamic Forces of a Micro Aerial Vehicle," *Sensors and Actuators A: Physical*, Vol. **139** (1-2), pp. 95-103.
[19] Berg, C. V. D., and Ellington, C., 1997, "The Vortex Wake of a 'Hovering' Model Hawkmoth," *Philos Trans Roy Soc Lond Ser B-Biol Sci*, Vol. **352** (1351), pp. 317-328.
[20] Ellington, C., Berg, C. V. D., Willmott, A., and Thomas, A., 1996, "Leading-Edge Vortices in Insect Flight," *Nature*, Vol. **384** (6610), pp. 626-630.
[21] Birch, J., and Dickinson, M., 2001, "Spanwise Flow and the Attachment of the Leading-Edge Vortex on Insect Wings," *Nature*, Vol. **412** (6848), pp. 729-733.
[22] Dickinson, M., Lehmann, F., and Sane, S., 1999, "Wing Rotation and the Aerodynamic Basis of Insect Flight," *Science*, Vol. **284** pp. 1954-1960.
[23] Dickinson, M., and Gotz, K., 1993, "Unsteady Aerodynamic Performance of Model Wings at Low Reynolds Numbers," *Journal of Experimental Biology*, Vol. **174** pp. 45-64.
[24] Wang, Z., Birch, J., and Dickinson, M., 2004, "Unsteady Forces and Flows in Low Reynolds Number Hovering Flight: Two-Dimensional Computations Vs. Robotic Wing Experiments," *Journal of Experimental Biology*, Vol. **207** pp. 449-460.
[25] Weis-Fogh, T., 2005, "Quick Estimates of Flight Fitness in Hovering Animals, Including Novel Mechanisms for Lift Production," *Journal of Experimental Biology*, Vol. **59** (1973), pp. 169-230.
[26] Hsu, C.-K., Evans, J., Vytla, S., and Huang, P., 2010, "Develoment of Flapping Wing Micro Air Vehicles - Design, Cfd, Experiment and Actual Flight," Orlando, Florida.
[27] Breugel, F. V., Teoh, Z. E., and Lipson, H., 2009, *Flying Insects and Robots*, Springer Berlin Heidelberg,
[28] Mueller, D., Gerdes, J., and Gupta, S., 2009, "Incorporation of Passive Wing Folding in Flapping Wing Miniature Air Vehicles," San Diego, CA.
[29] Billingsley, D., Slipher, G., Grauer, J., and Hubbard, J., 2009, "Testing of a Passively Morphing Ornithopter Wing," AIAA Paper Number 2009-1828.
[30] Billingsley, D., and Hubbard, J., 2007, "Passive Wing Morphing for Improved Lift in Flapping Wing Ornithopters," *Proceedings of the AIAA Student Conference Region I-MA*,
[31] Tsai, B.-J., and Fu, Y.-C., 2009, "Design and Aerodynamic Analysis of a Flapping-Wing Micro Aerial Vehicle," *Aerospace Science and Technology*, Vol. **13** (7), pp. 383-392.
[32] Malolan, V., Dineshkumar, M., and Baskar, V., 2004, "Design and Development of Flapping Wing Micro Air Vehicle," Reno, Nevada.
[33] Ornithology, C. L. O., 2003, Baltimore Oriole, March 17, http://www.birds.cornell.edu/AllAboutBirds/BirdGuide/Baltimore_Oriole.html
[34] Olszewski, A., 1997, The Canary Faq, March 19, http://www.upatsix.com/faq/canary.htm
[35] Harper, E. J., Lambert, L., and Moodie, N., 1998, "The Comparative Nutrition of Two Passerine Species: The Canary (*Serinus Canarius*) and the Zebra Finch (*Poephila Guttata*)," *The Journal of Nutrition*, Vol. **128** pp. 2684S-2685S.
[36] Hoyo, J. D., Elliott, A., and Christie, D. A., 1992, *Handbook of the Birds of the World*, Barcelona.

[37] Suarez, R., 1992, "Hummingbird Flight: Sustaining the Highest Mass-Specific Metabolic Rates among Vertebrates," *Cellular and Molecular Life Sciences*, Vol. **48** (6), pp. 565-570.
[38] Pearson, O., 1950, "The Metabolism of Hummingbirds," *The Condor*, Vol. **52** (4), pp. 145-152.
[39] 2009, Northern Cardinal, March 17, http://www.birds.cornell.edu/AllAboutBirds/BirdGuide/Northern_Cardinal.html
[40] Sl Halkin, S. L., 1999, "Northern Cardinal (Cardinalis Cardinalis)," *The Birds of North America*, Vol. **440** (32),
[41] Berg, C. V. D., and Ellington, C., 1997, "The Three-Dimensional Leading-Edge Vortex of a 'Hovering' Model Hawkmoth.," *Philos Trans Roy Soc Lond Ser B-Biol Sci*, Vol. **352** (1351), pp. 329-340.
[42] Wu, P., and Ifju, P., 2010, "Micro Air Vehicle Flapping Wing Effectiveness, Efficiency and Aeroelasticity Relationships," *Proceedings of the 48th AIAA Aerospace Sciences Meeting Including the New Horizons Forum and Aerospace Exposition*, Orlando, Florida,
[43] Conn, A. T., Burgess, S. C., and Ling, C. S., 2007, "Design of a Parallel Crank-Rocker Flapping Mechanism for Insect-Inspired Micro Air Vehicles," *Journal of Mechanical Engineering Science*, Vol. **221** (10), pp. 1211-1222.
[44] Galinski, C., and Zbikowski, R., 2007, "Materials Challenges in the Design of an Insect-Like Flapping Wing Mechanism," *Materials & Design*, Vol. **28** (3), pp. 783-796.
[45] Banala, S., and Agrawal, S., 2005, "Design and Optimization of a Mechanism for out-of-Plane Insect Wing-Like Motion with Twist," *Journal of Mechanical Design*, Vol. **127** (4), pp. 841-844.
[46] Madangopal, R., Khan, Z. A., and Agrawal, S. K., 2004, "Energetics Based Design of Small Flapping Wing Air Vehicles," *Proceedings of the IEEE International Conference on Robotics and Automation*, 3, pp. 2367-2372.
[47] March 4, 2010, http://www.omega.com/Pressure/pdf/LCFD.pdf
[48] March 9, 2010, http://www.edmundoptics.com/onlinecatalog/displayproduct.cfm?productID=1618
[49] March 17, 2010, http://www.wes-technik.de/English/Motors-Brushless.htm
[50] June 19, 2010, www.microinvent.com
[51] March 19, 2010, http://www.bphobbies.com/view.asp?id=V253880&pid=D2635028&img=l
[52] March 20, 2010, www.matweb.com
[53] Gouker, R. M., Gupta, S. K., Bruck, H. A., and Holzschuh, T., 2006, "Manufacturing of Multi-Material Compliant Mechanisms Using Multi-Material Molding," *International Journal of Advanced Manufacturing Technology*, Vol. **30** (11-12), pp. 1049-1075.